

**Radiolabelled iododeoxyuridine for experimental targeted  
radiotherapy of glioma**

**ALI NESHASTEHRIZ**

**BSc., MSc.**

**A thesis presented for the degree of Doctor of Philosophy,**

**Faculty of Medicine, University of Glasgow**

**Department of Clinical Physics and Bio-engineering &**

**Department of Radiation Oncology, CRC Beatson Laboratories**

**University of Glasgow**

**July 1997**

ProQuest Number: 13832094

All rights reserved

INFORMATION TO ALL USERS

The quality of this reproduction is dependent upon the quality of the copy submitted.

In the unlikely event that the author did not send a complete manuscript and there are missing pages, these will be noted. Also, if material had to be removed, a note will indicate the deletion.



ProQuest 13832094

Published by ProQuest LLC (2019). Copyright of the Dissertation is held by the Author.

All rights reserved.

This work is protected against unauthorized copying under Title 17, United States Code  
Microform Edition © ProQuest LLC.

ProQuest LLC.  
789 East Eisenhower Parkway  
P.O. Box 1346  
Ann Arbor, MI 48106 – 1346

Thesis 10994  
Copy 1



## ABSTRACT

Gliomas are the most common primary tumours arising in the human brain. The most malignant glioma, the glioblastoma, represents 5000 new cases per year in the United States. Despite surgery, chemotherapy, and radiotherapy, glioblastomas are almost always fatal, with a median survival of less than a year and a 5-year survival rate of 5.5% or less. After treatment, recurrent disease often occurs locally; systemic metastases are rare. Neurologic dysfunction and death are from local growth. No therapeutic modality has substantially changed the outcome of patients with glioblastoma. Therefore, we have explored a novel form of treatment: targeted radiotherapy using radioiododeoxyuridine, a thymidine analogue that is intended to destroy glioma cells yet spare normal brain tissue. Radiolabelled IUdR is an appropriate targeting vehicle for the delivery of radiation to proliferating tumour target tissue. This study included an investigation of the most suitable radioisotopes to conjugate to IUdR.

Heterogeneous proliferative activity of glioma cells (ie non-cycling cells) is one of the main barriers to the therapeutic potential of radiolabelled IUdR. Therefore, an important part of this work was obtaining appropriate models for the study of human gliomas *in vitro*. We thus employed spheroids derived from UVW, SB18 and U251 glioma cell lines, as well as cells in exponential monolayer growth and plateau phase for this evaluation. Multicellular spheroids grown from established cell lines have been shown to have growth kinetics similar to *in vivo* tumours. As with the clinical situation, in the spheroid model there is an increase in the number of resting cells as the size of the mass enlarges and also there are nonproliferating cells and necrosis in the more central hypoxic area. The UVW cell line was chosen because of its capability to grow as very large and regularly shaped spheroids. The karyotype analysis of UVW cell line revealed a highly

aneuploid cell line.

This cell line was also very radioresistant in both monolayer and spheroid cultures as determined by external beam radiation experiments. The survival fraction values obtained at 2 Gy ( $SF_2$ ) were 0.55 for exponential monolayer cells and 0.83-0.93 for spheroids gained from clonogenic assay and growth delay experiments respectively. These values place this cell line at the radioresistant part of the spectrum of human cell line radiosensitivity.

We assessed the effect of proliferative heterogeneity on the uptake of non-radiolabelled IUdR by studying different sizes of UVW human glioma spheroids and monolayer cell cultures in exponential and plateau phases, in conjunction with flow cytometry. The results of the study confirm that there is an inverse relationship between the proportion of cycling cells and spheroid diameter. In monolayer cultures more than 95% of exponentially growing cells and 62% of plateau phase cells were labelled with IUdR after one doubling time. However, the labelling index in the small spheroids (100-200 $\mu$ m) was approximately 76% and 28% for large spheroids (700-1000 $\mu$ m) after one volume doubling time incubation (52 hours). The proportion of cells that incorporate IUdR is small and large sizes of spheroids increased with increasing the period of incubation with IUdR from one to four volume doubling times.

The effect of spheroid size and incubation time on labelling index was also evaluated in conjunction with autoradiography and Ki67 immunostaining. In these experiments nuclear incorporation of [ $^{125}$ I]IUdR decreased markedly with increasing size of spheroid. The distribution of IUdR was uniform throughout small spheroids (<200 $\mu$ m), while the concentration of IUdR occurred predominantly in the peripheral cells of larger spheroids.

Radiopharmaceutical uptake corresponded closely to the regions of cell cycling as indicated by staining for the nuclear antigen Ki67. The IUdR uptake enhancement occurred by increasing the incubation time from 52 hours to 104 hours. It was concluded that a single injection of radioiodinated IUdR would be insufficient to sterilise all of the malignant cells. Therefore, to achieve maximal therapeutic benefit IUdR should be administered either by multiple injections or by slow release from polymers or slow-pump delivery.

As a possible approach to overcome this barrier of proliferation heterogeneity, the toxicities of three radioiodoanalogues of IUdR, [ $^{123}\text{I}$ ]IUdR, [ $^{125}\text{I}$ ]IUdR and [ $^{131}\text{I}$ ]IUdR were compared, using the human glioma cell line UVW, cultured as monolayers in exponential and plateau phase of growth and as multicellular spheroids using a clonogenic end point.

Both  $^{125}\text{I}$  and  $^{123}\text{I}$  are very short range Auger emitters while  $^{131}\text{I}$  is a  $\beta$ -emitter which will provide some 'cross fire' irradiation between cells. The experiments showed that [ $^{125}\text{I}$ ]IUdR (concentration resulting in 37% survival ( $C_{37}$ ) = 2.36 kBq/ml) was a more effective eradicator of clonogens in monolayers treated in exponential growth phase than [ $^{123}\text{I}$ ]IUdR and [ $^{131}\text{I}$ ]IUdR ( $C_{37}$  = 9.75 and 18.9 kBq/ml) respectively, whereas plateau phase monolayer cultures were marginally more susceptible to treatment with [ $^{123}\text{I}$ ]IUdR and [ $^{125}\text{I}$ ]IUdR (40% clonogenic survival) than [ $^{131}\text{I}$ ]IUdR (60% clonogenic survival). In glioma spheroids both [ $^{125}\text{I}$ ]IUdR and [ $^{123}\text{I}$ ]IUdR, were again more effective than [ $^{131}\text{I}$ ]IUdR at concentration up to and including 20 kBq/ml. However, at concentrations of 40 kBq/ml and higher, [ $^{131}\text{I}$ ]IUdR was superior in killing relative to the other isotopes, resulting in lower survival for [ $^{131}\text{I}$ ]IUdR than [ $^{123}\text{I}$ ]IUdR and [ $^{125}\text{I}$ ]IUdR. The clonogenic survival values at 100 kBq/ml were 13%, 45% and 28% for [ $^{131}\text{I}$ ]IUdR, [ $^{123}\text{I}$ ]IUdR and [ $^{125}\text{I}$ ]IUdR respectively. In conclusion, only cells which were in S phase during the period of incubation with radiopharmaceutical, were killed by IUdR conjugated Auger electron emitters ( $^{123}\text{I}$  and  $^{125}\text{I}$ ), whereas [ $^{131}\text{I}$ ]IUdR at higher concentration had superior toxicity to

clonogenic cells in spheroids due to cross-fire  $\beta$ -irradiation on  $G_0$  cells. These findings suggest that a combination of [ $^{131}\text{I}$ ]IUdR and [ $^{125}\text{I}$ ]IUdR or [ $^{123}\text{I}$ ]IUdR might be more effective than [ $^{125}\text{I}$ ]IUdR or [ $^{123}\text{I}$ ]IUdR alone for the treatment of residual glioma. Another therapeutic strategy may be based on combination of Auger emitters and  $\alpha$ -emitter radioisotopes like  $^{211}\text{At}$  in the form of [ $^{211}\text{At}$ ]AUdR and [ $^{125}\text{I}$ ]IUdR for eliminating untargeted cells.

***THIS THESIS IS DEDICATED TO MY WIFE TO WHOM  
I OWE MORE THAN I COULD EVER SAY***

## TABLE OF CONTENTS

Abstract . . . . .	I
Dedication . . . . .	V
Table of contents . . . . .	VI
Index of tables . . . . .	VIII
Index of figures . . . . .	X
Abbreviations . . . . .	XIII
Acknowledgements . . . . .	XVI
Declaration . . . . .	XVII
<b>Chapter one:</b>	
The biology and treatment of malignant glioma . . . . .	1
<b>Chapter two:</b>	
The radiobiology of glioma cells in culture . . . . .	30
<b>Chapter three:</b>	
Targeted radiotherapy . . . . .	57
<b>Chapter four:</b>	
General materials and methods . . . . .	80
<b>Chapter five:</b>	
Biology of human glioma cell lines . . . . .	97
<b>Chapter six:</b>	
Cellular radiosensitivity of the human glioma cell line UVW . . . . .	120
<b>Chapter seven:</b>	
Flow cytometric cell cycle analysis . . . . .	133

**Chapter eight:**

Incorporation of radiolabelled IUdR in spheroids of different size  
and monolayer cells . . . . . 149

**Chapter nine:**

Differential cytotoxicity of alternative radioiodoanalogues of IUdR  
to human glioma cells in monolayer or spheroid culture . . . . . 172

**Chapter ten:**

Conclusions and future work . . . . . 197

**References** . . . . . 205

## LIST OF TABLES

### **Chapter 1**

- 1.1 WHO histological typing of CNS tumours . . . . . 7
- 1.2 WHO grading system (malignancy scale) of CNS tumours . . . . . 9
- 1.3 Average annual age adjusted mortality rates per 100 000 for malignant neoplasms  
of brain in selected countries, by sex. 1960 and 1985 . . . . . 12
- 1.4 Comparison of five publications reporting the results of surgery (1937-1974) . . . 20

### **Chapter 2**

- 2.1 The GFAP status in established human malignant glioma cell lines . . . . . 35
- 2.2 *In vitro* cell survival curve parameters of malignant glioma cell lines . . . . . 49
- .

### **Chapter 3**

- 3.1 Currently promising approaches to targeted radiotherapy . . . . . 61
- 3.2 Physical properties of radionuclides of current interest for targeted therapy . . . . 63
- 3.3 Applications of spheroids in targeted radiotherapy research . . . . . 78

### **Chapter 5**

- 5.1 Phenotypic and genotypic characteristics of human glioma cell lines . . . . . 104
- 5.2 Growth curve parameters of glioma cell lines . . . . . 107
- 5.3 Karyotype analysis of the UVW glioma cell line . . . . . 111

### **Chapter 6**

- 6.1 Radiobiological survival curve parameters for UVW spheroids and  
exponentially growing monolayers . . . . . 127

## **Chapter 9**

9.1 Slope and $D_0$ of survival curve of UVW monolayer cells in exponential growth	178
9.2 Slope of the initial portion of the survival curves of UVW spheroids . . . . .	180
9.3 Comparison between labelling index studied by flow cytometry, autoradiography and cell killing by clonogenic assay . . . . .	182
9.4 Uptake of [ $^{125}\text{I}$ ]IUdR into UVW cells in exponential growth for different concentrations of the radiopharmaceutical in the medium . . . . .	183
9.5 Number of decays per cell for $^{123}\text{I}$ and $^{131}\text{I}$ relative to $^{125}\text{I}$ , integrated over incubation periods of 44 and 52 hours . . . . .	183

## LIST OF FIGURES

### Chapter 2

- 2.1 Properties of the multi-target model of radiation cell killing . . . . . 46
- 2.2 Form of the linear-quadratic survival equation . . . . . 47

### Chapter 3

- 3.1 Structures of IUdR and thymidine . . . . . 73
- 3.2 Salvage pathway for TdR and IUdR incorporation into DNA . . . . . 74

### Chapter 5

- 5.1 Phase contrast micrographs of morphology of (a) UVW monolayer cells and (b) UVW spheroids . . . . . 105
- 5.2 Phase contrast micrographs of morphology of monolayers cells of (a) U251, (b) SB18 . . . . . 106
- 5.3 Growth curves of glioma cell lines . . . . . 108
- 5.4 Spheroid growth curve . . . . . 109
- 5.5 Karyotype of the UVW cell line . . . . . 112
- 5.6 Flow cytometry analysis of UVW cells in exponential and plateau phase culture 114
- 5.7 A) Histogram of PI stained CEN.  
B) Ploidy study of UVW cells in monolayer exponential culture . . . . . 116

## **Chapter 6**

6.1 General principle of estimation of cell surviving fraction from spheroid regrowth curves . . . . .	125
6.2 Growth curves for UVW glioma multicellular spheroids treated with single dose irradiation . . . . .	128
6.3 Survival fraction of UVW spheroids obtained from regrowth delay and clonogenic assay methods . . . . .	129
6.4 Survival curves of UVW multicellular spheroids and monolayer cells calculated from clonogenic assay after external beam irradiation . . . . .	130

## **Chapter 7**

7.1 Concentration dependence of IUdR uptake in exponentially growing UVW cells after incubation with a range of concentrations of IUdR . . . . .	142
7.2 Concentration dependence of IUdR uptake in spheroids of different size . . . . .	143
7.3 Comparison between labelling index studied by flow cytometry of monolayer cells in exponential and plateau phase after one to three doubling times incubation . . . . .	144
7.4 Labelling indices of small and large spheroids after one to four volume doubling times incubation with non-radiolabelled IUdR . . . . .	145

## **Chapter 8**

8.1 Sections of (a) 1000 $\mu\text{m}$ diameter and (b) 250 $\mu\text{m}$ diameter spheroids, showing cells labelled with both Ki67 and IUdR . . . . .	160
--	-----

8.2 Total Ki67 and IUdR (52 and 104 hours incubation) labelling indices in the viable rim of spheroids as a function of spheroid diameter . . . . .	161
8.3 The relationship between Ki67 and IUdR labelling indices for 52 and 104 hour incubation periods . . . . .	162
8.4 Regional IUdR labelling indices for 52 and 104 hours incubation as a function of spheroid diameter in (a) outer, (b) middle and (c) inner 25µm cell layers . . . .	163

**Chapter 9**

9.1 Survival fraction of UVW monolayer cells in exponential growth phase after incubation with [ <sup>125</sup> I]IUdR, [ <sup>123</sup> I]IUdR and [ <sup>131</sup> I]IUdR . . . . .	184
9.3 Survival fraction of UVW monolayer cells in exponential growth phase after incubation with Na <sup>125</sup> I and Na <sup>131</sup> I] . . . . .	185
9.3 Survival fraction of UVW monolayer cells in plateau growth phase after incubation with [ <sup>125</sup> I]IUdR, [ <sup>123</sup> I]IUdR and [ <sup>131</sup> I]IUdR . . . . .	186
9.4 Survival fraction of UVW spheroids after incubation with [ <sup>125</sup> I]IUdR, [ <sup>123</sup> I]IUdR and [ <sup>131</sup> I]IUdR . . . . .	187
9.5 Survival fraction of spheroids after 52 and 104 hours incubation with [ <sup>125</sup> I]IUdR	187

## ABBREVIATIONS

$\alpha$	alpha
AT	ataxia telangiactasia
At	astatine
Bi	bismuth
Br	bromine
BUdR	bromodeoxyuridine
CEN	chicken erythrocyte nuclei
CNS	central nervous system
$^{\circ}\text{C}$	degrees centigrade
cm	centimeter
$\text{CO}_2$	carbon dioxide
CT	computed tomography
Cu	copper
DAB	diaminobenzidine
DNA	deoxyribonucleic acid
DPX	synthetic resin mountant
dTMP	deoxythymidine monophosphate
dTTP	deoxythymidine triphosphate
EDTA	ethylenediamine tetra-acetic acid
EGF	epidermal growth factor
EGFR	epidermal growth factor receptor
FGF	fibroblast growth factor
FITC	fluorescein isothiocyanate
GB	glioblastoma multiforme
GFAP	glial fibrillary acidic protein
Gy	gray
cGy	centigray
g	gram
HAMA	human anti-mouse antibody
HPLC	high performance liquid chromatography

H <sub>2</sub> O <sub>2</sub>	hydrogen proxide
IdUMP	iododeoxymonophosphate
IUdR	iododeoxyuridine
kb	kilo-base
kBq	kilobecquerel
kD	kilo-dalton
keV	kilo electron volt
LET	linear energy transfer
LOH	loss of heterozygosity
LQ	linear quadratic
mBq	milibecquerel
MEM	minimum essential medium
M phase	mitosis
mg	miligram
MIBG	meta-iodobenzylguanidine
min	minute
ml	milliliter
mm	millimeter
MBq	megabecquerel
MRI	magnetic resonance imaging
nM	nanomolar
n.c.a	no-carrier-added
NaI	sodium iodide
PBS	phosphate buffered saline
PCNA	proliferating cell nuclear antigen
PDGF	platelet derived growth factor
PE	plating efficiency
PLD	potentially lethal damage
PI	propidium iodide
SDS	sodium dodecyl sulphate
SLD	sub-lethal damage
SF2	surviving fraction at 2 Gy
t 1/2	half life

TBq	terabecquerel
TdR	thymidine
TE	Tris-EDTA
TK	thymidine kinase
TMPK	thymidylate kinase
TS	thymidylate synthetase
Ts	duration of S phase
Tpot	potential doubling time
μg	microgram
μl	microlitre
μm	micrometer
μM	micromolar
v/v	volume per volume
WHO	world health organization
w/v	weight per volume

## ACKNOWLEDGEMENTS

Firstly, I would like to thank the University of Medical Science of Iran for providing me with a PhD studentship. My special thanks are due to Dr Tom Wheldon and Dr Rob Mairs, my great supervisors, for making available all the facilities of their department, for their general guidance, support, friendship and encouragement during the course of this work. Also I would like to express my gratitude to Professor A.T. Elliott and Dr Roy Rampling for their support and concern over my project.

In particular, I am greatly indebted to Dr Wilson Angerson for his helpful discussion, and for help with statistical analysis and advice on my project.

Thanks also to Dr Jonathan Owens for his help in synthesising and labelling IUdR and also to Dr Peter Stanton for his friendly help on flow cytometry. Thanks also go to Drs Jonathan Reeves and Ian Freshney for their advice and technical expertise.

A special word of thanks to Dr Marie Boyd for her kindly help and encouragement during my writing up. Also I would like to thank Dr JH Mao who gave freely of his help and made valiant attempts to make me "computer literate"; to Ann Livingstone and Shona Cunningham for managing to drag me away from the computer for celebrations on various occasions during this time. I would like also to acknowledge the help in literary searches, received from our librarian, Mrs. Liz Gordon.

Last, but not the least, I wish to thank my children, Amir Reza and Amir Hossein for their loving pride and patience during the many long weekends and late evening I spent with my research. My final, heartfelt word of thanks goes to my wife for tolerating my anti-social hours and remaining my best friend, during what might have seemed at times, like my single-minded devotion to this piece of work. The warmth and support provided at home was my constant source of strength.

## DECLARATION

The work contained in this thesis was performed by myself with the following exceptions; the statistical analysis by Dr Wilson Angerson, Department of Surgery, Glasgow Royal Infirmary; Synthesis of the precursor and labelling by Dr Jonathan Owens, Department of Clinical Physics and Bio-engineering, Radionuclide Dispensary, Western Infirmary and flow cytometry analysis carried out in collaboration with Dr Peter Stanton, Department of Surgery, Glasgow Royal Infirmary. Karyotype analysis was carried out by the Department of Medical Genetics, Royal Hospital for Sick Children, Yorkhill, Glasgow.

# **Chapter 1**

## **The biology and treatment of malignant glioma**

<b>The biology and treatment of malignant glioma</b> . . . . .	1
<b>1.1 Historical background</b> . . . . .	3
<b>1.2 Classification</b> . . . . .	5
<b>1.3 Epidemiology of brain tumours</b> . . . . .	8
1.3.1 Incidence . . . . .	8
1.3.2 Mortality . . . . .	10
1.3.3 Age and sex distribution . . . . .	10
<b>1.4 Genetic factors</b> . . . . .	13
1.4.1 p53 gene . . . . .	13
1.4.2 Gene amplification and oncogene expression . . . . .	16
<b>1.5 Treatment of malignant glioma</b> . . . . .	18
1.5.1 Surgery in the treatment of malignant glioma . . . . .	18
1.5.2 Radiotherapy of brain tumours . . . . .	21
1.5.2.1 Altered fractionation schedules in brain tumour radiotherapy . . . . .	22
1.5.2.2 Radiosurgery . . . . .	23
1.5.3 Radiation modifiers . . . . .	24
1.5.4 Brachytherapy . . . . .	26
1.5.5 Chemotherapy . . . . .	27
1.5.5.1 Local chemotherapy and the potential for locally delivered targeted radiotherapy . . . . .	29

## 1.1 Historical Background

Malignant gliomas comprise more than 40% of central nervous system malignancies and are associated with a very poor prognosis (MacDonald, 1994). They also account for approximately 20% of all paediatric neoplasms of which approximately two-thirds are infratentorial. Gliomas present a supreme challenge to local modes of therapy (Kramer, 1975). In 1966, Bouchard reported that growth and extension of primary intracranial tumours is essentially a regional and localized neoplastic process (Bouchard, 1966). Although this tumour does not metastasise to distant sites, it undergoes diffuse local spread within the brain. Surgical resection with a generous margin of adjacent normal tissue is rarely feasible (Kramer et al., 1972).

The percentage of patients cured by surgery alone has not increased significantly despite the development of new diagnostic tools, improved surgical and anaesthetic techniques and earlier referral of patients for definitive treatment. As radiation therapy has improved, its role has expanded in the treatment of many types of central nervous system neoplasms (Rasmussen et al., 1966).

Shortly after the discovery of X-rays and of radioactivity, at the end of the 19<sup>th</sup> century, radiotherapy was applied to the treatment of brain tumours. It was the first modality to make a significant difference to the survival of patients with malignant intracranial lesions (Walker et al., 1978). In 1921, Ewing predicted the radiosensitivity of various brain tumours based on several histological criteria (Ewing, 1921). However, we nowadays consider that histological features may predict the speed of response to radiotherapy, rather than the magnitude of cell kill. Nordentoft (1922) reported the treatment with radiation therapy of nineteen clinically diagnosed brain tumours, nine of which regressed and ten

failed to respond. He concluded that those who failed to respond were incorrectly diagnosed.

In 1977, Sheline examined a number of published studies which compared the results of surgery alone to the use of surgery and postoperative radiation therapy (Sheline, 1977). He documented a benefit for the addition of radiation therapy in grade III tumours and a benefit in grade IV tumours for up to 4 years. Subsequently, it was demonstrated by a prospective randomized comparison, that an unequivocal benefit was derived from the addition of postoperative radiation therapy relative to surgical removal alone (Walker et al., 1978).

## 1.2 Classification of gliomas

Glia are the most numerous cells in the human brain, and comprise astrocytes, oligodendrocytes and ependymal cells. Astrocytes perform many essential functions, including participation in neuronal conduction and response to injury. Oligodendrocytes produce the myelin sheaths that facilitate conduction of neuronal impulses, while ependymal cells line the ventricles of the brain, and specialized ependymal cells in the choroid plexus regulate cerebrospinal fluid production. Malignant gliomas are divided into three histopathological grades. These include low grade astrocytoma (World Health Organization grade II), anaplastic astrocytoma (grade III) and GB (glioblastoma) (grade IV) (Kleihues et al., 1993). The most malignant form (GB), is thought to arise either *de novo* or secondarily from lower-grade glioma. The designation 'multiforme', used in older nomenclature, refers to the pathological heterogeneity characteristic of this tumour (Table 1.1). Secondary GBs characteristically occur in younger adults and can develop years after an initial diagnosis of a low-grade tumour. Alternatively, GB might occur in a so-called *de novo* form, where there is no clear history of a lower-grade precursor lesion, a scenario typically occurring in older adults (Morantz, 1995). Of the malignant gliomas that affect adults, the most prevalent are the astrocytomas and GB which greatly outnumber all other types, accounting for at least 70% of cases. The less common oligodendrogliomas and oligoastrocytomas each represent about 5 to 15% of the total number of cases. The prognosis in malignant glioma correlates with the patient's age and performance status, tumour grade and tumour type but in general, younger, fitter patients with lower-grade, non-astrocytic tumours have somewhat better prognoses. However, the lower-grade tumours display a remarkable tendency to undergo malignant transformation (Morantz, 1995) and younger patients with lower-grade tumours will frequently represent with higher-grade tumours with rapidly fatal consequences. For these reasons, there has

been interest in elucidating the biological basis of malignant progression in gliomas (Leenstra et al., 1994).

It is worth noting however, that any histologic grading system will suffer inaccuracies if insufficient or unrepresentative biopsy material is submitted for evaluation. This is especially true for gliomas, which have considerable intratumoral heterogeneity (Taratuto et al., 1991; Paulus and Peiffer, 1989).

**Table 1.1** WHO histological typing of CNS tumours (Kleihues et al., 1993)

Tumours of neuroepithelial tissue

Astrocytic tumours

Astrocytoma  
Variants: Fibrillary  
          Protoplasmic  
          Gemistocytic  
Anaplastic (malignant) astrocytoma  
Glioblastoma  
Variants: Giant cell glioblastoma  
          Gliosarcoma  
Pilocytic astrocytoma  
Pleomorphic xanthoastrocytoma  
Subependymal giant cell astrocytoma

Oligodendroglial tumours

Oligodendroglioma  
Anaplastic (malignant)  
oligodendroglioma

Ependymal tumours

Ependymoma  
Variants: Cellular  
          Papillary  
          Clear cell  
Anaplastic (malignant) ependymoma  
Myxopapillary ependymoma  
Subependymoma

Mixed gliomas

Oligo-astrocytoma  
Anaplastic (malignant)  
Oligo-astrocytoma  
Others

Choroid plexus tumours

Choroid plexus papilloma  
Choroid plexus carcinoma

Neuroepithelial tumours of uncertain origin

Astroblastoma  
Polar spongioblastoma  
Gliomatosis cerebri

Neuronal and mixed neuronal-glial tumours

Gangliocytoma  
Dysplastic gangliocytoma of cerebellum  
Desmoplastic infantile ganglioglioma  
Dysembryoplastic neuroepithelial tumour  
Ganglioma  
Anaplastic (malignant) ganglioma  
Central neurocytoma

Pineal parenchymal tumours

Pineocytoma  
Pineoblastoma  
Mixed/ transitional pineal tumours

Embryonal tumours

1. Medulloepithelioma
  2. Neuroblastoma  
   Variant: ganglioneuroblastoma
  3. Ependymoblastoma
  4. Retinoblastoma
  5. Primitive neuroectodermal tumours (PNET)  
   with multipotential differentiation-neuronal,  
   astrocytic, ependymal, muscle, melanocytic,  
   etc.
- a. Medulloblastoma  
   Variants: desmoplastic, medullomyoblastoma,  
   melanocytic medulloblastoma

## **1.3 Epidemiology of glioma**

### **1.3.1 Incidence**

Primary brain tumours, of which about 40% are gliomas, constitute 1-2% of all human tumours (Codd and Kurland, 1985; Laerum et al., 1978). The most malignant glioma, glioblastoma, represents 29% of all primary brain tumours or 5000 new cases per year in the United States (Mahaley et al., 1989). All gliomas are all malignant to some extent and about 50% fall into the WHO categories anaplastic astrocytoma and glioblastoma of grade III or IV. Table 1.2 shows the WHO grading system of CNS tumours (Kleihues et al., 1993).

**Table 1.2** World Health (1993) Organization grading system (malignancy scale) of CNS

tumours

<u>Tumour Group</u>	<u>Tmour Type</u>	Grade I	Grade II	Grade III	Grade IV
Astrocytic tumours	Subependymal-giant cell	*			
	Pilocytic	*			
	Low grade		*		
	Pleomorphic xanthoastrocytoma		*	*	
	Anaplastic			*	
	Glioblastoma				*
Oligodendrogliomas	Low grade		*		
	Anaplastic			*	
Oligo-astrocytomas	Low grade		*		
	Anaplastic			*	
Ependymal tumours	Subependymoma	*			
	Myxopapillary	*			
	Low grade Anaplastic		*		*
Choroid plexus- tumours	Papilloma	*			
	Carcinoma			*	*
Neuronal/glial tumours	Gangliocytoma	*			
	Ganglioglioma	*	*		
	Desmoplastic-infantile ganglioma	*			
	Dysembryoplastic neuroepithelial tumour	*			
	Central neurocytoma	*			
Pineal tumours	Pineocytoma		*		
	Pineocytoma / pineoblastoma			*	*
	Pineoblastoma				*
Embryonal tumours	Medulloblastoma				*
	Other PNETs				*
	Medulloepithelioma				*
	Neuroblastoma				*
	Ependymblastoma				*
Cranial & spinal nerve tumours	Schwannoma	*			
	Malignant peripheral nerve sheath tumour			*	*
Meningeal tumours	Meningioma	*			
	Atypical meningioma		*		
	Papillary meningioma		*	*	
	Hemangiopericytoma		*	*	
	Anaplastic-meningioma			*	
					*

### **1.3.2 Mortality**

The death rate for intracranial tumours is similar in most countries which produce mortality statistics, and ranges between 3.2-5.6 per 100,000 of population (Muir et al., 1994). Table 3.1 shows the comparison of mortality rates in 1960 and 1985.

### **1.3.3 Age and sex distribution**

Glioblastoma is a disease which affects children and adults of all ages with greater incidence in late middle age (Kornblith et al., 1987). The overall incidence of primary brain and central nervous system cancer ranges from six to sixteen per 100,000 (Polednak, 1991) and the age-adjusted incidence of primary brain tumours is rapidly increasing in the United States, especially in the elderly and has more than doubled over the past two decades (Desmeules et al., 1992). It was estimated that 17,500 Americans would develop malignant brain tumours in 1994 (Boring et al., 1994). The Connecticut Tumour Registry noted a significant increase in brain tumour incidence in age groups from 65 to 69 years and 80 to 84 years between the periods 1965 to 1969 and 1985 to 1988 (Polendak, 1991). In a study in Lothian Region in south-east Scotland in 1989 to 1990, among 106 patients, 60 (57%) were of working age (15 to 64 years). The average annual incidence of cerebral glioma in this age range was 5.9 per 100,000 per year. Overall it was reported that cerebral glioma will affect approximately 2100 people of working age in the UK every year (Grant et al., 1996).

The reason for the increase has not been determined, but dental radiographs and therapeutic radiation in childhood might be associated with slightly higher incidence

of brain tumours (Ryan et al., 1992). Some studies have also reported an increased incidence of primary brain tumours in individuals extensively exposed to electromagnetic fields (Feychting and Ahlbom, 1992). Others suggested etiological factors associated with increased CNS tumour risk include industrial chemicals, head injury and diet in childhood (Giles and Gonzales, 1995).

Brain tumours tend to occur most frequently at two distinct periods of life: in childhood and in late middle age. Posterior fossa tumours are commoner in children (e.g. medulloblastomas and cerebellar astrocytomas) whereas supratentorial hemisphere tumours are most common in adults (e.g. malignant astrocytomas). There is some evidence to suggest an unequal sex distribution of some tumour types. Glioblastomas and medulloblastomas being more common in males than females (1.5-2.3 :1), whilst meningiomas are more common in females (Laerum et al., 1978).

Location	1960		1985	
	Male	Female	Male	Female
Canada	4.3	3.0	4.9	3.3
Singapore	–	–	1.8	1.1
Israel	–	–	3.2	2.4
Finland	3.2	2.2	4.1	3.5
Norway	4.5	3.2	5.1	3.3
Sweden	3.6	2.5	4.5	3.5
Switzerland	4.1	2.6	4.9	3.1
UK, Scotland	4.2	2.7	4.6	3.2
New Zealand	5.0	3.3	5.4	3.7
USA	3.9	2.6	4.1	2.8

**Table 3.1** Average annual, age-adjusted, mortality rates per 100, 000 for malignant neoplasms of brain in selected countries, by sex for 1960 and 1985 (Muir et al., 1994).

## 1.4 Genetic factors

Over the past several years, some of the molecular abnormalities associated with primary brain tumours have been elucidated, but it is still unclear which genetic aberrations are the rate-limiting steps that lead to neoplastic transformation and progression to various malignant stages. The application of molecular biological techniques to the investigation of gliomas has greatly increased our understanding of changes that lead to their creation. This tumorigenic process involves an interplay between two classes of genes: oncogenes and tumour suppressor genes. It is believed that these genes exert a balance control on cell growth (Bigner et al., 1988; Weingerg, 1989). Cells can receive an exaggerated impulse to grow and divide either from oncogene activation or from tumour suppressor gene inactivation.

Various chromosomal abnormalities have been described in gliomas, most of which are associated with the most malignant form, glioblastoma multiforme. These include gain of chromosome 7 and loss of chromosomes 9p, 10p, 11p, 13p, 17p, or 22. The tumour-suppressor gene *p53* which is located on 17p (Fults et al., 1992a) is discussed below. Also in the low-grade gliomas, including oligodendrogliomas and mixed oligodendroglioma, double-minute chromosomes occur less frequently than in malignant gliomas.

### 1.4.1 The *p53* gene

The *p53* gene is located on the short arm of chromosome 17 and is composed of 11 exons that encode a 2.2 to 2.5-kb messenger RNA, producing a 53,000-D protein (Fults et al., 1992b). The protein has an acidic N terminal that forms an  $\alpha$  helical structure and a basic C terminal capable of binding DNA. The encoded protein of the wild-type *p53* gene has

been shown to function in a wide variety of biological processes including the suppression of cell transformation, but certain gene mutations result in loss of this function and increase the transformation potential of cells. It has been suggested that the *p53* gene acts as the 'guardian of the genome', repairing mutagenic alterations or mediating cell death (Lane, 1992). The wild-type *p53* protein may be involved in inhibition of DNA synthesis and G<sub>1</sub> phase arrest after cellular DNA damage (Kuerbitz et al., 1992). Such cell-cycle delays (checkpoints) provide opportunities for DNA repair before replication or segregation of the affected chromosomes (Hartwell and Weinert, 1989). Therefore, alterations of the *p53* gene are thought to cause genomic instability that may induce other genetic changes. In addition to cell cycle arrest, DNA damage may also induce apoptosis (programmed cell death) in multicellular organisms, thus eliminating cells in which damage is beyond repair, protecting the host organism at the expense of the individual cell (Enoch and Norbury, 1995). It has been suggested that in some cell types such as lymphocytes and bone marrow cells, *p53* is important for triggering both apoptosis and G<sub>1</sub> arrest following irradiation but that in others, such as fibroblasts, it is important only in initiating G<sub>1</sub> block (Slichenmyer et al., 1993). In lymphocytes, loss of wild type *p53* may lead to a decreased capacity for apoptosis which is manifested as increased radioresistance. However, in fibroblasts in which the *p53* signal is not important for apoptosis, loss of wildtype *p53* function may not affect radiosensitivity. Mutations of the *p53* gene occur in many diverse human tumour types, including gliomas. Loss of heterozygosity (LOH), a hallmark of loss of tumour suppressor gene activity, and the presence of mutations in *p53* have been confirmed in astrocytomas and anaplastic astrocytomas at a similar rate to that for glioblastomas (Von Deimling, 1992a). Such alterations are rare in low-grade gliomas but appear to occur with the same frequency in anaplastic astrocytomas and glioblastomas, indicating that they may signal the transition from low-grade to malignant forms (Fults et al., 1992b). Some studies have indicated that *p53* may be involved in tumour progression

because it is more common in glioblastomas than in anaplastic astrocytomas (Chung et al., 1991). Investigation of *p53* mutations in four glioma patients before and after malignant transformation showed mutations only in tumour recurrence (Hayashi et al., 1991). All *p53* mutations found so far in gliomas occur in exons 4 to 8, which represent highly conserved regions of the gene. The overall *p53* mutation frequency has been reported to be 37% in gliomas that retain both 17p alleles but 64% in tumours that lose a single allele of chromosome 17p (Frankle et al., 1992).

It appears that in low grade astrocytomas (grade II), mutations of the *p53* tumour suppressor gene with or without LOH on chromosome 17p, constitute the earliest detectable genetic alteration in diffusely infiltrating astrocytomas (Ohgaki et al., 1993), although isolated cases with LOH on chromosomes 13 and 22 have also been reported (James et al., 1988). Anaplastic astrocytomas (grade III) often develop over the course of several years from low grade astrocytomas, but may also arise *de novo*, that is without clinical or histopathological evidence of a preceding low grade glioma. In addition, more than 40% of anaplastic astrocytomas show LOH on chromosome 19p (Von Deimling et al., 1992b) and more than 70% of glioblastomas have LOH on chromosome 10 (Ransom et al., 1992).

Oligodendrogliomas and oligoastrocytomas are less common, and are not as well characterized as astrocytomas. Oncogene amplification has only rarely been noted in oligodendroglial tumours (Reifenberger et al., 1994). Most reports have emphasized that allelic losses in oligodendrogliomas and oligoastrocytomas occur preferentially on chromosomes 1p and 19p, affecting 40 to 80% of these tumour types (Bello et al., 1994). Due to the frequent loss of these loci in low-grade, as well as anaplastic, oligodendrogliomas and oligoastrocytomas, the putative 1p and 19p tumour suppressor genes are probably important early in oligodendroglial tumorigenesis. In contrast to

diffusely infiltrating astrocytomas, non-astrocytic brain tumours and pilocytic astrocytomas do not or very rarely contain *p53* mutations, thus suggesting a different genetic basis for these CNS neoplasms (Ohgaki et al., 1991).

#### 1.4.2 Gene amplification and oncogene expression

Several families of oncogenes may be involved in malignant glioma development. Many of these encode receptors for factors believed to be involved in glioma tumorigenesis (Maruno et al., 1991; Westphal and Herrmann 1989) such as epidermal growth factor (EGF), platelet derived growth factor (PDGF), insulin growth factor (IGF-1) and fibroblast growth factor (FGF) which have structural homologies (Cooper et al., 1991). Abnormalities of the epidermal growth factor receptor (EGFR) gene, including overexpression, amplification, and rearrangement, have been shown to occur frequently in glioblastoma (Ekstrand et al., 1992). The EGFR gene is located on chromosome 7 and encodes a transmembrane receptor protein with tyrosine kinase activity that becomes active upon receptor stimulation (Cooper et al., 1991). This would be expected to increase protein phosphorylation and, in turn, cell division. The loss of chromosome 10 has also been directly correlated with amplification of the EGFR gene (Von Deimling et al., 1992c).

In addition to EGFR gene amplification, gene rearrangement and altered expression are now being investigated in glioblastoma (Wong et al., 1992). Rearrangements and deletions on the EGFR gene in malignant glioma result in defects in the normal extracytoplasmic domain of the receptor and thus abnormal binding of its ligands (Humphrey et al., 1990). The amplified gene shows frequent deletions, including abnormal regions at both the 3' and 5' ends (Ekstrand et al., 1992). These alterations

may produce tumour-specific proteins that have biological or functional significance. EGFR amplification has been found in 33% of all grades of astrocytomas. Patients with gene amplification had worse prognosis than did those without amplification, indicating that amplification may be a significant prognostic factor (Hurt et al., 1992). In a study of 103 cases using immunohistochemical staining for EGFR, the authors found heterogeneous labelling of tumour cell cytoplasm in 37% of glioblastomas but in no other grade of astrocytomas (Agosti et al., 1992). The specific association of EGFR overexpression with glioblastoma may be useful in histochemically differentiating these tumours from anaplastic astrocytomas when the biopsy tissue is limited and nonrepresentative (Agosti et al., 1992).

From the above studies it can be concluded that in gliomas, which are the most common cerebral neoplasms, loss of *p53* gene function appears to be an early event associated with malignant transformation and progression. Loss of genetic information from chromosome 9p is common in anaplastic astrocytomas. Furthermore, *p53* mutations, loss of heterozygosity on chromosome 10 and amplification of EGFR gene are events associated with progression of anaplastic astrocytoma to the most malignant form of glioma-glioblastoma. Less well-defined abnormalities are associated with other primary brain tumours such as oligodendrogliomas, ependymomas, medulloblastomas and meningiomas.

## **1.5 Treatment**

Malignant gliomas constitute the bulk of the intrinsic intraparenchymal tumours of both the brain and spinal cord which occur either as single or multifocal lesions. They rarely metastasize outside the CNS. These tumours, which arise from distinct types of glial cells, are the most difficult to treat. Regardless of the location of the malignant glioma, the prognosis has not changed greatly in the last 15 years (Bleehan and Stenning, 1991). It is not firmly established at present if treatment of the low-grade astrocytomas improves survival. Despite optimal treatment with surgery, radiotherapy and chemotherapy, median survival is approximately 6-8 years for low-grade gliomas, 3 years for anaplastic astrocytomas and one year for glioblastoma (Leibel et al., 1994; MacDonald, 1994). Survival is also influenced by histologic type and tumour grade, proliferative index, post surgical tumour volume, age and performance status of the patient, and type of chemotherapy used. Fundamental problems include the limitations of current diagnostic techniques such as CT and MRI to localize the extent of tumours and the difficulty of their total removal and effective radio sterilization. These problems stimulate urgent research for alternative diagnostic procedures and treatment modalities. Selective radiopharmaceutical uptake and killing of glioma cells may improve therapy and will be the subject of this thesis.

### 1.5.1 Surgery in the treatment of malignant glioma

The first surgical removal of glioma was done by Rickman Godlee over 100 years ago (Bennet and Godlee, 1884). The value and role of surgery in patients with glioma remain contentious (Kreth et al., 1993). Surgical management is directed towards two goals. Firstly, to confirm the histological diagnosis and secondly to achieve tumour debulking. Internal decompression or near complete surgical extirpation of the tumour

produce more prolonged relief from the effects of tumour bulk and allow further treatment to be more effective. Because of the location within the brain and their diffuse mode of local spread, complete surgical excision can not be achieved.

The diagnosis is confirmed by biopsy, guided either by intuition if the tumour is large enough (although this approach is accompanied by significant mortality), or by a stereotactic technique. A surgical reduction of at least 90% of tumour volume, (more than 1 log of cell kill) is required for a measurable increase in survival. Patients with malignant glioma rarely survive more than three months after treatment by burr hole biopsy or external decompression. Table 1.4 gives a summary of the published results of such surgery covering the period 1937 to 1974.

## **Chapter 2**

### **The radiobiology of glioma cells in culture**

<b>The radiobiology of glioma cells in culture.</b> . . . . .	30
<b>2.1 <i>In vitro</i> cell biology of human glioma.</b> . . . . .	32
2.1.1 Karyotypic abnormalities . . . . .	33
2.1.2 Cytological morphology . . . . .	33
<b>2.2 Characteristics of established brain tumour cell lines</b> . . . . .	34
<b>2.3 Growth kinetics of human brain tumours <i>in vitro</i> and <i>in vivo</i></b> . . . . .	36
<b>2.4 Multicellular tumour spheroid model</b> . . . . .	39
<b>2.5 Radiobiological studies on human tumours</b> . . . . .	41
2.5.1 Single hit killing . . . . .	42
2.5.2 Multitarget model . . . . .	43
2.5.3 Linear-quadratic model . . . . .	44
<b>2.6 Radiosensitivity of brain tumours</b> . . . . .	48
2.6.1 Radiobiological factors . . . . .	52
2.6.2 Cellular recovery phenomena . . . . .	55
2.6.3 Potentially lethal damage repair (PLD) . . . . .	55
2.6.4 Sub lethal damage (SLD) . . . . .	56
<b>2.7 Why are we exploring targeted radiotherapy ?</b> . . . . .	56

## 2.1 *In vitro* cell biology of human glioma

*In vitro* models have played an important role in studies of brain tumour biology and experimental therapy (Ponten and Macintyre., 1968; Rosenblum et al., 1975; Freshney, 1980; Laerum et al., 1985). Many brain tumours are capable of limited growth *in vitro* (Russell and Bland, 1933) and several specific phenotypic properties of cultures from human gliomas may be associated with the malignant origin of the cells. It was first established by Westermark (1973) and others (Maunoury, 1977; Ponten and Westermark, 1978) that glioma cultures grown as continuous cell lines would reach a higher saturation density in culture than finite cell lines derived from normal brain. About 80% of glioma biopsies can be grown in short-term culture and about 40% give rise to established cell lines (Westermark et al., 1973). In contrast, although 50% of biopsy samples from medullablastoma will grow in short-term culture, few (less than 1%) will establish in long-term culture (Freshney, 1980; Hill, 1985; Bloom et al., 1986).

The Courtenay soft agar system has been used to grow colonies from brain tumours (Deacon et al., 1985). Soft agar is used to suppress the growth of connective tissue cells and also prevents migration of cells between adjacent colonies. Using a low concentration of oxygen in the gas phase allows approximate, physiological, oxygen tension in the medium and the addition of rat red blood cells (RBC) to the culture medium supplies labile growth factors (Courtenay, 1976; Courtenay and Mills, 1978).

Brain tumours have also been cultured as multicellular spheroids in suspension culture. In these cultures, brain tumour cells are able to reaggregate and form complex histiotypic patterns which show characteristics of their tissue of origin (Schwachofer et al., 1989).

### 2.1.1 Karyotypic abnormalities

Karyotypic heterogeneity of glioma cell lines is common, with the number of chromosomes per cell ranging from 37 to over 208. Karyotype analysis often shows aneuploidy with different modal numbers in various glioma cell lines and instability in the stem-line (Westermarck et al., 1973; Kawamoto et al., 1979; Shapiro et al., 1981). There are some non-random chromosome alterations in cultured malignant glioma; in particular losses of chromosomes 10 and 22 and gain of chromosome 7 (Bigner et al., 1986; Rey et al., 1987). James et al. (1988) compared the loss of heterozygosity between grade IV and grade III gliomas for loci on each chromosome. They found loss of heterozygosity affecting chromosome 10 sequences in samples from grade IV tumours, but not in samples from tumours of lesser malignancy.

### 2.1.2 Cytological morphology

The morphological heterogeneity of malignant glioma *in situ* is well known. This is reflected in a considerable degree of morphological heterogeneity in cultures from these tumours. Bigner et al. (1981) have suggested that well established cell lines can be classified on the basis of their morphological appearance in confluent cultures identifying a range of forms that he called fibroblastic, fascicular, epithelial and glial.

## **2.2 Characteristics of established brain tumours cell lines**

A high proportion of cultured human gliomas have been established as permanent lines (Manuelidis, 1969; Westermark et al., 1973). Five cell lines established from a series of 50 human primary intracranial tumours were reported by Maunoury (1977). These included 4 malignant gliomas and one meningeal sarcoma. These five cell lines were injected subcutaneously into both flanks of athymic nude mice but only two gave rise to tumours. Only one of the five cell lines was occasionally positive for glial fibrillary acidic protein (GFAP). GFAP is a cytoskeletal protein which is considered to be a marker of the astrocytic lineage (Bignami et al., 1972). However, a high proportion of cell lines derived from human malignant glioma do not express GFAP (Kennedy et al., 1987). Collins (1983) has summarised the characteristics of 42 human glioma cell lines. The tumour types included glioblastoma, malignant glioma, astrocytoma grade III and IV, giant cell glioblastoma, gliosarcoma and mixed anaplastic glioma. S-100 protein and GFAP expression was reported in 34 of the tumours, but only 8 cell lines were positive. S-100 protein is an acidic, calcium binding protein that is concentrated in the central nervous system and produced mainly by astrocytes (Donato, 1991). It was considered to be unique to the nervous system but it has now been found in a number of other cell types including cultured human melanoma cells (Gaynor et al., 1980) and skin cells (Cocchia et al., 1981).

Rutka et al. (1987) established and characterized five cell lines from human malignant gliomas. These cell lines grew both in monolayer and soft agar. The doubling time varied from 29-34 hours in monolayer culture. In the early-passage, cultures, only one cell line expressed GFAP, but lost this during serial passage apparently a common finding (Diserens et al., 1981; Westphal et al., 1990).

While there is limited experimental data suggesting that high levels of expression of GFAP might reduce the motility of malignant astrocytes, there is no consistent evidence that loss of this cytoskeletal protein defines a more malignant phenotype (Duffy et al., 1982). Studies of GFAP positivity are summarized in Table 2.2.

Authors	Number of cell lines	GFAP positive cell lines
Maunoury, 1977	5	1
Collins, 1983	34	8
Rutka et al., 1987	5	1

**Table 2.2** The GFAP status in established human malignant glioma cell lines.

### 2.3 Growth kinetics of human brain tumours *in vitro* and *in vivo*

The principal attributes of malignant solid tumour cell populations *in vivo* are:

- a) loss of normal growth control.
- b) ability to invade and metastasise.
- c) ability to induce angiogenesis.

Brain tumours have certain characteristics in common with other neoplasms. *In vitro*, some cells from malignant gliomas appear to be capable of unlimited proliferation, in contrast to normal adult glial cells for which the maximum number of passage is 15 (Pertuiset et al., 1985). When the concentration of serum supplement in the culture medium is reduced below 5%, proliferation of normal astrocytes rapidly stops whilst established glioma cell lines continue to proliferate in less than 1% serum. If serum is removed entirely, normal glial cell proliferation is arrested in the  $G_0/G_1$  phase of the cell cycle. It has been demonstrated that glioma cells remain in  $G_0$  in the absence of serum derived growth factors but are readily recruited into cycle after even short (one hour) exposure to serum, whereas up to 12 hours incubation is required to stimulate the growth of normal glia (Collins, 1983). This would seem to indicate that normal glial cells need a large number of growth factors in serum for continued proliferation, whilst glioma cells do not. There is now considerable evidence for the involvement of platelet-derived growth factor (PDGF) and other growth factors in the growth regulation of glial and glioma cells. PDGF stimulates proliferation of human glial cells (Heldin et al., 1980) and it has been reported that glioma cells express an oncogene which codes for PDGF (Grinspan et al., 1994).

The proliferative activity of neoplastic cells is an exciting field for histopathological investigation due to the suggested correlation between cell proliferation rate and biological

aggressiveness. Several techniques are available for evaluating cell kinetics including, immunostaining of cell cycle-related antigens such as Ki67 and proliferating cell nuclear antigen (PCNA), bromodeoxyuridine incorporation and determination of percentage of cells in S phase by flow cytometry (Hall and Levison, 1990).

The nuclear antigen Ki67 is perhaps the most widely used proliferation marker and is expressed in cell cycle phases G<sub>1</sub>, S, G<sub>2</sub> and mitosis but not in G<sub>0</sub> cells. It has recently been characterized as a highly protease-sensitive, nonhistone protein with an apparent molecular weight of 395 kD (Gerdes et al., 1984; 1991). Values of Ki67 labelling indices parallel the degree of histologic malignancy in many tumours including GB, anaplastic astrocytoma, pituitary adenoma and meningioma (Louis et al., 1991 ; Shibuya et al., 1992). Burger et al. (1986) have found that intensity of nuclear staining of gliomas for Ki67 corresponds with more malignant histologic appearance and faster growth characteristics.

Another immunohistochemical marker, PCNA, may have use as an index of proliferation rate and tumour aggressiveness (Prelich et al., 1987). PCNA expression is increased through G<sub>1</sub>, is at a maximum in early S phase, declines through G<sub>2</sub> phase, and reaches low levels at M phase and interphase. The monoclonal antibody PC10 binds to the PCNA epitope in both frozen and formalin-fixed paraffin-embedded tissue, thus allowing retrospective studies (Gelb et al., 1992). PCNA indices may be modified by the action of growth factors (PDGF, FGF, and EGF) or other exogenous agents (Bravo and McDonald, 1984; Jaskulski et al., 1988). Comparisons of PCNA with Ki67 labelling indices in primary brain tumours indicated that PCNA may be a more specific S-phase marker but a less accurate index of proliferation activity than Ki67 (Allegranza et al., 1991). However, Figge et al. (1992) reported that PCNA was not a useful prognostic parameter in determining survival in glioblastomas.

Monoclonal antibodies against bromodeoxyuridine (BUdR), a thymidine analogue incorporated during DNA synthesis, can be used to determine the S-phase fraction in cell populations. Bromodeoxyuridine labelling indices can be obtained by flow cytometry.

Glioma cell proliferation *in vitro* and *in vivo* has been studied mainly by labelling with BUdR and Ki67. Nishizaki et al. (1989) assessed cell proliferation potential by measuring the labelling indices of Ki67 and BUdR in 48 brain tumours. They showed both Ki67 and BUdR labelling indices correlated with the degree of malignancy estimated from conventional histological preparations. The mean BUdR labelling index in glioblastoma was 9.9% and the Ki67 labelling index was 13.5%. For anaplastic astrocytoma and astrocytoma the BUdR labelling indices were 4.3% and 1.6% and the Ki67 labelling indices were 5.2% and 2.2% respectively. Hoshino et al. (1992) studied cellular growth kinetics by *in situ* double labelling with BUdR and iododeoxyuridine (IUdR) in 57 patients with brain tumours including 29 gliomas, 23 meningiomas and 5 miscellaneous. The patients received infusions of intravenous IUdR and BUdR 1-5 hours apart shortly before tumour removal. Excised tumour specimens were stained sequentially for BUdR and IUdR. The percentage of BUdR-labelled cells was determined to establish the labelling index, or S-phase fraction, and the ratio of cells labelled only with IUdR to cells labelled with BUdR or with BUdR and IUdR was determined to calculate the duration of S-phase ( $T_s$ ) and the potential doubling time ( $T_{pot}$ ) of each tumour. The  $T_{pot}$  is defined as the time within which a cell population would double its number if cell loss did not occur. The BUdR labelling index varied from 1% to 20%, reflecting the malignancy of each tumour.  $T_s$  was  $8.7 \pm 2$  hours and  $T_{pot}$  varied from 2 days to more than one month. *In vitro* doubling times of glioma cells vary from 22 to 144 hours (Pertuiset et al., 1985). Perez et al. (1995) summarized available information on the IUdR labelling indices in xenograft models of seven well established cell lines originating from human malignant

gliomas. The mean  $T_{pot}$ ,  $T_s$  and labelling index were 4.9 days, 19.4 hours and 17.7% respectively. Several studies on the proliferation rate of brain tumours using Ki67 and other proliferative markers have been reported (Morimura et al., 1991; Schroder et al., 1991; Onda et al., 1994). The percentage of Ki67 positive cells (growth fraction) tended to reflect the histological grade of malignancy.

## 2.4 The multicellular tumour spheroid model

The major objective of the present investigation is an evaluation of the effect of proliferative heterogeneity of tumour cells on the therapeutic potential of the cycle-specific agent radiolabelled IUdR. Therefore an important part of this work was the evaluation of the appropriateness of different *in vitro* glioma models. Cultures in the form of three-dimensional multicellular spheroids are especially useful for the study of radiation responses.

Experimentally induced aggregates of animal cells have been in use since the pioneering studies of Holtfreter (1944). Studies were performed by Moscona (1961) to assess the capacity of embryonic and malignant cells for reaggregation, proliferation and differentiation. Due to their spherical shape, the aggregates were termed multicellular spheroids. The structure of spheroids is similar to that of solid tumour nodules, composed of dividing cells close to the capillaries, adjacent non-proliferating cells and more distant necrotic regions (Carlsson and Nederman, 1989). The cell survival curves obtained from radiation experiments either with aggregates or with solid tumours were similar (Sutherland et al., 1970; 1971). As spheroids enlarge, the external, well-nourished cells continue to divide but the internal cells, lacking nutrients, often exit the cell cycle and enter  $G_0$  or non proliferating state (Durand, 1990). Enlargement of spheroids can also be accompanied by

changes in ploidy (Olive et al., 1982), changes in extracellular matrix constituents (Grover et al., 1983), development of central necrosis (Inch, 1970), and development of hypoxia (Durand, 1984).

Multicellular tumour spheroids are a well-established model of prevascular microtumours that provide a means of studying the intratumoural distribution of therapeutic agents and of determining the effect of alternative schedules of administration on cellular incorporation. They have previously been used extensively in targeted therapy research to investigate diffusion gradients of alternative targeting agents (Langmuir et al., 1991; Mairs et al., 1991); to assess efficacies of alternative modalities (Rotmensch et al., 1994) and modulating agents (Langmuir and Medonca, 1992); to evaluate microdosimetry (Bardies et al., 1992), and to provide experimental model systems for testing hypotheses (Gaze et al., 1992). There are reported studies using glioma spheroids. For example the radiosensitivity of a human glioma cell line (Gronvik et al., 1996), the relation between radioresponsiveness and tumour differentiation (Stuschke et al., 1993), the effect of leukotriene and 5-lipoxygenase inhibitors on thymidine uptake (Gati et al., 1994) and the penetration of thymidine and thymidine-5-triphosphate in cellular spheroids (Nederman et al., 1988).

Tumour spheroids represent a useful *in vitro* model for the study of heterogeneity with respect to the effects of cytotoxic drugs. This is probably representative of the heterogeneity in real tumours which often have irregular vascularization. There are also cell type-dependent differences in the response to the cytotoxic agents which parallel the differences seen between different types of tumours. For these reasons we employed spheroids derived from glioma cell lines to evaluate incorporation and efficacy of the proliferation specific targeting agent IUdR.

## 2.5 Radiobiological studies on human tumours

Radiobiology is the study of the action of ionizing radiation on living things. There have been important developments in the radiobiology of human tumours in recent years. Exposure of cells to ionizing radiation results in molecular damage that can be expressed at the cellular, metabolic, or chromosomal level. The most extensively studied radiation effect is that of cell survival, assayed by determining the proportion of cells that can make colonies. The eradication of clonogenic cells is the major objective of therapeutic irradiation, therefore the use of such an *in vitro* endpoint is particularly relevant to the measurement of tumour response to radiation. The practical limitations of this experimental endpoint have become apparent due to increasing interest in measuring the radiosensitivity of human cells. Many normal human tissues have limited or no proliferative potential, and the low cloning efficiencies observed in primary tumour cultures are major barriers to the routine measurement of cellular radiosensitivity (Peters, 1990). Despite the practical difficulties inherent in the clonogenic cell assay, it has generated most of the currently available data on mammalian cellular radiosensitivity. It has the advantage of allowing the measurement of cellular radiation dose-response over a logarithmic range. This is possible because relatively high concentrations of viable cells ( $10^5$ - $10^6$ /ml) can be readily prepared from continuous cell lines.

A cell survival curve describes the relationship between the radiation dose on a linear scale and the proportion of clonogenic cells that survive on a log scale. Surviving fraction is calculated from the relationship:

$$\text{Surviving fraction} = \frac{\text{colonies counted}}{\text{cells seeded} \times (\text{PE}/100)}$$

where plating efficiency (PE) of the experiment is the percentage of cells forming colonies in control plates. The mathematical models of radiation most commonly used to quantify cellular radiosensitivity are described below.

### 2.5.1 Single hit killing

Many different mathematical models have been proposed to define the shapes of survival curves. All of these are based on the concept of the random nature of energy deposition by radiation.

The earlier models, which are discussed in detail by Elkind and Whitmore (1967), were based on the idea that a specific target had to be inactivated for cells to be killed. According to this model the number of targets ( $dN$ ) inactivated by a small dose of radiation ( $dD$ ) should be proportional to the initial number of targets  $N$  and to  $dD$ , therefore

$$dN \propto N dD \text{ or } dN = - (1/D_0) N dD,$$

where  $1/D_0$  is a constant of proportionality and the negative sign is introduced because the number of active targets  $N$  decreases with increasing dose. This equation can be integrated to give

$$N = N_0 e^{(-D/D_0)},$$

where  $N_0$  is the number of active targets present at zero dose. If it is assumed that cells contain only a single target that must be inactivated then the surviving fraction is given by  $N/N_0 = e^{(-D/D_0)}$ . This also represents the probability that any individual cell will

survive the radiation dose  $D$ . This equation gives a straight line on a semilogarithmic plot representing a surviving fraction of 1 at zero dose.

If  $D$  equals  $D_0$  in the above equation, then  $N = N_0 e^{-1} = 0.37 N_0$ . Therefore  $D_0$  represents the dose required to reduce cell survival from  $N$  to  $0.37 N$  which is a measure of the slope of the line. However, most survival curves in practice show a 'shoulder' or have continuously bending shapes which requires the use of more sophisticated mathematical models, as described below.

### 2.5.2 Multitarget Model

This is an alternative mathematical model which generates survival curves of characteristic shapes for mammalian cells *in vitro*. At low doses there is an initial shoulder, followed by a portion which becomes almost straight on a semilogarithmic plot (Figure 2.1).

The model postulates that the cell contains " $n$ " sensitive targets each of which must be hit for sterilisation. Therefore the probability of inactivating one target is given by:

$$P_1 = (1 - e^{-D/D_0}),$$

where  $D$  = dose. The probability of a cell surviving a given dose (all " $n$ " targets hit) would be:

$$S(D) = 1 - (1 - e^{-D/D_0})^n$$

At high doses the survival curve predicted from this model approximates to a pure exponential, appearing as a straight line on a log-linear plot, with a slope of  $-1/D_0$ .

The multitarget parameters are  $D_0$ ,  $n$  and  $D_q$ .  $D_0$  is the dose of radiation that is required, on the exponential part of the curve, to reduce cell survival to 37%. The extrapolation number ( $n$ ) is the intercept when the survival curve is extrapolated back to where it cuts the Y axis at zero radiation dose, and the  $D_q$  is the X-axis intercept. Both  $D_q$  and  $n$

provide estimates of the shoulder size. These three parameters are related by the expression:

$$\text{Log}_e n = Dq/D_0$$

However, the multitarget equation has the property of zero initial slope at zero dose.

Much mammalian cell survival data do not appear to support a zero initial slope at zero dose, leading to the modification of the basic multitarget equation to include a single event component at low doses:

$$S(D) = e^{-D/D_s} [1 - (1 - e^{-D/D_0})]^n,$$

where  $d$  is given dose,  $D_0$  is the reciprocal final slope,  $D_s$  is the reciprocal initial slope, and  $n$  the extrapolation number. However, this more sophisticated model requires estimation of an additional parameter ( $D_s$ ).

### 2.5.3 Linear-quadratic model

Another approach to fitting survival curve data that is in common use is the linear-quadratic equation (Kellerer and Rossi, 1972). It was developed on the basis of a proposed relationship between dose-related induction of double strand breaks within DNA and was popularised by the work of Keller and Rossi (1973).

The model is described by the equation:

$$S(D) = e^{-(\alpha D + \beta D^2)},$$

where  $S(D)$  is the survival fraction after a dose  $D$ , and the exponential component ( $\alpha$ ) and the bending component ( $\beta$ ) are constants. The components of cell killing that are proportional to dose and to the square of the dose are equal when

$$\alpha D = \beta D^2 \text{ or } D = \alpha/\beta$$

The  $\alpha/\beta$  ratio represents the radiation dose at which the cell kill achieved by  $\alpha$  and  $\beta$  events is equal. As a ratio its numerical value is independent of those obtained for both

$\alpha$  and  $\beta$ . Human cells of high radiosensitivity are usually observed to have  $\alpha/\beta$  ratios of greater than 8Gy, whilst only the most resistant cells have values of less than 5Gy (Williams et al., 1985). It is believed that recovery from radiation damage affects only the  $\beta$ -component (Peacock, 1988). For instance, when the dose rate is lowered the survival curve becomes shallower and straightens, until it appears to coincide with the linear component of the acute curve (Steel et al., 1986) (Figure 2.2). Therefore it may be appropriate, to regard the linear portion as a component of non-recoverable damage (Steel and Peacock, 1989).

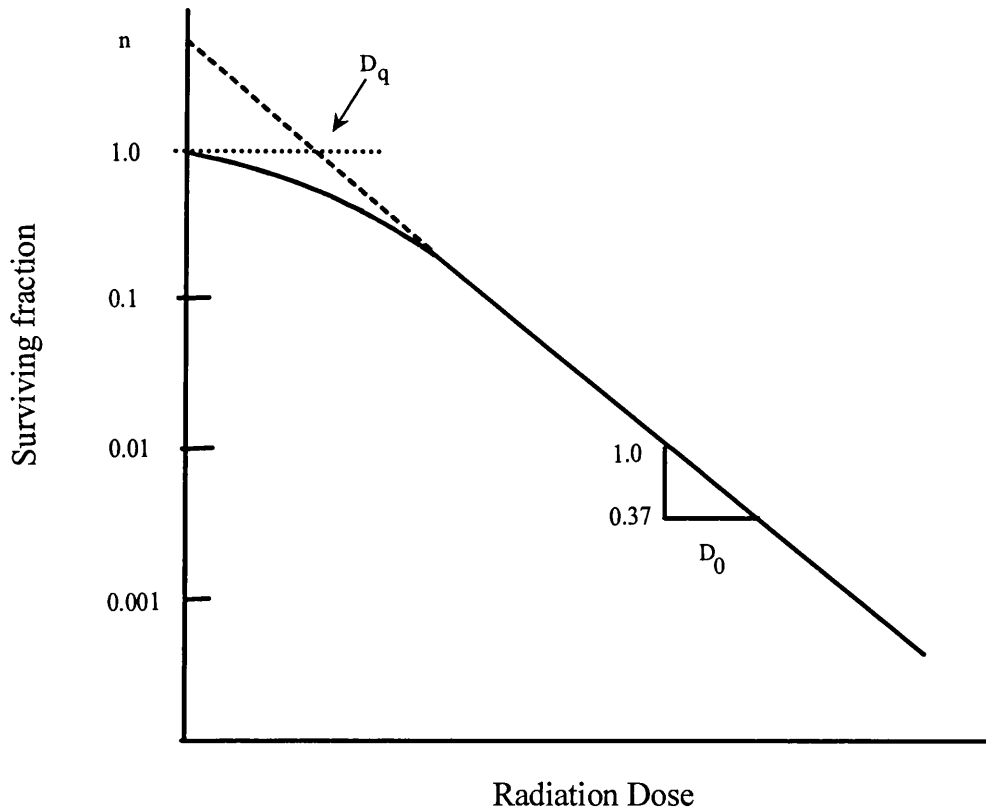


**Figure 2.1** Typical survival curves for mammalian cells exposed to radiation. The fraction of surviving cells is plotted on a logarithmic scale against dose on a linear scale. The curve is characterised by two parameters; the 37% dose slope,  $D_0$ , of the straight portion and the extrapolation number,  $n$ , which is measured of the width of the initial shoulder. Alternatively, the width of the shoulder may be specified in terms of the quasithreshold dose.  $D_q$ , which is the dose at which the extrapolated straight portion of the dose-response curve cuts the dose axis.

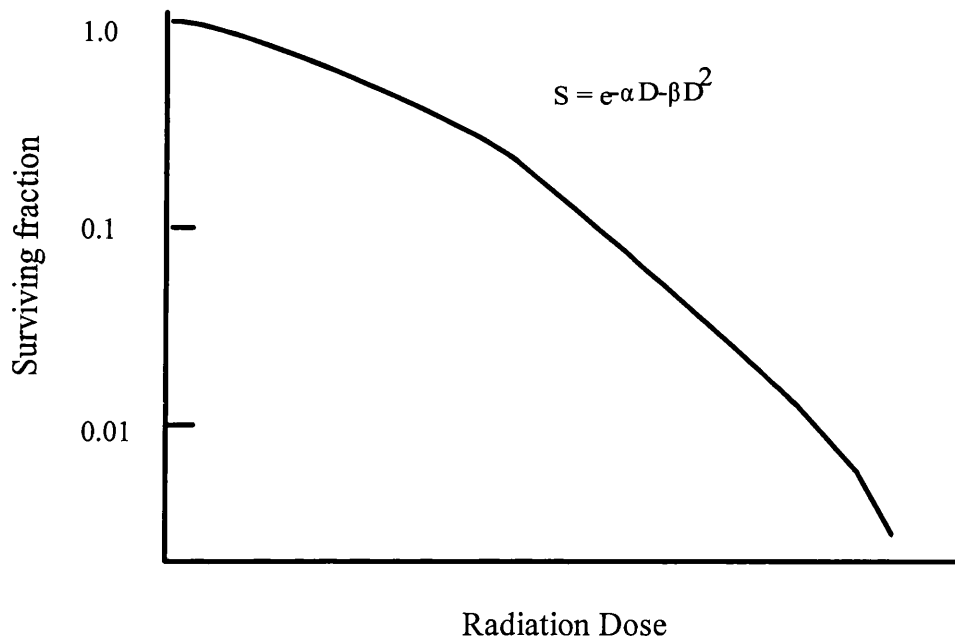


**Figure 2.2** Form of the linear-quadratic survival equation. The experimental data are fitted to a linear-quadratic function (shown on the curve). There are two components of cell killing: one is proportional to dose ( $\alpha D$ ), while the other is proportional to the square of the dose ( $\beta D^2$ ).

## 2.6 Radiosensitivity of brain tumours

Glioma is one of the most radioresistant human tumours. Resistance may be caused by one or more factors. These include inherent cellular radiation sensitivity, efficient repair of radiation damage, high hypoxic fraction and rapid proliferation between fractions of radiation (Taghian et al., 1993). Human glioma cell lines have been available for *in vitro* studies since the late 1960s and the dependence of radiosensitivity on dose rate has been widely studied. This has practical significance for clinical radiotherapy. Several reviews documented the radioresistance of human glioma cell lines (Raaphorst et al., 1989; Taghian et al., 1992; Gupa et al., 1996).

In 1981 Fertil and Malaise published the results of their re-analysis of published human cell survival curves. Their review led to the use of the surviving fraction at 2Gy ( $SF_2$ ) as the best way of describing radiosensitivity among human cell lines. Deacon et al. (1984), described five categories of clinical radioresponsiveness, ranging from the most responsive (Group A) to the least responsive (Group E). Gliomas were placed in group E, whose average  $SF_2$  was 0.52. A good correlation was seen between cellular radiosensitivity ( $SF_2$  value) and category (A-E) of clinical radioresponsiveness. The *in vitro* radiation sensitivity of different human glioma cell lines has been measured using colony formation as the end-point of cell viability. The survival curve parameters ( $SF_2$ ,  $\alpha$ ,  $\beta$ ,  $D_0$ ,  $n$ ) have been determined for single dose irradiation of exponential phase cells by different research groups and are summarised in table 2.3.

**Table 2.3** *In vitro* cell survival curve parameters of malignant glioma cell lines.

<u>Cell line</u>	<u>D<sub>0</sub></u>	<u>n</u>	<u>α(Gy<sup>-1</sup>)</u>	<u>β (Gy<sup>-2</sup>)</u>	<u>SF<sub>2</sub></u>	<u>Ref</u>
KNS-42	1.9	11.6	0.3	0.063		Masuda, 1983
U-118	1.3	8.5				Millar and Jinks1985
U-87	1.02	38	0.02	0.06	0.8	Raaphorst,1989
U-138	1.14	14	0.056	0.057	0.7	"
MMC2	1.29	4.5	0.34	0.029	0.45	Taghian, 1992
A7	1.56	5.9	0.22	0.022	0.53	"
D54MG	1.05	10.5	0.266	0.0449	0.54	"
T98G	1.61	8.3	0.092	0.0292	0.88	"
WF	1.92	2.3	0.32	0.012	0.47	"
IJK	2.17	6.7	0.076	0.024	0.82	Ross, 1992
CCM	1.67	8.78	0.22	0.048	0.58	"
U-251	1.69	3.11	0.21	0.051	0.56	"
SB-18	2.38	8.13	0.10	0.026	0.77	"

The survival curve parameters (SF<sub>2</sub>, α, β, D<sub>0</sub>, n) obtained by different research groups.

These parameters are defined in section 2.5.3.

Rutka et al. (1996) compared the intrinsic radiation sensitivity parameters of seven human soft tissue sarcoma and eight human breast carcinoma with nine human malignant glioma cell lines *in vitro* by clonogenic assays under aerobic conditions on cells in exponential phase of growth. The results for soft tissue sarcoma and breast carcinoma cell lines showed the mean surviving fraction at 2Gy about 0.39 and 0.37 respectively while it was 0.50 for malignant glioma cell lines. They concluded that cells of sarcomas and breast carcinoma did not show unusual radiation resistance compared with malignant glioma and the success rate for radiation applied against sarcomas and breast carcinoma of comparable size could be similar.

The radiosensitivity of the human glioma cell line U-343MGa, growing as spheroids and as conventional monolayers, was the subject of a study by Gronvik et al (1996). The spheroids were first irradiated with  $^{60}\text{Co}$  photons, and the radiosensitivity was then analyzed in different cell layers of varying proliferative activity. High radioresistance was found in all cell layers and the inner, mainly quiescent cells, were as resistant as the outer proliferating cells. The studied glioma cells were equally radioresistant under all tested proliferative conditions when conventional low LET radiation was applied.

The induction and repair of DNA double-strand breaks in glioma cells were studied by Allalunis-Turner et al. (1995). They used the cells of two isogenic human malignant glioma cell lines which vary in their  $\text{SF}_2$  values by a factor of approximately 30. M059J cells were radiosensitive ( $\text{SF}_2 = 0.02$ ) and M059K cells were radioresistant ( $\text{SF}_2 = 0.64$ ). Their experiments indicated that equivalent numbers of DNA lesions were produced by ionizing radiation in M059K and M059J cells but more double-strand breaks were repaired by 30 min in M059K cells than in M059J cells. They concluded that deficient DNA repair processes may be a major determinant of radiosensitivity in M059J cells.

The split dose recovery of cells of seven early-passage glioblastoma multiforme (GB) cell lines and six cell lines derived from tumours of a type frequently treated successfully (two squamous cell carcinomas of head and neck, three breast cancers and one low-grade astrocytoma cell line) was studied by Taghian et al. (1993). They measured *in vitro* split-dose recovery using colony formation. Results were presented in terms of recovery ratio: the ratio of the mean inactivation dose of split-dose radiation to that of single-dose radiation. Their data showed a significantly higher recovery ratio for GB than for the other cell types.

The cellular response to ionising radiation is beginning to be understood at the molecular level. Gupa et al. (1996) studied the effect of *p53* gene on G<sub>1</sub>-phase cell cycle checkpoint after radiation to test whether repair occurs in the additional time provided by *p53* activation. Two different glioma cell lines were used: U87-175.4, which carried a dominant-negative *p53* construct and lacked an X-ray-induced G<sub>1</sub>-phase cell cycle arrest and U87-lux.8, which carried only wild-type *p53* and demonstrated an X-ray-induced G<sub>1</sub>-phase cell cycle arrest. U87-lux.8 cells remained in G<sub>1</sub>-phase for 48 hours post irradiation while U87-175.4 accumulated to a much lesser extent in G<sub>1</sub>-phase after irradiation. Cells lacking the G<sub>1</sub>-phase checkpoint showed increased survival at all radiation doses. There was no significant difference in repair ability nor in rate of chromosomal aberration between the two cell lines. They concluded that G<sub>1</sub>-phase arrest by *p53* may reduce the overall degree of survival by stimulating other G<sub>1</sub>-phase events.

The association between *p53* gene mutation and radiosensitivity is controversial. Several investigators have shown that *p53* mutation does not correlate with radiosensitivity and that the expression of mutated *p53* gene increases radiosensitivity (Brachman et al., 1993; Biard

et al., 1994). Others have argued that expression of wild-type *p53* gene increases the susceptibility to radiation and induces apoptosis, *p53* mutant lines therefore being more resistant (Lee and Bernstein, 1993; McIlwrath et al., 1994). However, the radiobiology of human gliomas demonstrates that there are multiple biological factors involved in clinical radioresponsiveness.

### 2.6.1 Radiobiological factors

Radiation treatment of cancer is usually given as a series of daily fractions of 2Gy. The use of fractionated treatment arose from studies of the French radiobiologist Regaud in the early part of the century. He demonstrated that, with fractionated treatment to a ram's testes, it was possible to achieve sterilization without significant damage to the scrotal skin. This strategy was soon applied to the treatment of cancer. Each daily dose (fraction) kills the same proportion of cells, reducing cell survival to about 50%. A series of fractionated doses amplifies the therapeutic differential between normal tissue and tumour by several mechanisms, easily remembered as the 5Rs: repair of cellular injury, repopulation by surviving viable cells, redistribution within the division cycle, reoxygenation of the tumour, and radiosensitivity.

a) *Repair*: DNA repair is completed over a few hours but the extent of repair is not equal in all tissues. In general, slowly responding normal tissues such as connective tissue and spinal cord are capable of greater repair than malignant tissues (Withers, 1992). Thus, by spacing dose fractions by at least 6 hours the recovery in slowly responding normal tissue is greater than that in tumours.

b) *Repopulation*: As cellular damage and cell death occur during the course of the fractionated treatment, the tissue may respond with an increased rate of cell proliferation (Tannock, 1996). The effect of cell proliferation during treatment, known as repopulation or regeneration, will be to reduce the overall response. This is most important in early-responding normal tissues such as skin or gastro-intestinal tract or tumours whose stem cells are capable of rapid proliferation and will be of little consequence in late-responding slowly proliferating tissues like kidney or liver which do not suffer much early cell death and hence do not produce an early proliferative response to the radiation treatment. During fractionated treatment, therefore, repopulation will decrease the damage to early-responding normal tissue to a greater extent than late-responding normal tissue. The mechanisms underlying the accelerated regrowth of tumour cells are unknown, just as they are for normal tissue. It seems reasonable to assume that growth factors are involved, and that their effects may be supplemented by improved vascularization of residual tumour as it shrinks. Repopulation is likely to be more important toward the end of a course of treatment, when sufficient damage has accumulated to induce a regenerative response.

c) *Redistribution*: During a course of fractionated treatment, proliferating cells may move from one phase of cell cycle to another between the radiation doses. This leads to two effects that can make the cell population more sensitive to a subsequent dose of radiation. First radiation typically induces a G<sub>2</sub> block in cell cycle progression which is usually a sensitive phase. Secondly, some of the surviving cells will redistribute into more sensitive parts of the cell cycle. These effects make the whole population more sensitive to fractionated treatment compared to a single dose.

d) *Reoxygenation*: When solid tumours grow, they often outstrip their blood supply and acquire areas of hypoxia and necrosis. Hypoxic cells are two-to-three times as

radioresistant as normal cells (Withers, 1992). During the interval between dose fractions, killed normal cells are eliminated and the previously hypoxic cells gain better access to oxygen (Kallman, 1988). This process of reoxygenation limits the negative effect of hypoxic cells on radiocurability during fractionated radiotherapy.

e) *Radiosensitivity*: The study of the radiobiology of human tumours has led to the realization that cells from different types of tumour differ markedly in their inherent radiosensitivity; that is the steepness of the oxic, cell survival curve. This was shown for the initial part of the survival curve by Fertil and Malaise (1981). Work on a representative group of human tumour cell lines has confirmed that the differences in the oxic cell survival curves among human tumours are considerable, and large enough to explain the clinically observed differences in curability (Steel et al., 1987). The term radiosensitivity can have a number of meanings. The most direct is the steepness of the acute radiation survival curve. The most clinically relevant parameter is the survival curve at low dose rate, whose steepness may approximate to the initial slope of the acute cell survival curve. It is not known with certainty what factors are responsible for radiation sensitivity or resistance. However, DNA is considered to be the major target for reproductive cell death (Hagen, 1990), and differences in damage induction (Peacock et al., 1989) and /or repair (Ward, 1990) of DNA damage are involved.

### 2.6.2 Cellular recovery phenomena

The damage to mammalian cells produced by irradiation has been divided theoretically into three categories:

- 1) Lethal damage; irreversible and irreparable lesions leading to cell death.
- 2) Sublethal damage (SLD); non-lethal cellular injury that can be repaired, or accumulate

with further dose to become lethal.

3) Potentially lethal damage (PLD); This damage is potentially lethal (if cells divide soon afterwards), but may be repaired if division is delayed. The kinetics of entry of cells into the cycle is therefore important and is a function of the post irradiation environment.

All three are simply operational terms, because in mammalian cells the mechanisms of repair and radioresistance are not fully understood. The comparative ability of human tumours to recover has been obtained using observation of post irradiation events at the DNA or chromosomal level (Steel, 1991).

#### 2.6.3 Potentially lethal damage repair (PLD)

Repair is found in almost all tumour cell lines in which it has been sought. Potentially lethal damage repair (PLD), has been shown to vary considerably from one cell line to another (Weichselbaum and Little, 1982) and to correlate with clinical radiocurability. The less curable tumours show the greatest degree of PLD recovery. There is general agreement that PLD is repaired and the fraction of cells surviving a given dose is enhanced if post irradiation conditions are suboptimal for growth, so that cells do not have to attempt the complex process of mitosis while their chromosomes are damaged. If mitosis is delayed by suboptimal growth conditions, DNA damage can be repaired.

#### 2.6.4 Sublethal damage (SLD)

This damage can be repaired under normal circumstances in hours unless additional sublethal damage, incurred by a second dose of radiation, is suffered. Additional radiation can interact with SLD to form lethal damage. Sublethal damage repair, therefore, is

evident by the increase in survival observed when a dose of radiation is divided into two fractions separated by a time interval. It was observed that the surviving fraction of irradiated cells increased with prolongation of the split dose interval from 0 to 3 hours, then reaching a plateau (Elkind and Whitmore, 1967). However, SLD repair occurs slowly in tissues. SLD repair is most often seen in the cells whose survival curves show large shoulders (large  $n$  value on the multitarget model) which occurs for many glioma cell lines *in vitro* (Taghian et al., 1993).

## **2.7 Why are we exploring targeted radiotherapy ?**

Due to fundamental problems such as limitation of current diagnostic techniques, localisation of malignant glioma and difficulty of total removal or effective sterilization of the tumour, prognosis has not changed greatly in the last 15 years. The low median survival motivates the search for alternative diagnostic procedures and treatment modalities that will allow selective killing of glioma cells. Such is the promise of targeted radiotherapy using radiolabelled IUdR.

## **Chapter 3**

### **Targeted radiotherapy**

<b>3.1 Targeted radiotherapy</b>	59
3.1.1 Targeting agents	60
3.1.2 Radionuclides	62
<b>3.2 Radiobiological factors in targeted radiotherapy</b>	64
<b>3.3 Specific targeting vehicles</b>	67
3.3.1 Antibody targeting	67
3.3.1.1 Radioimmunoconjugates	68
3.3.1.2 Use of MAbs in solid tumours	68
3.3.2 Metaiodobenzylguanidine (MIBG)	70
3.3.3 Novel targeting vehicle	71
3.3.4 Iododeoxyuridine (IUdR)	72
<b>3.4 Applications of the spheroid model in targeted radiotherapy research</b>	77
<b>3.5 Project aims</b>	79

### 3.1 Targeted radiotherapy

One of the most generally useful modalities in oncology is ionising radiation. Though variation of intrinsic cellular radiosensitivity between tumours may be of major importance in clinical outcome, the range of variability observed is much less than for sensitivities to cytotoxic drugs. However, conventional radiotherapy unavoidably involves irradiation of normal organs and tissues. It is the vulnerability of critical normal tissues, rather than the existence of highly radioresistant tumour cells, which ultimately limits the effectiveness of radiation treatment. Targeted radiotherapy utilises a radionuclide-conjugated molecular vehicle which localises on the surface of malignant cells or is selectively accumulated within them. This enables preferential irradiation of tumour cells, relative to critical normal tissues. In recent years, monoclonal antibodies attracted most attention as potentially selective delivery vehicles, but advances in tumour and molecular biology are now providing a much wider choice of molecular species. Targeted radiotherapy has features in common with conventional radiation treatment (e.g cell kill will be governed by the 5Rs of radiobiology), but also important differences. These differences are related to specificity, uptake and penetration of the targeting agent, intracellular distribution of cellular receptors and the finite range of nuclear particles emitted during radionuclide disintegration. A wide range of radionuclides with differing physical properties is available for conjugation to diverse targeting agents (Table 3.1). The experimental investigation of targeted radiotherapy requires a three dimensional tumour model for which monolayer cultures are inappropriate but spheroids are more realistic.

### 3.1.1 Targeting agents

For many tumours, monoclonal antibodies or antibody fragments represent the only means of targeting radionuclides to malignant cells (Vaeth and Meyer, 1990). Although monoclonal antibodies now have demonstrable usefulness in pathological diagnosis, they are still very limited in therapy. The evidence of therapeutic efficacy of antibody targeting for glioma will be discussed in following sections. However, a range of small molecular weight compounds with specific tumour affinities is becoming available. These targeting agents exploit differences in metabolism or receptor expression between tumour and normal cells (Table 3.1). In principle, many radionuclides are available for targeted radiotherapy but only  $^{131}\text{I}$  and  $^{90}\text{Y}$  have been significantly used in clinical practice. An important consideration is the range of the emitted particle. Even if the distribution of the targeting agent is uniform, small microtumours and spheroids will be underdosed if their size is less than the particle range, allowing much of the radiation energy to escape from the tumour surface (Humm, 1986). Heterogeneous uptake of targeting agents can also lead to underdosing of untargeted cells if there is insufficient cross-fire irradiation from targeted cells. This problem will be minimal when the bound radionuclide is a long range  $\beta$ -emitter like  $^{131}\text{I}$  or  $^{90}\text{Y}$  but the cross-fire dosage to surrounding normal tissue may then be substantial.

Conversely, strategies based upon the incorporation of ultra short range Auger electron emitters should reduce damage to adjacent organs but may fail to sterilise all clonogens if cellular uptake is not completely uniform.

<u>Tumour</u>	<u>Target</u>	<u>Targeting agent</u>	<u>Radionuclide</u>
Lymphoma	Antigen	Antibody	<sup>131</sup> I (beta)
Neuroblastoma	Noradrenaline receptor	MIBG	<sup>131</sup> I (beta)
		MABG	<sup>211</sup> At (alpha)
Melanoma	Metabolic pathway	Melanin precursor	<sup>131</sup> I, <sup>211</sup> At (beta, alpha)
Glioma, squamous carcinoma	EGF receptor	EGF	<sup>131</sup> I, <sup>123</sup> I (beta, Auger)
Proliferating cells (eg glioma)	Replicating DNA	IUdR	<sup>125</sup> I, <sup>123</sup> I (Auger)
Breast cancer	nuclear receptor	oestradiol	<sup>125</sup> I, <sup>123</sup> I (Auger)
Various	gene mutation	oligonucleotide	<sup>125</sup> I, <sup>123</sup> I (Auger)

**Table 3.1** Currently promising approaches to targeted radiotherapy (Mairs and Wheldon, 1995). The type of emission are shown in the brackets.

### 3.1.2 Radionuclides

Criteria for radionuclide selection for targeted radiotherapy have been discussed by several authors (Hofer, 1980; Wessels and Rogus, 1984; Humm, 1986; Wheldon, 1994). Table 3.2 summarizes the physical properties of some radionuclides that may have applications in targeted radiotherapy. In choosing a radionuclide for targeted radiotherapy consideration must be given to its feasibility of conjugation to the targeting vehicle, physical half life, particle range and its radiobiological effectiveness. In practice, clinical experience with targeted radiotherapy is largely reliant on  $\beta$ -emitters, particularly  $^{131}\text{I}$  and to a lesser extent,  $^{90}\text{Y}$ . An important concept is that of cross-fire, i.e. the irradiation of untargeted cells by radionuclides bound to neighbouring targeted cells. The particle range of long range  $\beta$ -emitters means that considerable cross-fire will occur with possible sterilization of untargeted cells, both neoplastic and normal.

$\alpha$ -emitters have high radiobiological effectiveness and short range emissions with a typical range of several cell diameters but are difficult to obtain and have inconveniently short half lives. Encouraging laboratory experience with targeted  $\alpha$ -emitters has nevertheless been reported (Vaidyanathan et al., 1996; Strickland et al., 1994).

Auger emitters are radionuclides with even shorter-range emissions (1 to 3nm) and are of high LET quality. The potential use of Auger emitting radionuclides for cancer therapy has been under investigation for many years (Hofer and Hugues, 1971; Adelstein, 1993) but practical difficulties have delayed their clinical introduction. Auger cascades are generated by some radionuclides such as  $^{123}\text{I}$  /  $^{125}\text{I}$  or  $^{99\text{m}}\text{Tc}$  after decay by electron capture and internal conversion. Extremely low energy electrons (less than 1keV) deposit their energy in the vicinity of the nuclear disintegration producing  $10^5$  to  $10^9$  cGy absorbed dose per decay in 20-60 nm spheres (Kassis et al., 1987a; Makrigiorgos et al., 1989).

<u>Radionuclide</u>	<u>Half life</u>	<u>Emitted particles</u>	<u>Mean range of particles</u>
<sup>90</sup> Y	2.7 days	β	5 mm
<sup>131</sup> I	8 days	β	0.8 mm
<sup>67</sup> Cu	2.5 days	β	0.6 mm
<sup>199</sup> Au	3.1 days	β	0.3 mm
<sup>211</sup> At	7 hours	α	0.05 mm
<sup>212</sup> Bi	1 hour	α	0.05 mm
<sup>125</sup> I	60 days	Auger Electron	1-3 nm
<sup>123</sup> I	13.2 hours	Auger Electron	1-3 nm

**Table 3.2** Physical properties of radionuclides of current interest for targeted therapy (Wheldon, 1994).

The long half life of  $^{125}\text{I}$  (60 days) poses problems when considered in the context of radionuclide therapy.  $^{123}\text{I}$  which has a half life of 13.2 hours also emits Auger electrons. Approximately 11 of these electrons are emitted for each nuclear disintegration compared with 20 for  $^{125}\text{I}$  (Sastry and Rao, 1984). Experiments have shown that the decay of  $^{125}\text{I}$  in the DNA of mammalian cells leads to efficient production of DNA double-strand breaks (DSB) [one decay gives rise to about one DSB] (Painter et al., 1974), while  $^{123}\text{I}$ , on average, produces 0.74 DSB per decay (Makrigiorgos et al., 1992). The radiotoxicity of Auger-emitting radionuclides may depend on the precise molecular localization of the radionuclide in relation to the DNA double helix (Kassis et al., 1987a,b). For all short-range-emitters, heterogeneity of radionuclide deposition within the tumour is a potentially serious problem.

### **3.2. Radiobiological factors in targeted radiotherapy**

In this section we address radiobiological problems likely to arise in targeted radiotherapy. Emphasis is placed on radiobiological considerations which are different from those occurring in more conventional forms of radiotherapy.

The biological effectiveness of targeted radiotherapy will depend on radiobiological factors as well as on the physics of dose absorption. The 5Rs of radiobiology will be involved to a greater or lesser extent.

*Intrinsic radiosensitivity* is an important factor. Due to the limited uptake of targeting agents at present, only tumour types with high intrinsic sensitivity will be sterilized by targeted radiotherapy alone. High LET agents ( $\alpha$  and Auger emitters) have the potential to overcome the problem of intrinsic radioresistance.

*Repair* is believed to be important because of the usually low and exponentially depreciating dose rate at which most of the treatment is given. In tumours for which the  $\alpha/\beta$  ratio exceeds 10 Gy, such as neuroblastoma, the sparing due to low-dose rate will probably not be great. Fowler (1990), calculated that an extra 10 to 20% dose would have to be given by targeted radiotherapy compared with fractionated external-beam radiotherapy. For glioma, however, with lower  $\alpha/\beta$  ratio, considerable dose-rate sparing could occur. It is calculated that for biological isoeffect in late-responding tissues, the component of targeted radiotherapy may be reduced several-fold relative to single-dose irradiation at high dose rate (Wheldon and O'Donoghue, 1990). However, this mostly applies to low LET radiation. For Auger electrons, of high LET quality, dose rate effects will be less important. Other radiobiological factors are probably of lesser importance.

*Redistribution*: radiation typically induces a  $G_2$  block in cell cycle progression. Decreasing dose-rate could lead to a release of this block with progression of cells into more sensitive phases of the cycle. This 'inverse dose-rate effect', if it exists, may to some extent compensate for the decreasing radiobiological effectiveness of the diminishing dose-rate.

*Reoxygenation*: it is difficult to predict whether hypoxia and reoxygenation will be important in targeted radiotherapy or not. Most of the radiation dose delivered by targeted radiotherapy will usually be given within a week, due to biological clearance of the agent and radioactive decay. This short time may not be sufficient for complete reoxygenation. However, the low dose-rate could result in a low oxygen enhancement ratio (OER), thereby reducing the importance of hypoxia (Langmuir and Medonca, 1992).

*Repopulation*: In the first week of treatment by targeted radiotherapy more than 90% of total dose will have been received by the tumour. Therefore, repopulation is unlikely to

be an important factor in tumour or normal tissue. When the dose-rate drops below 2-3 Gy/h (Fowler, 1990), a certain amount of 'dose-wastage' will occur. Therapy using radionuclides with short half lives is therefore preferable to those with long half lives (O'Donoghue and Wheldon, 1996). Repopulation may play a more important role if targeted radiotherapy comes to be used in fractionated mode.

An additional important consideration is heterogeneity of distribution of targeting agents in tumours. Most analyses have assumed for simplicity, that the targeted agents were distributed uniformly throughout the tumour. In fact, for larger tumours, this is most unlikely to happen. Reasons for heterogeneity of radionuclide deposition include limited penetration of the agent into solid tumours as well as heterogeneous expression of the molecular targets themselves throughout the cells. Heterogeneity of radionuclide deposition has been shown by several experimental and clinical studies (Moyes et al., 1989; Olea et al., 1992). Whether non-uniform deposition of targeted agents translates into heterogeneity of absorbed dose depends on the spatial distribution of the radionuclide in relation to the particle range. Small changes in deposition over dimensions less than the particle range will tend to be smoothed out by crossfire from radionuclides targeted to nearby cells. However, changes which are greater than the mean path length of the emitted particles will increase survival of tumour cells in the regions receiving less dose deposition. Heterogeneity will be most serious for short-range Auger and  $\alpha$ -emitters and least serious for long  $\beta$ -emitters.

### **3.3 Specific targeting vehicles**

#### **3.3.1 Antibody targeting**

Monoclonal antibodies (MAbs) have been used since Kohler and Milstein's (1975) seminal observation that monoclonal antibodies with precise target specificity could be produced by fusing B lymphocytes from an immunized host to an immortalized myeloma-cell line. MAbs can achieve antitumour effect by several mechanisms including complement or antibody-dependent cytotoxicity, binding to growth factors or growth factor receptors, signalling of apoptosis through cell-surface molecules, and as immunoconjugates passively delivering radioisotopes, toxins or chemotherapeutic agents to the tumour site (Goldenberg, 1993). Problems which are recognised include the failure to find epitopes (specific molecular groups on the cell surface) unique to tumour cells, heterogeneity of expression of epitopes, limited penetration of antibodies into solid tumours and, more generally, low levels of absolute antibody uptake. Approaches have been developed to improve the localization of radiolabelled MAbs in experimental tumours. These approaches involve three general strategies: a) modifying antibodies or radiolabelling techniques; b) increasing the clearance of radiolabelled MAbs; and c) modifying tumour delivery, tumour antigen expression or increasing tumour vascular permeability or blood flow (Buchsbaum, 1995).

To enhance the cytotoxicity of monoclonal antibodies against human tumours, a variety of cytotoxic agents have been conjugated to the antibody. The antibody serves as a targeting mechanism and agents such as radioisotopes, plant or bacterial toxins and drugs have been identified as potential therapeutic modalities in these immunoconjugates.

### 3.3.1.1 Radioimmunoconjugates

Radioisotope selection is critical. Isotopes with  $\alpha$ -decay have very short ranges of penetrance and require antibodies that bind to surface antigens in order to bring the isotope into close approximation with the cell nucleus.  $\beta$ -decay is associated with long path lengths and relatively confined radiation exposure to the sites of isotope deposition.  $\gamma$ -decay produces high-energy photons which attenuate exponentially. Approximately 50% of the  $\gamma$ -decay photons are absorbed by normal human tissues distant from the binding sites and 50% of these photons escape to the environment surrounding the patient. The toxicities of the various immunoconjugates must be compared with the benefits of the possible elimination of antigen-negative neoplastic cells in tumours.

### 3.3.1.2 Use of MAbs in solid tumours

MAB therapy for solid tumours has progressed rather slowly owing to a number of factors:

- a) Many of these tumours are radioresistant.
- b) Patients with solid tumours frequently generate human antimouse antibodies (HAMA) after a single exposure, which could abrogate the effect of repeated MAbs infusions (Jeffers et al., 1986).
- c) Tumour penetrance by the immunoconjugate is less compared with lymphoma and leukaemia owing to differences in the vascular availability in solid tumours.

Radioimmunotherapy has been evaluated in malignant gliomas. Some human gliomas amplify and rearrange the EGFR gene, resulting in generation of truncated EGFR proteins. Antibodies generated against these truncated proteins could be ideal candidates for antibody guided imaging and therapy of gliomas (Humphrey et al., 1990). Systemic and intracarotid administration were evaluated in ten patients with grade III or IV glioma

(Kalofonos et al., 1989) using an antibody to EGFR labelled with 40-140 mCi of  $^{131}\text{I}$ . Six patients showed clinical improvement, with one patient remaining in remission for 3 years. Since gliomas remain confined to the brain, intratumoural administration has been considered as an alternative approach. Autoradiographic studies have shown that the antibody is able to diffuse from the site of injection to more remote tumour islands (Rowlinson-Busza et al., 1991a). Papanastassiou et al. (1993) treated patients with malignant gliomas by placing a  $^{131}\text{I}$ -labelled MAb into the resection cavity. The systemic uptake was 0.13% to 14.8% of injected dose. The cause of these results may in fact lie not so much in the nature of the applied antibody but in the nature of the addressed target (Kuzel and Rosen, 1994). A critical issue for the MAbs therapy is the accessibility of tumour cells in solid tumours. An increasing amount of experimental data demonstrates that macromolecules including MAbs do not penetrate well into solid tumour tissues. Barriers to penetration are surrounding basement membranes and poor vascularization of tumours (Jain, 1991). Raben et al. (1996) have sought to address the poor intratumoural antigen expression by enhancement of radiolabel binding and tumour localization. They focused on gene transfer methods and showed that human glioma cells that do not express carcinoembryonic antigen (CEA) can be transduced *in vitro* with recombinant replication-defective adenovirus encoding human CEA, which renders them susceptible to binding by radiolabelled anti-CEA antibodies. An advantage of radiolabelled MAbs is that they can be active on the cells in proximity of the antigen-positive target cell irrespective of their antigen status. In preclinical comparative studies, the  $^{125}\text{I}$ -labelled EGFR MAbs have shown more significant anti-glioma effect than  $^{131}\text{I}$ -labelled EGFR MAbs (Bender et al., 1992). Brady et al. (1990) evaluated an  $^{125}\text{I}$ -labelled EGFR MAbs delivered intraarterially in 15 patients with recurrent, malignant astrocytomas. One patient showed a surgically documented complete response, and two patients achieved a partial response. Comparative study of the intra-carotid versus intravenous administration of radiolabelled

MAbs in glioma patients did not show a significant advantage for either delivery modality in terms of immunoglobulin uptake in the tumour (Zalutsky et al., 1990). More promising results were obtained by Riva et al. (1994) who used direct intratumoural injection of <sup>131</sup>I-anti-tenascin MAbs in a series of 24 patients suffering from recurrent malignant gliomas. Tenascin is an antigen specifically expressed in the glioma stroma but not in normal brain tissue. A clear therapeutic effect was obtained in 6/17 patients (35%) and the median survival (16 months) was longer than that generally expected with other treatment modalities. The radiation doses delivered to the tumours were higher than those obtained by traditional external radiation therapy. In conclusion, clinical trials to date using MAbs for treatment of malignant gliomas have had only limited success. However, controlled studies are needed to evaluate the true value of these therapeutic strategies alone or in combination with other conventional treatment modalities.

### 3.3.2 Meta-iodobenzylguanidine (MIBG)

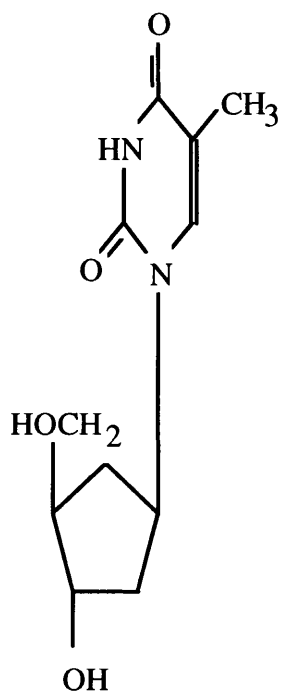
A promising targeting agent is the radiopharmaceutical meta-iodobenzylguanidine (MIBG) which is preferentially taken up by catecholamine-synthesising cells of the sympathetic nervous system. Malignant tumours of sympathetic nervous tissues, particularly neuroblastoma and pheochromocytoma, often retain the property of high MIBG uptake, allowing this agent to be used as a means of delivery of radio-iodine, for both diagnostic and therapeutic purposes (Voute et al., 1991; Lewis et al., 1991).

### 3.3.3 Novel targeting vehicles

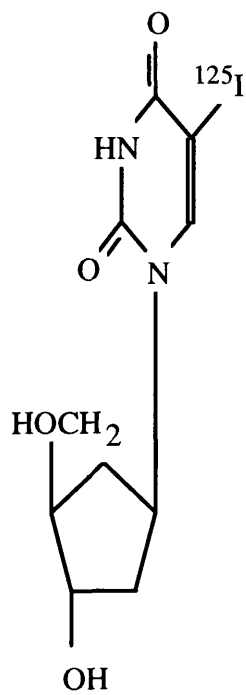
Many other potential targeting agents are now being studied. These include a variety of growth factors that might be used against tumours whose cells have been found to over-express the receptor for the appropriate growth factor (Capala and Carlsson, 1991; Mairs et al., 1991). It is now well-established that an important group of tumours, including gliomas and squamous carcinomas, characteristically over-express the cellular receptor for epidermal growth factor (EGF) (Bigner et al., 1988; Ozanne et al., 1986). Theoretically, administration of radiolabelled EGF should lead to at least partially selective radionuclide delivery to these tumours. Experimental studies have shown that it is possible to achieve preferential cell kill *in vitro* of cells over-expressing the EGF receptors by means of <sup>131</sup>I labelled EGF (Capala and Carlsson, 1991). Some of the potential problems are also addressed by this work which shows the rapid turnover of EGF internalized by cells, and possible ways to avoid this problem such as conjugation of EGF to more stable molecules to slow its intracellular breakdown (Andersson et al., 1992). However, the most important progress in the molecular biology of tumours has been the discovery of oncogenes, abnormal tumour suppressor genes and incidental genetic aberrations in particular tumour types. The challenge for targeted therapy is to make use of this knowledge to effect tumour cell kill or gene inactivation by means of highly selective DNA targeting of radionuclides with subnuclear ranges of emission for example Auger emitters.

### 3.3.4 Iododeoxyuridine (IUdR)

A novel treatment approach for glioma involves DNA targeted Auger electron emitters, bound to iododeoxyuridine. Iododeoxyuridine (IUdR), in which the 5-methyl group is replaced by an iodine is an analog of thymidine (TdR) (Figure 3.1). Since a methyl group and an iodine atom have similar van der Waals radii, the substitution produces a compound that behaves like the natural pyrimidine nucleoside (Eidinoff et al., 1959; Morris and Cramer, 1966). IUdR is a suitable competitor of TdR for incorporation into the DNA of replicating cells (Halperin et al., 1988). The nucleoside salvage enzyme, thymidine kinase (TK), phosphorylates both TdR and IUdR (Bresnick and Thompson, 1965), to TdR monophosphate (dTMP) and IUdR monophosphate (IdUMP) respectively. dTMP is then phosphorylated to thymidine diphosphate (dTDP), by means of the thymidylate kinase (TMPK) catalyzed reaction, and in turn to thymidine triphosphate (dTTP) which is incorporated into DNA. On the other hand, IdUMP may be phosphorylated by the same enzyme-catalyzed pathway or dehalogenated by thymidylate synthetase (TS) to dUMP and then converted to dTMP (by the *de novo* TS pathway) and subsequently phosphorylated to dTDP (Garret et al., 1979) (Figure 3.2).



Thymidine



<sup>125</sup>I-iododeoxyuridine

**Figure 3.1** The structures of thymidine and <sup>125</sup>I-iododeoxyuridine

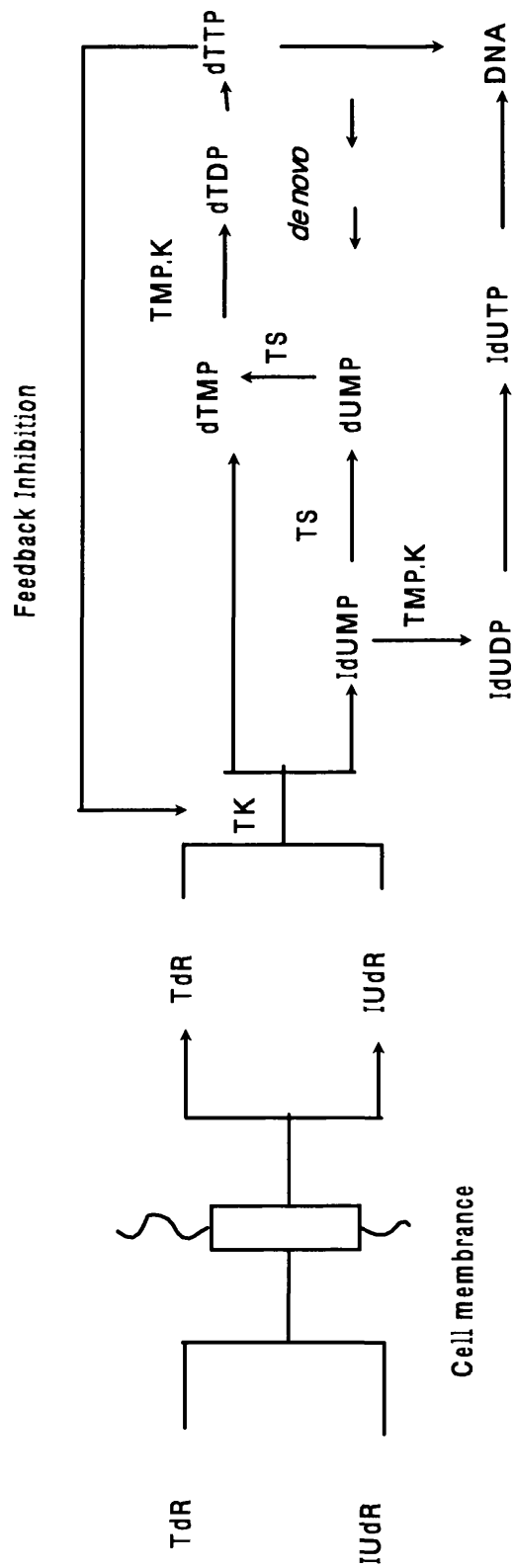


Figure 3.2 Salvage pathway for TdR and IUdR incorporation into DNA (Kassis et al., 1991)

Pioneering radiobiological experiments using the  $^{125}\text{I}$ -labelled thymidine precursor, [ $^{125}\text{I}$ ]IUdR, were performed in the 1970's by several investigators (Hofer and Hugues, 1971; Burki et al., 1973). Radiolabelled IUdR is an appropriate targeting vehicle for the delivery of radiation to proliferating tumour target tissue. *In vitro*, uptake of IUdR is progressive with time over several cell cycles and linear with extracellular concentration (Baranowska-Kortylewicz et al., 1988). It is well known that IUdR labelled with the Auger-emitting radionuclides  $^{123}\text{I}$ ,  $^{125}\text{I}$  and  $^{77}\text{Br}$  is highly toxic to mammalian cells (Kassis et al., 1989). Because IUdR is a cell cycle-dependent agent, only cells which are in, or enter, S phase during the period of exposure to the drug can be effectively targeted. The rate of incorporation into DNA of radiopharmaceutical depends on the rate of proliferation.

Four conditions must be met for IUdR, conjugated to short range emitters (alpha and Auger) to be used for therapy:

- (a) the agent must be capable of penetrating the tumour.
- (b) the IUdR must be taken up preferentially in the DNA of tumour cells.
- (c) the agent should not reach proliferating normal tissue (eg. gastrointestinal tract, bone marrow).
- (d) if the agent diffuses out of the target area, it must be converted quickly into an inactive/nontoxic form and be excreted rapidly from the body (Kassis et al., 1990). IUdR may be an agent that meets these requirements for targeting glioma.

The use of IUdR *in vivo* is associated with several problems. Firstly, deiodination: IUdR is extremely stable *in vitro* (Kassis and Adelstein, 1996) but quite unstable *in vivo*. The half life of IUdR in the circulation in humans is less than 5 min (Rey and Kinsella, 1991) and 7 min in mice (Prusoff, 1963). Since IUdR belongs to the class of drugs undergoing rapid first-pass hepatic degradation (Clifton et al., 1963), most of the tracer passing

through the liver is rapidly deiodinated and radioactivity is released into the circulation in the form of free iodide which is excreted in the urine. Secondly, IUdR uptake by actively proliferating normal cells may cause normal tissue toxicity. These problems might be overcome by loco-regional intracavity administration which enhances availability of the drug to tumour cells, while taking advantage of dilution and rapid metabolic breakdown to reduce uptake in distant normal cells. A third problem arises from S phase specific labelling. Malignant cells which are not synthesising DNA during the time of exposure to IUdR, labelled with  $^{125}\text{I}$  or  $^{123}\text{I}$ , will be spared. Enhanced tumour cell uptake may be achieved by continuous or intermittent infusion.

Clinical evaluation of radiolabelled IUdR for the treatment of malignancies other than brain tumour has demonstrated therapeutic benefit. Mariani et al. (1993) found that injection of [ $^{125}\text{I}$ ]IUdR into colorectal tumours resulted in high values of mean uptake in the tumour and high tumour to non-tumour ratios. Microautoradiography confirmed that the fraction of cells with intranuclear uptake was also high close to the injection site. With respect to macroscopic and microscopic scales, uptake was very heterogeneous. Therefore they concluded that loco-regional methods of delivery would be required for therapeutic effect. In a clinical study (Kassis et al., 1996), single intracerebral injections of [ $^{123}\text{I}$ ]IUdR were given to patients suspected of having primary gliomas in order to determine the biodistribution of radiopharmaceutical and to calculate dose estimates to the tumour and normal tissue. They demonstrated by scintigraphic imaging that the distribution of radiolabelled IUdR was mainly limited to the tumour, stomach and bladder. The optimal use of IUdR in treatment of glioma has yet to be defined.

### **3.4 Applications of the spheroid model in targeted radiotherapy research**

Spheroids were first used for targeted radiotherapy studies in the 1980s as *in vitro* micrometastases models (Sutherland et al., 1987; Walker et al., 1988; Kwock et al., 1989). Since then a large number of experimental studies have been reported, employing the three dimensional structure of spheroids to investigate diffusion gradients of alternative targeting agents, efficacies of alternative modalities and modulating agents, to evaluate microdosimetry and provide experimental model systems for testing hypotheses. Some examples of important applications are shown in Table 3.3.

Application	Example
Factors governing antibody binding	Carlsson et al.,1989; Langmuir et al.,1991.
Relative diffusion of antibodies and small molecules	Mairs et al.,1991; Petterson et al.,1992; Lindstorm and Carlsson, 1993.
Comparison of cell killing by X-rays, chemotherapy and targeted <sup>131</sup> I	Rotmensch et al.,1994.
Comparative radioimmunotherapy using alternative antibodies	Langmuir et al., 1992a.
Comparative radioimmunotherapy using alternative isotopes	Langmuir et al., 1992b.
Microdosimetry of radionuclide therapy	Bardies et al., 1992; Langmuir et al.,1992b.
Experimental test of microdosimetric hypotheses	Gaze et al., 1992.
Evaluation of radiosensitisers in radioimmunotherapy	Langmuir and Medonca, 1992.

**Table 3.3** Applications of spheroids in targeted radiotherapy research

## PROJECT AIMS

The goals of this study were as follows:

- (a) To establish an *in vitro* model for IUdR mediated therapy, based on human glioma cell lines grown as monolayers and as multicellular tumour spheroids.
  
- (b) To determine the uptake of IUdR in cultured cells and spheroids using flow cytometric DNA analysis.
  
- (c) To determine the effect of proliferative heterogeneity and incubation time on the uptake of IUdR in different sizes of spheroids using flow cytometry.
  
- (d) To examine the influence of proliferative heterogeneity and incubation time on cellular incorporation of [<sup>125</sup>I]IUdR, using localization of the cycle-specific nuclear antigen Ki67 and autoradiography.
  
- (e) To study the effect of external beam irradiation by clonogenic assay in both monolayer cells and spheroids and by growth delay in spheroids.
  
- (f) To compare the therapeutic potential of IUdR labelled with different radioisotopes (<sup>123</sup>I, <sup>125</sup>I and <sup>131</sup>I) using glioma cells cultured as monolayers in exponential or plateau phase of growth, and spheroids.

The results of these studies will form a basis for the evaluation of this therapeutic approach, which will be extended to animal models and ultimately human clinical studies.

## **Chapter 4**

### **General materials and methods**

<b>4.1 Cell culture conditions</b>	82
4.1.1 Cell storage and handling of stock	83
4.1.2 Mycoplasma testing	83
<b>4.2 Cell line characterisation</b>	83
4.2.1 Continuous lines	83
<b>4.3 Plateau phase culture</b>	84
<b>4.4 Spheroid culture</b>	84
<b>4.5 Analysis of DNA using IUdR</b>	84
<b>4.6 Clonogenic cell survival assay after external beam irradiation</b>	86
4.6.1 Determination of feeder cell requirements and linearity of plating efficiency	86
4.6.2 Cell monolayers	86
4.6.3 Spheroids	88
<b>4.7 Synthesis of precursor of radiolabelled IUdR</b>	88
4.7.1 Preparation of 5-(tributylstannyl)-2'-deoxyuridine	88
4.7.2 High performance Liquid Chromatography (HPLC)	89
4.7.3 HPLC analytical method	89
4.7.4 HPLC preparative method	90
4.7.5 Radiochemistry	90
4.7.6 Radioiodination method	91
4.7.7 HPLC analysis for deiodination of IUdR	91
<b>4.8 Clonogenic assay following targeted radiotherapy</b>	92
4.8.1 Monolayer	92
4.8.2 Spheroids	93
<b>4.9 Incorporation of IUdR into DNA</b>	93
<b>4.10 Solutions and reagents</b>	95

## 4.1 Cell culture conditions

All tissue culture was carried out in a class 2 microbiological safety hood, with vertical laminar air flow. Non-disposable equipment was sterilised by dry heat at 160°C for 1 hour. Heat stable solutions were sterilised by autoclaving at 120°C for 40 minutes.

Cells were maintained subconfluent in appropriate tissue culture medium by incubation at 37°C, in an atmosphere of 5% CO<sub>2</sub>, 20% O<sub>2</sub>.

Human glioma lines, continuous and primary, were maintained in Eagle's minimum essential medium (MEM) with 10% (v/v) fetal bovine serum, penicillin/streptomycin (100 I.U/ml), fungizone (2µg/ml) and glutamine (200 mM). All the reagents were purchased from GibcoBRL (Paisley, Scotland).

Routine cell counting was performed on a Coulter counter, with settings calibrated separately for each cell line.

#### 4.1.1 Cell storage and handling of stock

All continuous cell lines were stored in liquid nitrogen, suspended in complete medium, with 10% (v/v) dimethyl sulphoxide (DSMO). Cells were frozen at  $1 \times 10^6$  per ml. To avoid genetic drift, new cultures were initiated from frozen stocks every 6 weeks.

Stocks of each cell line were grown at the start of this project and frozen to provide material of similar passage level through the research.

#### 4.1.2 Mycoplasma testing

All lines were screened for mycoplasma contamination monthly, and prior to freezing. Cells were fixed at 50% confluence in Petri dishes, with 25% (v/v) acetic acid in methanol, and incubated with the fluorescent DNA stain Hoechst 33258 at 0.05mg per ml, for 15 minutes at room temperature. Cells were then screened by fluorescence microscopy for the extra-nuclear DNA pattern indicative of mycoplasma infection.

### **4.2 Cell line characterisation**

#### 4.2.1 Continuous lines

The following human glioma cell lines were established in this laboratory by previous workers: G-CCM, G-UVW, G-U251 and IP-SB18. The clinical origins of these were anaplastic astrocytoma, grade III and IV glioma.

At the time of undertaking the present studies all four lines had undergone more than 100 passages.

### **4.3 Plateau phase culture**

$10^5$ /ml cells were seeded into 24-well plates (Corning, UK), (1ml/well) each well containing a 13-mm-diameter coverslip. After incubation in a humidified CO<sub>2</sub> incubator for 1 to 3 days, the coverslips were transferred to 9-cm Petri dishes containing 20 ml medium and returned to the CO<sub>2</sub> incubator. Medium was changed every two days after the cells become confluent on the coverslips. After 12 days, cell growth ceased and two sequential counts showed no significant increase.

### **4.4 Spheroid culture**

One million cells were harvested from exponential monolayer cultures, seeded into biological Petri dishes (Bibby Sterilin Ltd., Ston, Staffs, U.K) containing 15 ml of medium and kept in a 5% CO<sub>2</sub> incubator for 48 hours. Cells were then transferred to spinner flasks (250ml) (Techne, Cambridge, UK) containing 100 ml medium in 5% CO<sub>2</sub> at 37°C and cultured until spheroids of the required size were obtained. Each of the cell lines when cultured as described above, grew as spheroids, but for the widest range of size of spheroids (100µm to 1000µm) UVW was used.

### **4.5 Analysis of DNA using IUdR**

Flow cytometry was performed on monolayer cells in exponential and plateau growth phases and also on single cells derived from multicellular spheroids. Spheroids were treated with 0.5 ml of phosphate buffered saline (PBS) containing 0.25% (v/v) trypsin and 1mM EDTA for 10 min at 37°C. After the addition of 0.5 ml of medium to neutralise the trypsin, the spheroids were mechanically disaggregated and finally passed through a

25 gauge hypodermic needle. Microscopic examination confirmed that the cell preparations were free from clumps. The proportion of labelled cells was determined according to the following method. The cells were harvested and centrifuged at 2000g for 5 min. After removal of the supernatant, the cells were dehydrated and fixed in 70% (v/v) ice cold ethanol. DNA was denatured by the addition of 1ml of 2M HCl followed by centrifugation at 2000g for 5 min. The preparation was then neutralized by the addition of 1ml of Borax buffer pH 8.5. After 2.5 min the cells were centrifuged and washed with 1ml of PBS and 1ml of PBT (PBS + 0.5% (w/v) bovine serum albumin + 0.05% (v/v) Tween 20) for 5 min. 100µl of a 1/30 dilution (see section 4.10) of anti-BudR antibody (Dako, Ltd, UK) in PBT was added to the cells, which were incubated for 1 hour at room temperature before washing three times in PBS. The supernatant was removed and 100µl of a 1/40 dilution (see section 4.10) of anti-mouse FITC-conjugated antibody (Dako, Ltd, UK) in PBT was added to the cells prior to incubation for 30 min at room temperature. After washing three times in PBS, 1ml of propidium iodide from a working solution (10ml PBS, 300µl Propidium iodide (PI), 1mg RNase, 25µl Triton X-100) was added to the cells which were left for 30min at room temperature. After centrifugation and removal of the supernatant, the cells were resuspended in 1ml of PBS. Flow cytometry analysis was performed using an Epics Coulter (Florida, USA), which has a 15 mW argon laser emitting at 488 nm.  $10^4$  cells were analyzed using a peak versus area fluorescence histogram to gate out debris and cell clumps. Cell cycle distribution was analyzed off line using Multicycle 2.5 software (Phoenix Flowsystems, San Diego, USA). This work was carried out in collaboration with Dr Peter Stanton (Department of Surgery, Glasgow Royal Infirmary).

## **4.6 Clonogenic cell survival assay after external beam irradiation**

### 4.6.1 Determination of feeder cell requirements and linearity of plating efficiency

Pilot experiments were performed on an experimental, continuous cell line (UVW) to establish the range of linearity of plating efficiency, ascertain feeder layer requirements, and determine the optimal incubation period to obtain colonies of greater than 50 cells.

### 4.6.2 Cell monolayers

The colony forming ability of tumour cells irradiated *in vitro* was examined according to the following protocol. Exponential cultures of adherent monolayer tumour cells were trypsinised, harvested in complete culture medium and mechanically disaggregated by pipetting followed by passage through a 25 gauge hypodermic needle. The quality of the single cell suspension was assessed by microscopy, and cell numbers counted using a haemocytometer. Cells were subcultured into 25cm<sup>2</sup> culture flasks at varying cell densities. A low density feeder layer comprising 10<sup>4</sup> heavily irradiated homologous cells (50Gy single dose irradiation) was added to each flask.

Flasks containing test and feeder layers were equilibrated with 5% CO<sub>2</sub> and returned to the hot room where they were maintained at 37°C for a period of 4 hours prior to the treatment, to minimise potential interactions of trypsin and radiation lesions.

Megavoltage irradiation was carried out using a Mobaltron cobalt-60 (Thompson, Versailles, France) therapy source, at room temperature. Doses of 1-10Gy were used, at a dose rate of 1.3-1.15Gy per minute, using full dose build up, and back scatter.

The cultures were returned to a 37°C hot room within minutes of irradiation, then left undisturbed for a period of 9 to 11 days. The cultures were then washed and stained with 10% (v/v) Carbol Fuchsin (Ziehl-Neelsen, London) and air dried before counting. The ability of single cells to form colonies greater than fifty cells was considered to indicate clonogenic survival. An automatic colony counter (Artec system Corporation Farmingdale, USA) was used. This was calibrated against a representative plate counted by eye.

The plating efficiency (PE) was calculated as:

$$\text{PE} = \frac{\text{Number of colonies obtained}}{\text{Number of cells plated}}$$

The surviving fraction (SF) at each dose was then calculated as:

$$\text{SF} = \frac{\text{Plating efficiency of treated cells}}{\text{Plating efficiency of control cells}}$$

The surviving fraction of cells at each dose point was plotted on a logarithmic scale, against dose in Gray (Gy) on a linear scale.

### 4.6.3 Spheroids

Spheroids of 100-180  $\mu\text{m}$  diameter were placed in Petri dishes coated with 1% (w/v) agar. This treatment prevented the attachment of spheroids to the bottom of the Petri dishes. The spheroids were then irradiated using a Cobalt-60 therapy source. Doses of 2-10 Gy were delivered using customised wooden and plastic blocks to provide build-up and back scatter radiation. They were then treated with 0.5ml of PBS containing 0.25% (v/v) trypsin and 1mM EDTA for 10 minutes at 37°C. After the addition of 0.5 ml of medium to neutralise the trypsin, the spheroids were mechanically disaggregated. Microscopic examination confirmed that the cell preparations were free of clumps. The same protocol for seeding, staining and calculation of surviving fraction were used as described above.

## **4.7 Synthesis of precursor of radiolabelled IUdR**

The preparation of radioiodinated (no-carrier-added) IUdR required the production of a trialkyltin derivative, 5-(tributylstannyl)-2'-deoxyuridine, as substrate for the radiosynthesis. This precursor can be readily synthesised from IUdR by a palladium catalysed substitution of the iodine for a tributyltin moiety (Baranowska-Kortylewicz et al., 1994).

### 4.7.1 Preparation of 5-(tributylstannyl)-2'-deoxyuridine

Tetrakis (triphenylphosphine) palladium (5 mg, 0.004 mmol) was added to 5-iodo-2'-deoxyuridine (0.1 g, 0.28 mmol) dissolved in 4.5 ml anhydrous dioxane. Hexabutyltin (0.35 g, 0.61 mmol) was introduced and the reaction mixture heated to 60°C under a nitrogen atmosphere for 18 hours. The solution was evaporated to dryness on a rotary evaporator and the dark coloured residue purified by column chromatography on silica gel

eluting with a 92:8 (v/v) mixture of  $\text{CHCl}_3$  /  $\text{CH}_3\text{OH}$ . Fractions containing the product were evaporated to dryness. 5-(tributylstannyl)-2'-deoxyuridine was obtained in a 48% yield (0.069 g) as a clear pale yellow oil.  $^1\text{H}$  nmr ( $\text{CDCl}_3$ ) 8.88 (s, 1H, NH); 7.23 (d, 1H, CH6); 6.10 (t, 1H, CH1O); 4.58 (m, 1H, CH3O); 4.02 (m, 1H, CH4O); 3.82 (s 2H, CH5O); 3.21 (s, 1H, OH3O); 2.99 (s, 1H, OH5O); 2.39 (m, 2H, CH2O); 1.64 - 0.83 (m, 27H, 3nBu).

#### 4.7.2 High performance Liquid Chromatography (HPLC)

All HPLC studies employed the following solvent system: solvent A: methanol, solvent B: water. All solvents were passed through  $0.45\mu\text{m}$  Milipore filters before use and maintained under a helium atmosphere during use. Confirmation of the identity of the radiopeak from IUdR was obtained by coelution of an authentic sample of IUdR whose retention time on the HPLC column was determined by UV spectroscopy (280nm). Prior to further use, radioiodinated IUdR was purified to remove unreacted 5-(tributylstannyl)-2'-deoxyuridine. The effect of 5-(tributylstannyl)-2'-deoxyuridine on the uptake of IUdR into cells is unknown.

#### 4.7.3 HPLC analytical method

Analytical HPLC was carried out using an LKB 2000 series controller with 2 pumps, and high pressure mixer detection was achieved with an LKB UV spectrophotometer at 280 nm. Radioflow detection was carried out using a Packard Radiomatic 500TR flow monitor. A  $5\mu\text{m}$  Kromasil RPC18 column (4.6 X 150 mm) with 10 mm guard cartridge was used with isocratic elution of 15% solvent A and 85% solvent B at a flow rate of 1ml/min. Data was analyzed using Packard FLO-ONE software.

#### 4.7.4 HPLC Preparative method

Purification of products was carried out on a system comprising a Waters 600 series pump and controller and a Wisp715 autosampler. Detection was achieved with a Waters 490 UV spectrophotometer at 280 nm. Radiodetection was carried out using a modified NaI crystal and a J and P Engineering MS310 ratemeter. Purification was carried out on a 5 $\mu$ m Kromasil RPC18 column (10 X 250 mm) with 10 mm guard cartridge. A gradient elution profile was used as defined by the following time points:- 0 min, 15% A / 85%B; 20 min, 15% A / 85%B; 25 min, 85% A / 15%B; 40 min, 85% A / 15%B. All gradients were linear. The flow rate was 3 ml/min. Data was analyzed using Waters Baseline software.

#### 4.7.5 Radiochemistry

Electrophilic iododemallation provides a well validated method for the introduction of iodine into complex organic molecules at high specific activities. In order to maximise radiochemical yield, the oxidant and the pH of the reaction must be determined with care. Products formed in these reactions must be separated from the metallo precursor which is normally present in large excess to drive the reaction to completion. The radioiodination of 5-(tributylstannyl)-2'-deoxyuridine was achieved by an electrophilic iododestannylation reaction using peracetic acid as an oxidant and semipreparative HPLC allowed us to readily separate the radiolabelled compound from the tin precursor. Unlike other oxidising agents used in the preparation of radioiodinated species by electrophilic iododemallation, peracetic acid does not generate chlorinated side products. Peracetic acid compared favourably with a range of oxidants. It delivered products of consistent purity with high radiochemical yield.

#### 4.7.6 Radioiodination method

Aliquots of a solution containing 50 µg of 5-(tributylstannyl)-2'-deoxyuridine in chloroform were added to 300 µl V-vials (Aldrich, Dorset) and evaporated to dryness under a stream of nitrogen. Stored under nitrogen at -20°C, the 5-(tributylstannyl)-2'-deoxyuridine was stable for several months. Peracetic acid was prepared from 2ml of 35% (v/v) hydrogen peroxide, 1ml of glacial acetic acid and 30 µl of 98% (v/v) sulphuric acid. This mixture was allowed to equilibrate for 2 hours before use. To a 300 µl V-vial containing 50 µg of 5-(tributylstannyl)-2'-deoxyuridine, 155 to 178 µl of acetic acid, 7.4 MBq of Na<sup>125</sup>I, 230 MBq of Na<sup>123</sup>I or 74 MBq of Na<sup>131</sup>I (Amersham, International, UK) and 20 µl of peracetic acid was added. This reaction mixture was incubated at room temperature for 5 minutes before injecting the total volume on to a semipreparative HPLC column. The 6 ml fraction containing the radiolabelled IUdR was collected and evaporated to dryness in vacuo. The radiochemical yield of labelled IUdR in the reaction was consistently more than 95% which after HPLC purification gave isolated yields of IUdR between 60-70%. The IUdR was reconstituted in normal saline and sterilised by 0.22 µm filtration. Radiolabelled IUdR was stored at 4°C and aliquots of the reconstituted material were analysed prior to use by analytical HPLC as described previously. Synthesis of the precursor and labelling was carried out by Dr Jonathan Owens, Department of Clinical Physics and Bio-engineering, Radionuclide Dispensary, Western Infirmary.

#### 4.7.7 HPLC analysis for deiodination of IUdR

Evaluation of deiodination kinetics was attempted using HPLC analysis. However, the HPLC results proved too unstable for reliance to be placed as the data, which are therefore not included here.

## 4.8 Clonogenic assay following targeted radiotherapy

The effect of radioiodinated IUdR on clonogenicity of UVW cells was determined for cultures treated in exponential growth phase, in plateau growth phase and growing as multicellular spheroids.

### 4.8.1 Monolayers

Aliquots consisting of  $10^4$  exponentially growing monolayer cells were seeded into 24 multiwell plates (Corning, New York) containing 1ml of complete MEM and incubated at  $37^\circ\text{C}$  with 5%  $\text{CO}_2$  for 2 days. The medium was then removed and replaced with 1ml of medium containing a range of concentrations of  $^{123}\text{I}$ IUdR,  $^{131}\text{I}$ IUdR,  $^{125}\text{I}$ IUdR,  $\text{Na}^{125}\text{I}$  or  $\text{Na}^{131}\text{I}$ . Controls contained equimolar non-radiolabelled IUdR or medium in place of radioiodinated reagents. Cell cultures in plateau growth phase were established as described in section 4.3 and treated similarly. The cultures were incubated at  $37^\circ\text{C}$  with 5%  $\text{CO}_2$  for 44 hours (one doubling time for exponentially-growing cells). The radioactive medium was removed, and the cells were washed with PBS until no further soluble radioactivity could be eluted. They were then trypsinised, serially diluted and seeded into  $25\text{ cm}^2$  tissue culture flasks in triplicate. The number of cells seeded was chosen to yield 30 to 260 colonies after 10 days. A low-density feeder layer, containing  $10^4$  heavily irradiated cells, was added to each flask. This procedure was shown in preliminary experiments to enhance plating efficiency.

#### 4.8.2 Spheroids

Spheroids of 100 to 200µm diameter were transferred from bacteriological Petri dishes into 1% (w/v) agar base-coated 6-well plates (35mm diameter) containing 4 ml medium. Each well contained several spheroids. These were incubated with varying concentrations of [<sup>123</sup>I]IUdR, [<sup>125</sup>I]IUdR or [<sup>131</sup>I]IUdR at 37°C in 5% CO<sub>2</sub> for 52 hours (one volume doubling time). The spheroids were washed several times in culture medium until no further soluble radioactivity could be eluted. They were then treated with 0.5 ml of PBS containing 0.25% (v/v) trypsin and 1mM EDTA for 10 minutes at 37°C. After the addition of 0.5 ml of medium to neutralise the trypsin, the spheroids were mechanically disaggregated. Microscopic examination confirmed that the cell preparations were free of clumps. The protocol for seeding, staining and calculation of surviving fraction was as described in section 4.6.2.

#### **4.9 Incorporation of IUdR into DNA**

DNA was extracted from the UVW glioma cells according to the protocol described by Laird et al, (1991). Cells in exponential growth phase were incubated with different activity concentrations of [<sup>125</sup>I]IUdR from 1kBq/ml to 100kBq/ml for one doubling time (44 hours) at 37°C. The unbound radiolabelled IUdR was removed after several washes with PBS. Then cells were trypsinized and a known number of cells were placed into a microfuge tube containing 0.5 ml lysis buffer (100 mM Tris.HCl pH 8.5, 5mM EDTA, 0.2% (w/v) sodium dodecyl sulphate (SDS), 200 mM NaCl). Proteinase K (Gibco, UK) was added at a final concentration of 100 µg/ml and incubated at 55°C overnight. Following complete lysis, the tubes were vortexed and were then centrifuged for 10 minutes. The supernatants were then poured into prelabelled tubes containing 0.5 ml of

isopropanol. The samples were mixed by hand until a DNA precipitate was visible. The DNA was recovered by lifting the aggregated precipitate from solution using a disposable yellow tip. Excess liquid was removed and the DNA was dissolved in 1x TE buffer (10 mM Tris.HCl, 0.1 mM EDTA, pH 7.5). The tube contents were incubated at 37°C overnight to ensure the DNA was properly dissolved. Cellular uptake was measured as DNA-associated activity per cell by gamma counting (Cobra II, Canberra, Packard).

#### **4.10 Solutions and reagents**

Antibodies: Dako, Ltd, UK

Autoradiography: Kodak, IBI Limited, England

Iododeoxyuridine: Sigma, USA

Radiochemicals: Amersham International, UK

Tissue culture plastics from Falcon, Nunc, Denmark; Corning, UK.

Media and supplements from Gibco, Paisley.

#### **DNA Isolation Reagents:**

Lysis buffer (100 mM Tris.HCl pH 8.5, 5mM EDTA, 0.2% (w/v) SDS, 200 mM NaCl)

TE buffer (10 mM Tris.HCl, 0.1 mM EDTA , pH 7.5)

#### **Autoradiography:**

D19 developer: 2g metol, 8g hydroquinone, 90g anhydrous sodium sulphite, 45g anhydrous sodium carbonate, 5g potassium bromide, 1000 ml distilled water.

Kodak Fixer, prepared according to manufacturer's instructions.

#### **Ki67 Reagents:**

Blocking serum: 25% (v/v) normal human serum, 25% (v/v) normal swine serum and PBS.

Primary antibody: 10% (v/v) normal human serum, 10% (v/v) normal swine serum, PBS, rabbit anti-human Ki67 (1:100) diluted from supplied stock (Dako, Ltd, Code, A 0047).

Control antibody: 10% (v/v) normal human serum, 10% (v/v) normal swine serum, PBS, normal rabbit immunoglobulin diluted 1/400 from supplied stock (Dako, Ltd, Code, E 353).

Secondary antibody: 10% (v/v) normal human serum, 10% (v/v) normal swine serum, biotinylated pig anti-rabbit immunoglobulin diluted 1/400 from supplied stock (Dako, Ltd,

Code, 353).

sABC reagent (strep Avidin Biotin- peroxidase Complex): prepared 30 min prior to use by diluting in PBS containing 2% (v/v) normal human serum.

Diaminobenzidine (DAB): 0.05% (w/v) (diaminobenzidine tetrahydrochloride containing 0.01% (v/v) hydrogen peroxide (H<sub>2</sub>O<sub>2</sub>) in PBS.

**Flow cytometry reagents:**

propidium iodide (PI) stock solution (10ml PBS, 300µl PI, 1mg RNase, 25µl triton X-100)

PBT (PBS + 0.5%bovine serum albumin + 0.05% Tween 20)

Anti-BudR antibody, diluted 1/30 from supplied stock (Dako, Ltd, Code, M 744).

Anti mouse FITC antibody, diluted 1/40 from supplied stock (Dako, Ltd, Code, F 0479).

## **Chapter 5**

### **Biology of human glioma cell lines**

<b>5.1 Characterisation of human glioma continuous cell lines</b>	99
5.1.1 Introduction	99
<b>5.2 Methods and materials</b>	100
5.2.1 Morphology	100
5.2.2 Population doubling times in monolayer culture	100
5.2.3 Volume doubling time in spheroid culture	101
5.2.4 Glial fibrillary acidic protein (GFAP)	102
5.2.5 Karyotype analysis of UVW cells	102
5.2.6 Cell cycle analysis	102
5.2.7 Ploidy	103
<b>5.3 Results</b>	104
5.3.1 Morphology	104
5.3.2 Doubling time of glioma cell lines	107
5.3.3 Karyotypic analysis of UVW line	110
5.3.4 Cell cycle analysis	113
5.3.5 Ploidy	115
<b>5.4 Discussion</b>	117

## **5.1 Characterisation of human glioma continuous cell lines**

### **5.1.1 Introduction**

The human glioma cell line U251 used in this study was initially described by Ponten (1975). SB18 was established by Pilkington and Lantos (1982) and UVW was established in the Department of Medical Oncology, University of Glasgow. All were anaplastic astrocytoma, grade III and IV glioma.

The UVW cells line was chosen because of its ability to grow as very large and regularly shaped spheroids in comparison to other cell lines. Therefore, we decided to characterise the UVW cell line. The rationale for this was as follows.

The UVW human glioma cell line used in the present investigations, was established in this lab in the early 1980s as part of a study of the phenotypic differences between normal and malignant glia. This line was used as a tumour model as part of a research program on the mechanisms of human tumour chemoresistance (Merry et al., 1984). At the commencement of the project all glioma lines had been passaged more than 100 times and therefore a re-assessment of their biological characteristics was considered important.

## 5.2 Methods and materials

### 5.2.1 Morphology

The cell lines used in this study grew as adherent monolayer cultures on tissue culture grade plastic. Morphological examination was made in mid-log phase of growth using bright field microscopy.

### 5.2.2 Population doubling times in monolayer culture.

To determine the population growth curves for each cell line, cells from early-culture passage of monolayer growth were harvested and  $10^4$  cells were seeded into two individual 24 multiwell plates, and allowed to adhere. On the second day after seeding, 0.5 ml of 0.25% trypsin in 1mM EDTA was added to three wells and the cells were counted using a Coulter counter (Coulter Electronic, Luton, England) calibrated for each cell line. This procedure was repeated daily for 18 days. The medium was replaced every day with 1ml fresh medium to maintain the cells in exponential growth. The mean of three counts were used to calculate the doubling time. Preliminary growth curves showed that log phase growth started at day 2 or 3 and the cells reached a plateau between days 8 and 18. Terminal density was judged to have been achieved when cell counts remained constant over 3 consecutive days. Population doubling times were calculated from the exponential portion of the growth curves by means of the equation:

$$T_D = 0.693 / \lambda$$

Where  $T_D$  is the mean doubling time and  $\lambda$  is mean slope of the exponential portion of the growth curve.

### 5.2.3 Volume doubling time in spheroid culture

Spheroid growth rates were measured to provide a basis for the selection of incubation times for radiolabelled and non-radiolabelled IUdR. Cultures of spheroids were initiated by inoculating  $10^6$  cells into a bacteriological Petri dish containing 15 ml of medium. After two days of incubation in 95% air / 5% CO<sub>2</sub> at 37°C, cell aggregates of approximately 100 µm diameter were selected and transferred to 24-well plates coated with 1% (w/v) agar, containing 0.5ml of medium per well. Each well contained a single aggregate which subsequently grew as a tumour spheroid. 0.5 ml of fresh medium was added every 7 days.

At 2 to 4 day intervals, each spheroid was evaluated by measuring 2 perpendicular diameters, using an inverted, phase-contrast microscope connected to an image analyzer. The volume of the spheroids was calculated from the equation:

$$V = a \times b^2 \times \pi / 6$$

Where a and b are the longest and shortest diameters respectively. Growth kinetic data were fitted (using BMDP program 3R) to a Gompertzian equation, which is defined by the following relationship:

$$V(t) = V(0) \exp \left[ \left( \frac{A}{\alpha} \right) (1 - \exp[-\alpha t]) \right]$$

where V(t) and V(0) are the volume of the spheroid at times t and 0, respectively and A and  $\alpha$  are parameters. UVW glioma spheroids initially grew exponentially but then underwent a progressive reduction in growth rate, and this pattern showed a good fit to a Gompertzian equation.

The volume doubling time of the initial exponential part of the growth curve, calculated as  $\ln 2 / A$ , was 52 hours.

#### 5.2.4 Glial fibrillary acidic protein (GFAP)

To determine expression of the astrocytic lineage marker, GFAP,  $10^4$  UVW tumour cells were seeded in 100 $\mu$ l of medium onto polylysine-coated sterile coverslips in 24 well plates, and allowed to adhere. The cells were fixed with ice-cold methanol, and left for 15 minutes, at -20°C, prior to brief rehydration with Hanks staining medium. Rabbit anti-human GFAP (Dako, Ltd, UK) was added in 50 ml Hanks medium, and left for 45 minutes. Coverslips were then washed in Hanks medium, and a goat anti-rabbit polyclonal second antibody conjugated to fluorescein (Southern Biotechnology) was added. Coverslips were treated with Cityflor antifade, and mounted cell-down on microscope slides, sealed with nail varnish to prevent movement, and dried. Cells were then examined for fluorescence using a Reikert Polyvar microscope. The percentage of total stained cells was then estimated. The human lung carcinoma line, A549, was used as a negative control.

#### 5.2.5 Karyotype analysis of UVW cells

Karyotype analysis was carried out by the Department of Medical Genetics, Royal Hospital for Sick Children, Yorkhill, Glasgow.

#### 5.2.6 Cell cycle analysis

Cells were grown as monolayers in exponential or plateau phases as described in sections 4.1 and 4.3. They were then trypsinised, rinsed well in PBS and fixed in 70% (v/v) ethanol. Before analysing, cells were pelleted by centrifugation, resuspended in 1.6 ml of PBS, 0.2 ml

RNase (1mg/ml) (Sigma) and 0.2 ml propidium iodide (PI) (400 $\mu$ g/ml). PI is a stoichiometric DNA dye suitable for monitoring the percentage of cells in the G<sub>1</sub>, S, and G<sub>2</sub>/M phases of the cell cycle on the basis of the cellular DNA content (Pucillo et al, 1990). After incubation for 30 min at 37°C, cells were pelleted by centrifugation, and resuspended in PBS. The cells were analysed using a Coulter Epics Profile II (Epics Coulter corporation, Florida, USA). Each analysis was the result of 10,000 nuclear counts on each sample. S phase fraction was then calculated by offline analysis using Multicycle software (Phoenix Flowsystems, San Diego, USA).

### 5.2.7 Ploidy

Flow cytometric analysis of cellular DNA content was used to establish cell line ploidy. For this purpose UVW nuclei were gently vortexed and one drop of chicken erythrocyte nuclei (CEN) (Becton Dickinson, Erembodegem, Belgium) was dispensed into the tube, to which 1ml of PI stain solution was then added. CEN act as internal reference standards for the determination of G<sub>0</sub>/G<sub>1</sub> cell DNA content. The tube was capped, gently vortexed and incubated for 10 minutes at room temperature, protected from the light. Cytometry was performed on a Becton Dickenson Florecent Activated Cell Sorter (FACS) using control aliquots of the suspension of PI stained nuclei. Each analysis was the result of 10,000 nuclear counts on each sample.

## 5.3 Results

### 5.3.1 Morphology

The morphology of the glioma cell lines growing in monolayer culture are shown in Figures 5.1-5.4. The morphological features, phenotypic and genotypic characteristics of the three continuous glioma lines are summarised in Table 5.1.

**Table 5.1** Phenotypic and genotypic characteristics of human glioma cell lines.

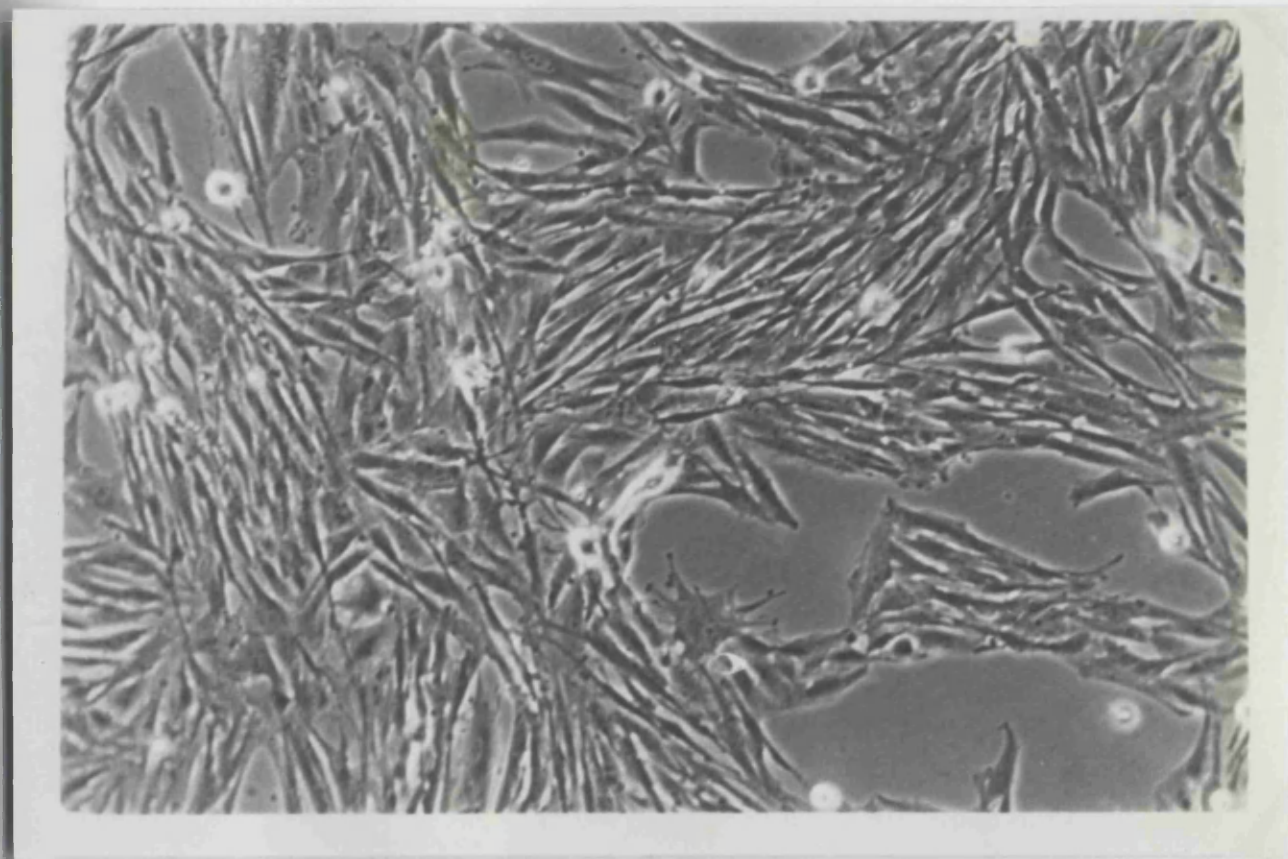
Cell line	UVW	U251	SB18
Passage level	>100	>100	>100
Morphology	fusiform	epithelioid	fusiform
Doubling time (hrs)	44	32	39
Monolayer	+	+	+
Spheroid	+	+	+
GFAP	-	+	+
DNA index	2.9	ND*	ND*
S phase fraction	13.6	19.6	16.5
G <sub>0</sub> /G <sub>1</sub>	70.8	74	79.3
G <sub>2</sub> /M	15.6	6.4	4.2

\*ND = Not determined

**Figure 5.1** Phase contrast micrographs of (a) UVW monolayer and (b) UVW spheroid.

200 $\mu$ m spheroid.

**A**



**B**

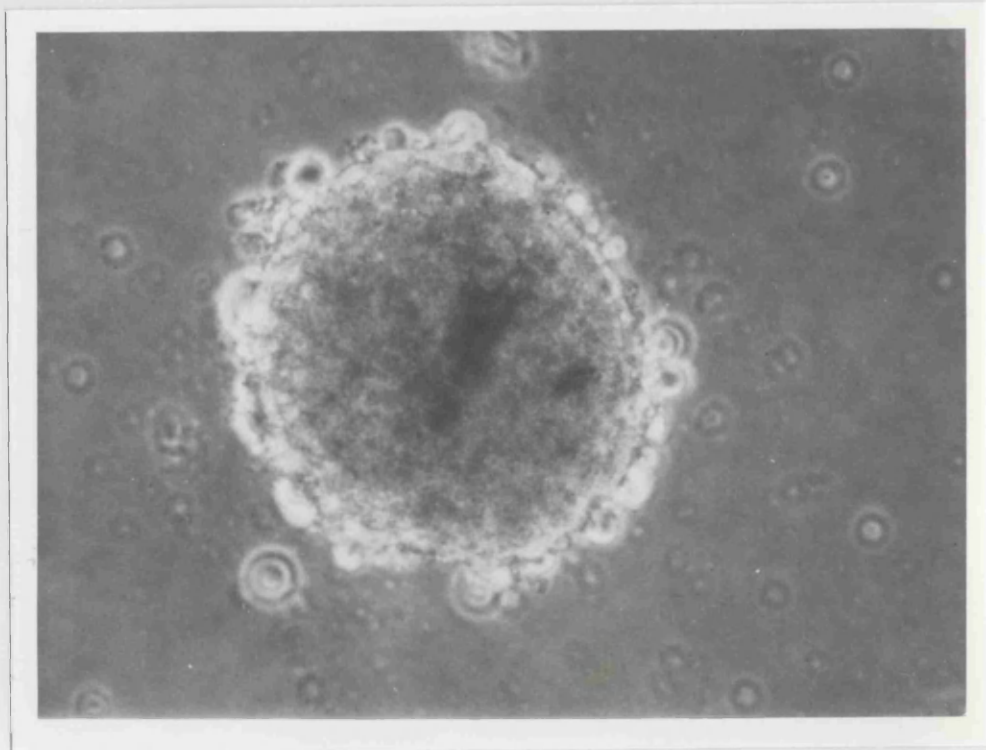
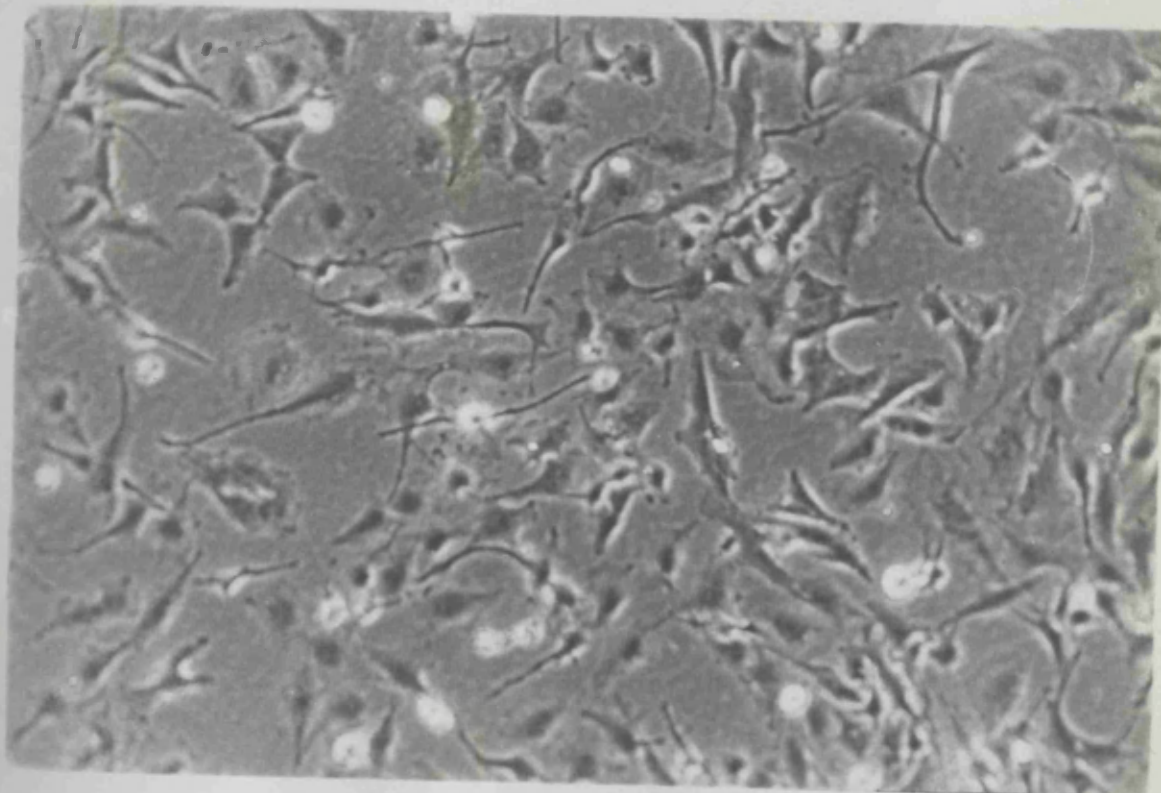


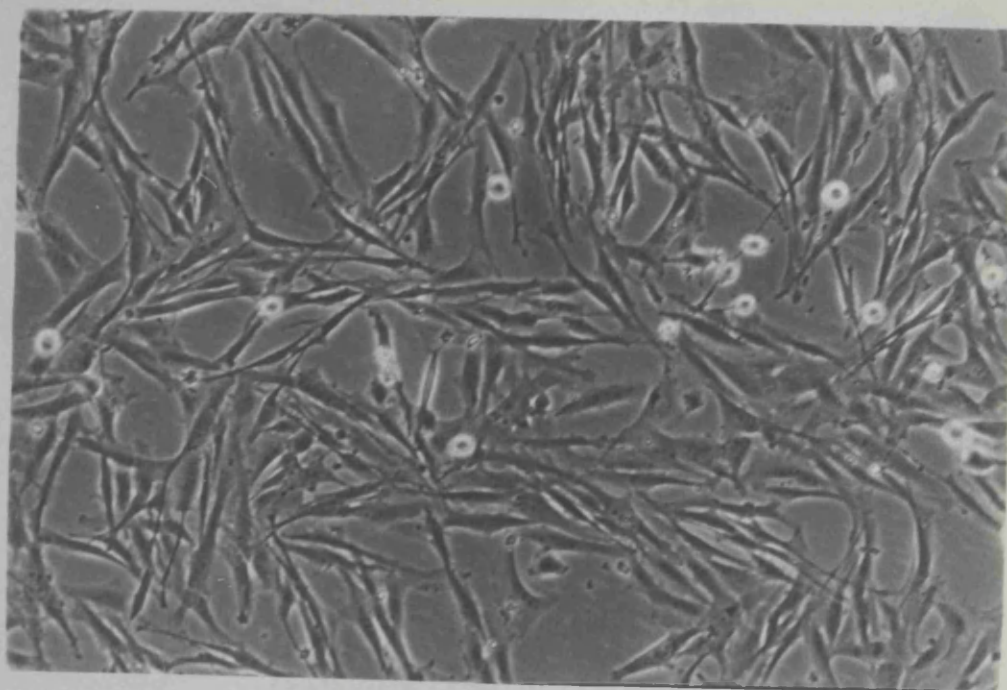
Figure 5.2 Phase contrast micrographs of monolayer (a) U251, and (b) SB18.

Magnification: x 150

**A**



**B**



### 5.3.2 Doubling time of glioma cell lines

Glioma cell lines showed a lag phase of 24-48 hours before achieving exponential growth. The population doubling times ( $T_D$ ), calculated from the slopes ( $\lambda$ ) of the exponential part of the growth curves, of cell lines SB18, U251 and UVW, were 39 hrs, 32 hrs and 44 hrs respectively. This data is summarized in Table 5.2.

Cell lines	$\lambda$ ( $\text{day}^{-1}$ ) ( $\pm$ SEM)	$T_D$ (hrs)
SB18	0.426 $\pm$ 0.03	39
U251	0.513 $\pm$ 0.04	32
UVW	0.376 $\pm$ 0.07	44

**Table 5.2** Growth curve parameters of glioma cell lines calculated by linear regression analysis using SPSS (statistical package) (SPSS Inc, USA) .

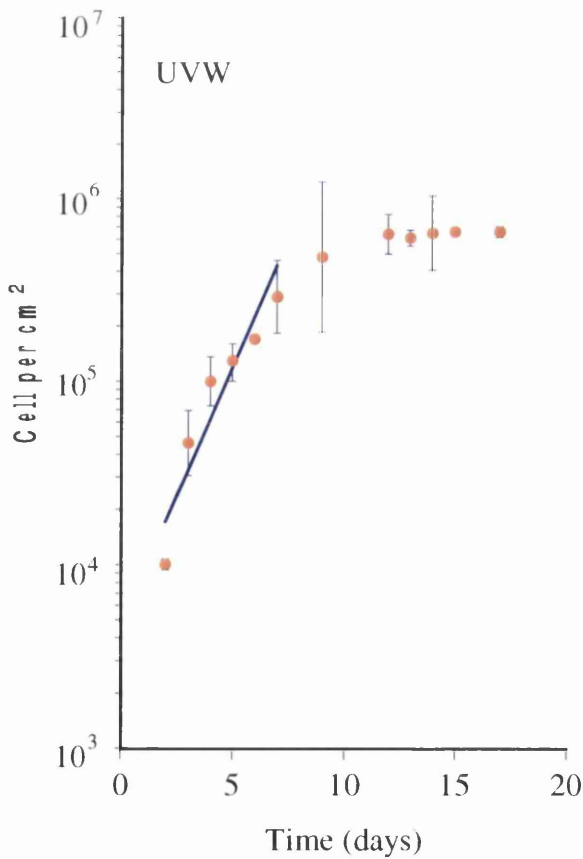
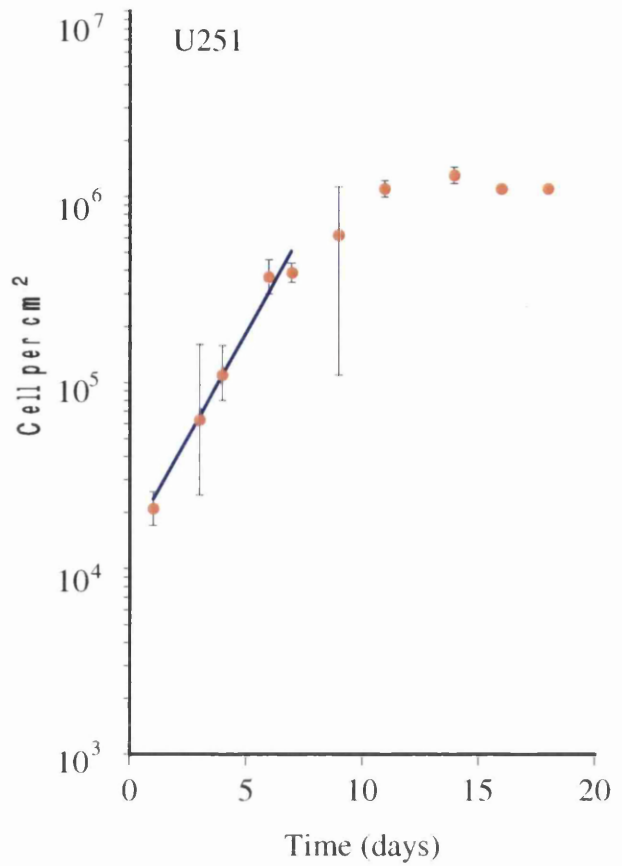
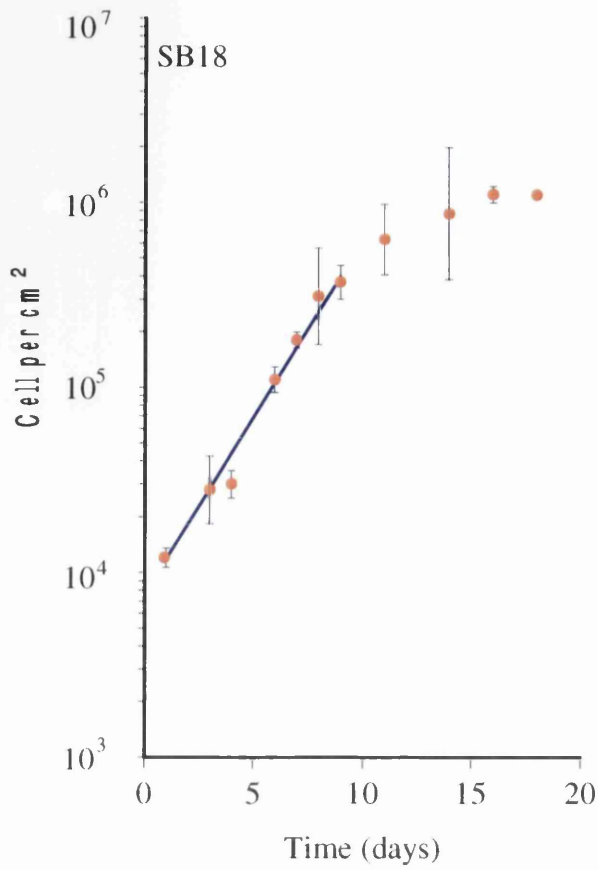


**Figure 5.3** Growth curves of glioma cell lines fitted by linear regression analysis using the statistical package SPSS. Each point represents the mean  $\pm$ SEM of estimations performed in triplicate.

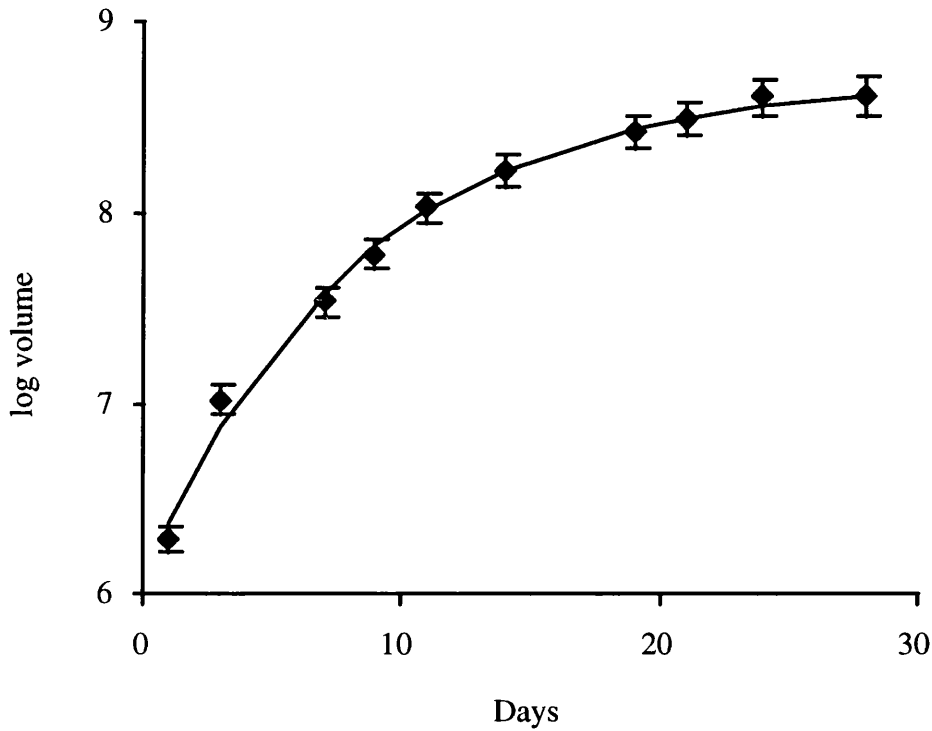


**Figure 5.4** Spheroid growth curve. The ordinate is the common logarithm of spheroid volume in  $\mu\text{m}^3$ . Each point represents the mean ( $\pm$ SEM) of at least 13 values, calculated from measured cross sectional area. The curve represents a Gompertzian equation fitted to the data by the relationship:

$$V(t) = V(0) \exp \left[ \frac{A}{\alpha} (1 - \exp[-\alpha t]) \right]$$

where  $V(t)$  and  $V(0)$  are the volume of the spheroid at times  $t$  and  $0$ , respectively and  $A$  and  $\alpha$  are parameters. The parameters of the fitted curve are  $V(0) = 6.08 \log \mu\text{m}^3$ ,  $A = 0.319 \text{ day}^{-1}$ ,  $\alpha = 0.122 \text{ day}^{-1}$ .

### 5.3.3 Karyotypic analysis of UVW line

Three cells from this line have been karyotyped from photomicrographs. Table 5.2 shows the three cells (A,B, and C) with the number of normal homologues of each chromosome followed by any structural abnormalities involving that chromosome. Any additional or missing material is denoted as + or -, and its position as to whether it is on the short arm (p) or long arm (q) has been noted. Due to the highly rearranged nature of these cells it was not possible to fully characterise all the chromosomes and those in which the centromere could not be identified have been classed as 'Markers'.

Chromosome	1	2	3	4	5	6	7	8	9	10	11
A	1	2	3	4	5	6	7	8	9p+	10	11
	1	2	3	4	5	6	7	8	9p+	10	11
		2	3	4q+	5	6q-	7	8p+		10	11q+
						6q-	7				
B	1	2	3	4	5	6	7	8	9p+	10	11
	1	2	3	4	5	6q-	7	8p+	9p+	10	11
		2	3p-	4q+	5	6q-	7		9p+	10	11q+
							i(7)p				
C	1	2	3	4	5	6	7	8	9p+	10	11
	1q-	2	3	4q+	5	6	7	8	9p+	10	11
		2	3		5	6q-	7		9p+	10	11q+
						6q-	7		9p+		
							i(7)p				

Chromosome	12	13	14	15	16	17	18	19	20	21	22
A	12	13	14	15	16	17	18	19q+	20	21	22
	12	13	14	15	16	17	18	19q+	20	21	22
	12			15		17		19q+		21	
						17					
B	12	13	14	15	16	17	18	19q+	20	21	22
	12	13	14	15		17	18	19q+	20	21	22
						17		19q+	20	21	
C	12	13	14	15	16	17	18	19q+	20	21	22
	12	13	14	15	16	17	18		20	21	22
				15		17	18		20	21	22
										21	22
										21	

Chromosome	X	Y	Markers	Count
A	Xp+ Xp+	Y	12	78
B	Xp+ Xp+	Y	12	72
C	Xp+ Xp+	Y	10	74

**Table 5.3** Karyotype analysis of UVW glioma cell line. Any additional or missing material is denoted as + or -, and its position as to whether it is on the short arm (p) or long arm (q) has been noted. Those chromosomes in which the centromere could not be identified have been classed as 'Markers'.

NAME ..... 74 ©  
LAB REF. No. ....

ROYAL HOSPITAL FOR SICK CHILDREN YORKHILL GLASGOW G3 8SJ

MEDICAL GENETICS UNIT

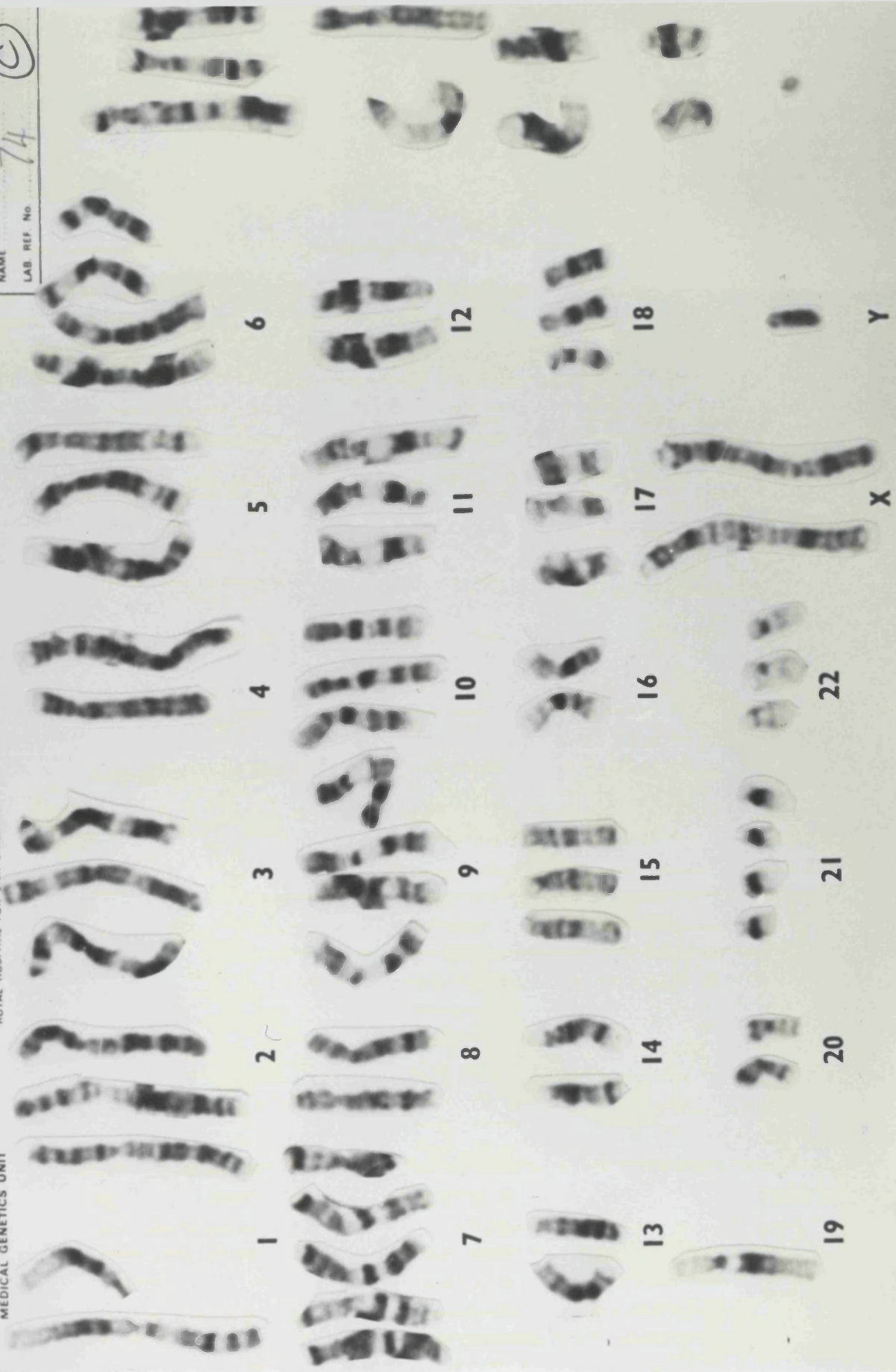
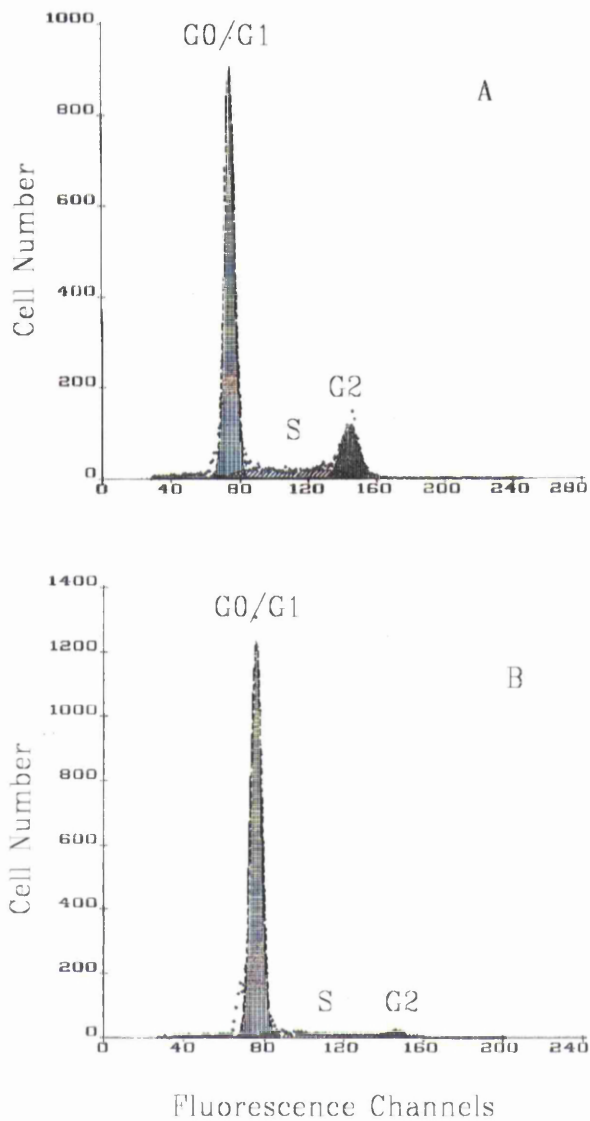


Figure 5.5 Photograph showing the karyotype of the UVW cell line.

#### 5.3.4 Cell cycle analysis

The percentage of cells in S phase, measured by flow cytometry, in exponentially growing cells and cells in plateau phase of growth was 13.6% and 7.4% respectively. Histograms are shown in Figure 5.6.



**Figure 5.6** Flow cytometry analysis of UVW cells in exponential and plateau phase culture.

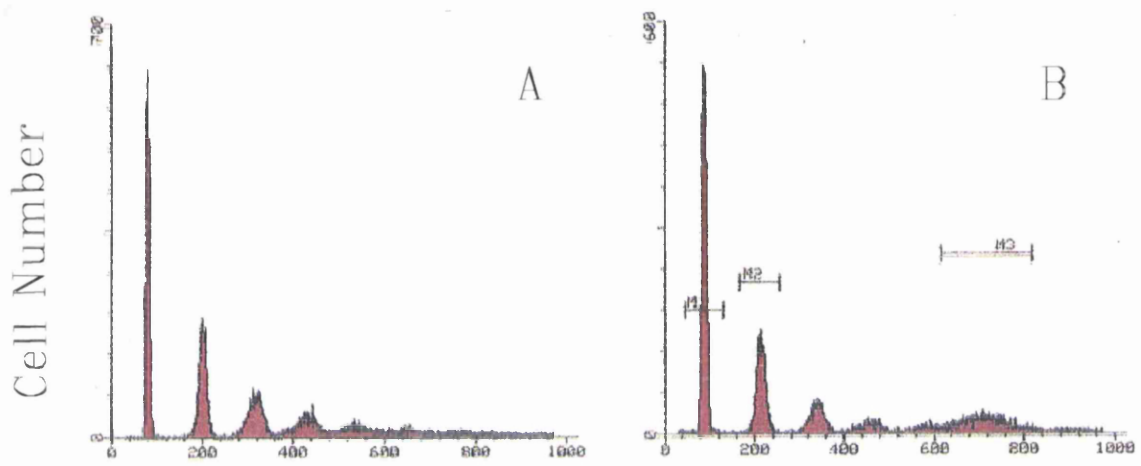
The Y axis indicates the number of cells. The number of fluorescence channels is indicated on the X axis.

(A) Exponential growth phase. (B) Plateau growth phase.

The percentage of cells in S phase in exponentially growing cultures was nearly twice as high as the percentage in plateau phase cultures.

### 5.3.5 Ploidy

The DNA content of the tumour cells relative to the normal cells can be expressed in terms of the DNA index. This is the ratio between the DNA content of the tumour  $G_0/G_1$  cells and the normal  $G_0/G_1$  cells. In this experiment, chicken erythrocyte nuclei (CEN) form peaks on the FL2-Area histogram at channels 87, 200 and 300. The human diploid peak should fall between channels 200-315. The UVW peak was collected at channel 707, giving a DNA index between 2.3 and 3.5, which represents a hypertetraploid DNA content.



### Fluorescence Channels

**Figure 5.7** (A) Histogram of PI stained CEN demonstrating resolution and linearity. (B) Ploidy study of UVW cells in monolayer exponential culture. The Y axis indicates the number of cells against typical CEN and UVW cells peak channels on the X axis.

## 5.4 Discussion

The aim of this project was to determine the effect of heterogeneous proliferative activity of cells on the therapeutic potential of radioiododeoxyuridine. An important part of this work was therefore obtaining appropriate models for the study of human gliomas *in vitro*. As a tool in the study of radiation responses of tumour cells, these cells can be cultured in the form of three-dimensional multicellular spheroids. The use of spheroids as a tumour model is described in detail in section 2.4.

The human glioma cell lines used in this study were UVW, SB18 and U251. They exhibited a heterogeneous range of phenotypic characteristics and displayed colony formation in monolayer culture with plating efficiencies ranging from 10-25%, using 10% (v/v) fetal calf serum and a low density feeder layer of homologous, heavily irradiated cells.

The three human glioma lines were compared for their suitability for the assessment of radiolabelled IUdR in the treatment of human glioma. The continuous line UVW was established in this lab before advent of this study and had been used previously by other groups (Freshney, 1984; MacDonald et al., 1985). All cell lines grew as spheroids but the UVW cell line was regarded as the most satisfactory *in vitro* model because of its capability to grow as very large and regularly shaped spheroids. The latter characteristic was essential for our study of the effect upon targeted radiotherapy of proliferative heterogeneity, which increases with spheroid size. The phenotype and genotype of the UVW glioma cell line was determined. This cell line lost its ability to express glial fibrillary acidic protein (GFAP) (see section 2.3), a cytoskeletal protein which is considered to be a marker of the astrocytic

lineage (Bignami et al., 1972). The pattern of expression of this marker is progressively altered with serial passage (Frame et al., 1984) and is likely to be heavily influenced by culture conditions. Many researchers have reported the loss of GFAP positivity within the first few early passages of malignant glial culture (Kennedy et al., 1987; Westphal et al., 1990).

The analysis of cellular DNA content provides information about the proliferative state of cell populations and about cell responsiveness to various stimuli. For example, tumour cell ploidy, and DNA index may be used as prognostic factors (Dressler et al., 1989). The UVW cell line was highly aneuploid and contained populations of cells which were sub-tetraploid by karyotype analysis. Flow cytometric analysis of UVW cells indicated a range of ploidy from sub-tetraploidy to hyper-tetraploidy confirmed that UVW is a highly aneuploid cell line.

Flow cytometric analysis of the UVW cell line cultured as monolayer in exponential growth or plateau phase showed the percentage of cells in S phase in exponentially growing culture to be 13.6%, while it was 7.4% in plateau phase cultures (Figure 5.6). Toward the end of the log phase, the culture became confluent when all the available growth surface was occupied and all the cells were in contact with surrounding cells. Following confluence, the growth rate of cultures was reduced, and in some cases, cell proliferation ceased almost completely after one or two doubling times. The reduction of the growth after confluence was not due only to contact but may also have involved reduced cell spreading (Folkman and Moscona, 1978), depletion of nutrients, and particularly growth factors (Holley et al., 1978), a reduction in cellular proliferation rate, a decrease in extracellular pH, oxygen tension and an increase in lactic acid and catabolite concentration (Bhuyan et al., 1977). Plateau growth

does not imply complete cessation of cell proliferation but represents a steady state where cell division is balanced by cell loss. These characteristics of plateau-phase culture, closely resemble those found within the hypoxic microenvironment of tumours, whereas cells in exponential growth exist in conditions that are analogous to cells growing close to blood vessels. These differences between plateau-phase and exponentially growing phase cells, provide a foundation for the development of an approach for glioma treatment using radiolabelled IUdR.

## **Chapter 6**

### **Radiosensitivity of the human glioma cell line UVW**

<b>6.1 Aims</b>	122
<b>6.2 Introduction</b>	122
<b>6.3 Methods and materials</b>	123
6.3.1 Spheroid culture	123
6.3.2 Spheroid growth delay after external beam irradiation	123
6.3.3 Clonogenic cell survival assay after external beam irradiation	126
<b>6.4 Results</b>	126
6.4.1 Spheroid growth delay	126
6.4.2 Clonogenic assay	126
<b>6.5 Discussion</b>	131

**6.1 Aim:** The aim of this study was to assess the effect of external beam irradiation on UVW cells in both monolayer and spheroid culture, in order to determine the radiosensitivity of this cell line under different conditions of culture. In particular we wished to establish a dose response for uniform irradiation for comparison with the response to IUdR targeted radiotherapy.

## **6.2 Introduction**

The vast majority of glioblastomas will recur in the irradiated field because this highly malignant glioma is radioresistant at a dose level which is at the limit of tolerance of normal brain tissue (Wallner et al., 1989). Several mechanisms could contribute to this clinical radiation resistance, such as efficient repair of radiation damage, a high intrinsic cellular radiation resistance and /or a rapid repopulation between fractions (Taghian et al., 1993). In order to establish the sensitivity of UVW cells to conventional radiotherapy by a standard technique, and to provide a basis for comparison of the efficacy of DNA-targeted radiotherapy, experiments were carried out to study the effect of single dose irradiation on UVW spheroids and monolayer cells. The radiation effect was evaluated by the assessment of regrowth delay and clonogenic assay in spheroids and by clonogenic assay in monolayer cultures.

## **6.3 Methods and materials**

### **6.3.1 Spheroid culture**

Spheroids were cultured according to the method described in section 4.4.

### **6.3.2 Spheroid growth delay after external beam irradiation**

Spheroids of 100-180  $\mu\text{m}$  diameter were placed in Petri-dishes coated with 1% (w/v) agar and irradiated using a cobalt-60 therapy source (Thompson, Versailles, France). Doses of 2-10Gy were delivered using customised wooden and plastic blocks to provide build-up and back scatter radiation. Spheroids were then placed individually into the wells of multiwell plates containing 0.5 ml of medium and coated with 1% (w/v) agar. This treatment prevented the attachment of spheroids to the bottom of the wells. Care was taken to ensure that approximately the same size of spheroids were used in control and test plates.

Spheroid growth was monitored by an Image Analyzer (Analytical Measuring System, Saffron, Essex) three times per week and 0.5 ml of fresh medium was added every 7 days. One 24 well plate was used for each dose point. Using a computer programme, (Dr G.M. Ford, Department of Clinical Physics and Bio-engineering, Glasgow) each measured area was converted into volume on the assumption that the spheroids were perfect spheres. Spheroid growth delay is presented in terms of specific growth delay, (Steel, 1984). This expresses growth delay in terms of the number of additional doublings which treated spheroids must undergo to reach the same volume as untreated controls. Spheroid growth curves were obtained by calculating the median volume of the spheroids in each experimental group on

each day of measurement. The surviving fraction for each experimental group was estimated by extrapolation of the exponential portion of the regrowth curve to the Y axis and calculation of the difference between effective log volume (given by the intercept) and initial log volume as measured immediately before irradiation (Figure 6.1).

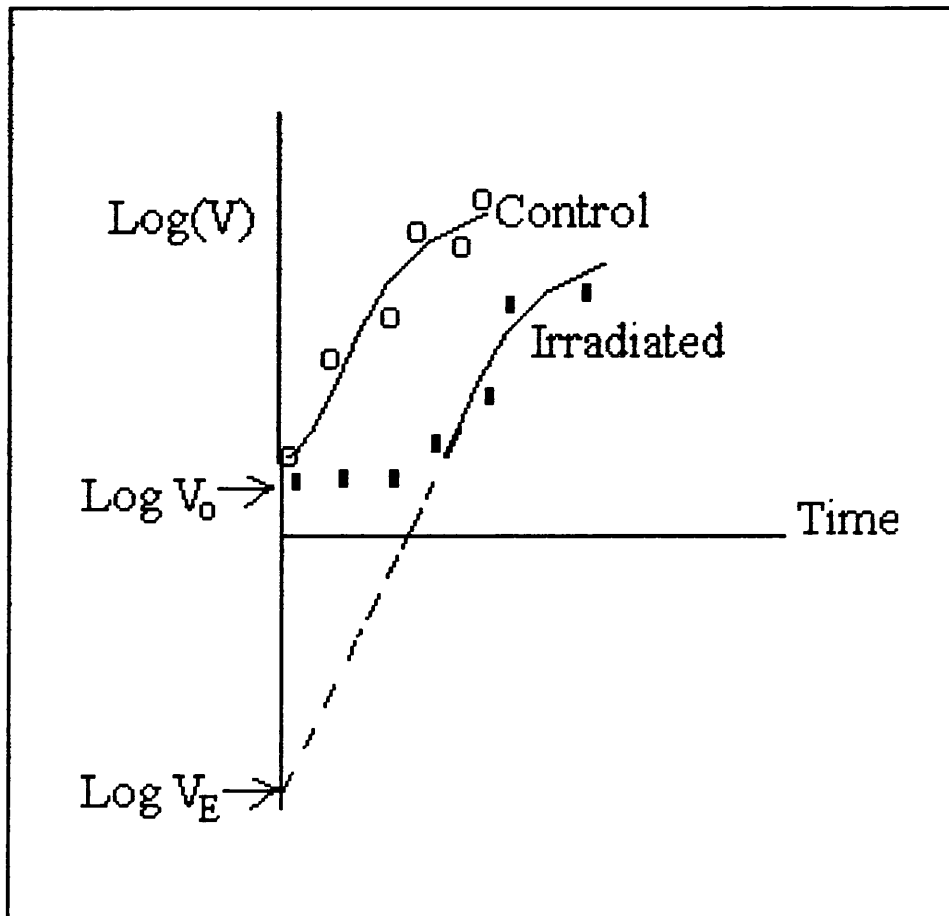


**Figure 6.1** General principle of estimation of cell surviving fraction from spheroid regrowth curve. Extrapolation of the regrowth curve to zero time yields an estimate ( $V_E$ ) of the 'effective volume' from which the spheroid appears to have regrown i.e. it represents the volume of viable cells following treatment. The ratio  $V_E$  to the measured volume  $V_0$  (representing the volume of all cells initially present) provides a measure of the cellular surviving fraction immediately following treatment.

### 6.3.3 Clonogenic cell survival assay after external beam irradiation

The radiation protocol and clonogenic cell survival assay for monolayers and spheroids were performed by the methods described in sections 4.6.

## **6.4 Results**

### 6.4.1 Spheroid growth delay

Figure 6.2 shows spheroid growth curves for the UVW cell line as a function of dose. The surviving fractions, calculated as described in section 6.3.2 and radiobiological surviving curve parameters are given in Table 6.1, where they are compared with the surviving fractions for spheroids as determined by clonogenic assay.

### 6.4.2 Clonogenic assay

Spheroids and monolayer experiments were performed with five and ten dose points respectively. The results are shown in Figure 6.3. Both survival curves were well fitted by the linear-quadratic equation (see chapter 2 for methodology) and the parameters of the curves are given in Table 6.1. The survival curves of spheroids had a greater degree of curvature than those of monolayers, corresponding to a larger  $\beta$  value for the fitted curve. Also shown in Table 6.1 are the survival fractions for monolayers and spheroids at a dose of 2Gy.

There was good agreement between the results of the growth delay and clonogenic assay experiments for the survival fraction for spheroids (Table 6.1, Figure 6.4).

**Table 6.1** Radiobiological survival curve parameters for UVW spheroids and exponentially growing monolayers calculated by regression analysis using the SPSS statistical package.

Cell culture	$\alpha$ Gy <sup>-1</sup> ( $\pm$ SEM)	$\beta$ Gy <sup>-2</sup> ( $\pm$ SEM)	SF <sub>2</sub>
monolayer	0.289 $\pm$ 0.03	0.023 $\pm$ 0.004	0.55
Spheroids (CA)	0.007 $\pm$ 0.05	0.045 $\pm$ 0.006	0.93
spheroids (GD)	0.007 $\pm$ 0.04	0.049 $\pm$ 0.004	0.83

The linear-quadratic components ( $\alpha$  and  $\beta$ ) show similar results for both clonogenic and regrowth delay techniques. SF<sub>2</sub> values (surviving fraction at 2Gy) are compared for both monolayers and spheroids cultures.

CA = Clonogenic assay

GD = Growth delay

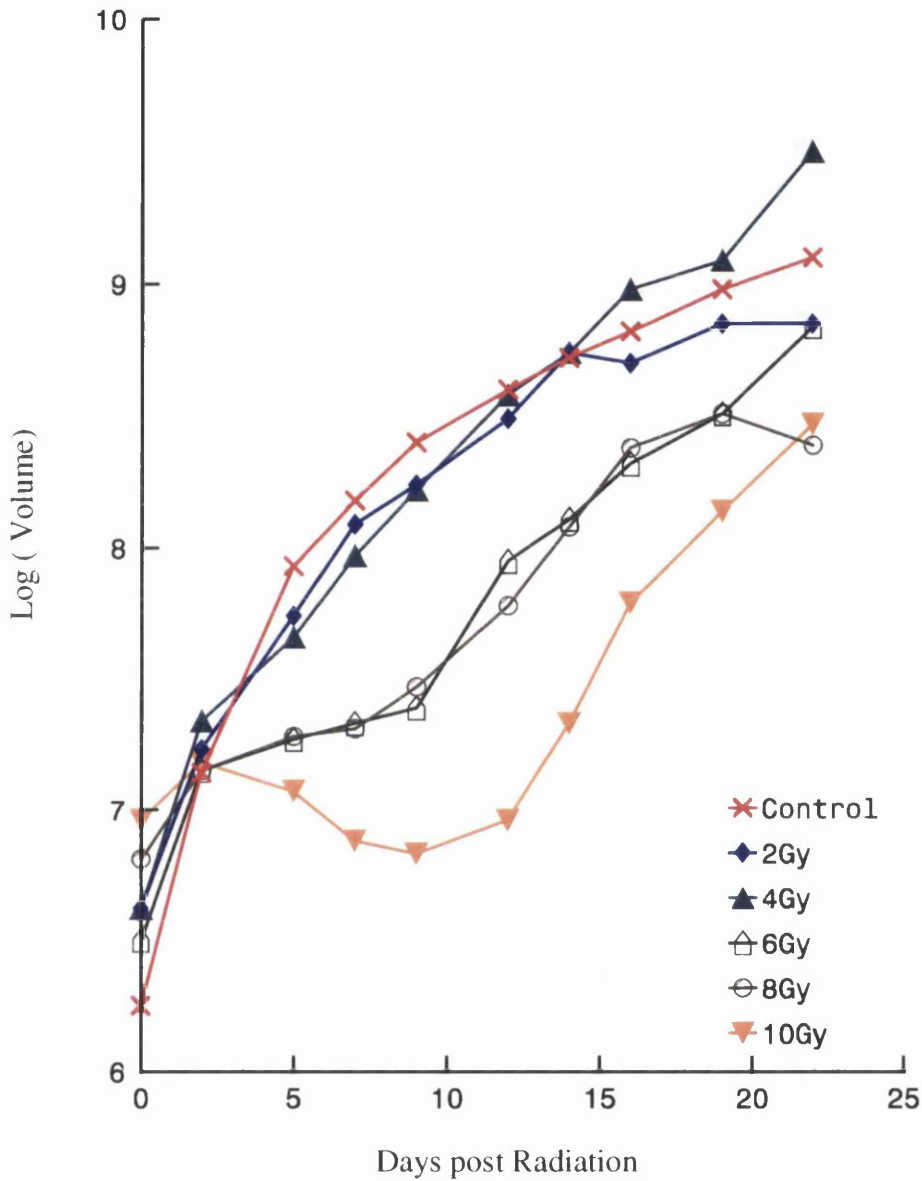


**Figure 6.2** Growth curves for UVW glioma multicellular spheroids treated with single dose irradiation. Different radiation doses (2 - 10 Gy) are shown by symbols. The relative radiation doses represented by each symbol are shown on the right hand corner of the graph.

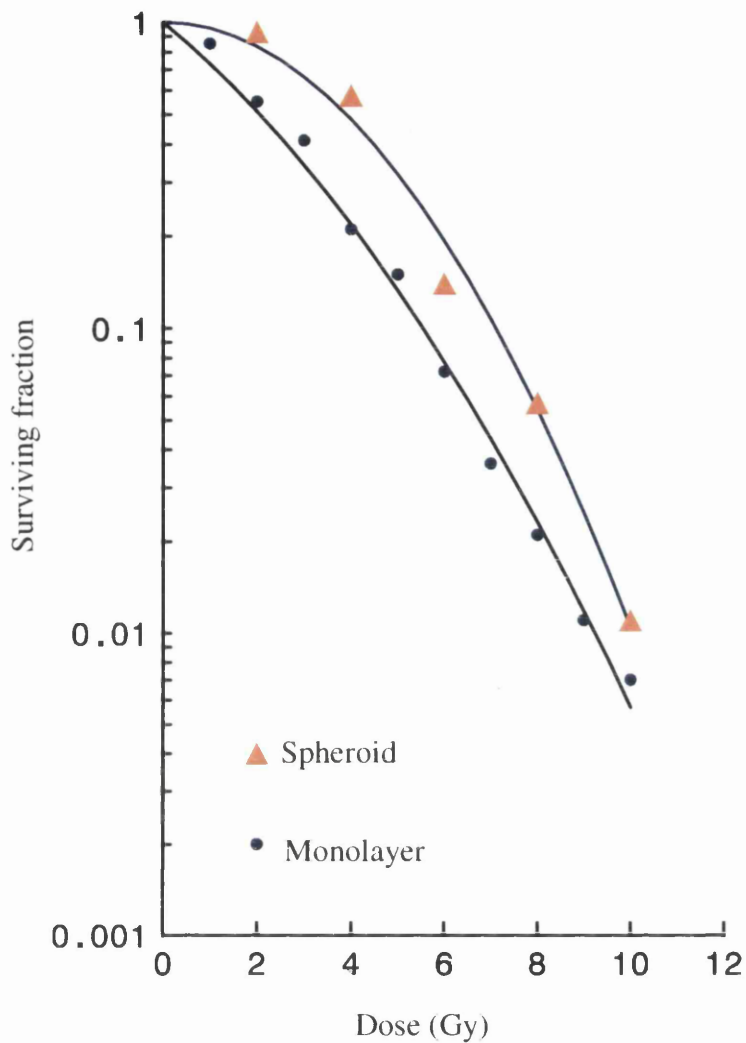


**Figure 6.3** Surviving curves of UVW multicellular spheroids and monolayer cells calculated from clonogenic assay after external beam irradiation. The fraction of surviving cells is plotted on a logarithmic scale against dose on a linear scale. The filled circles represent monolayer cultures and triangles the spheroid cultures.

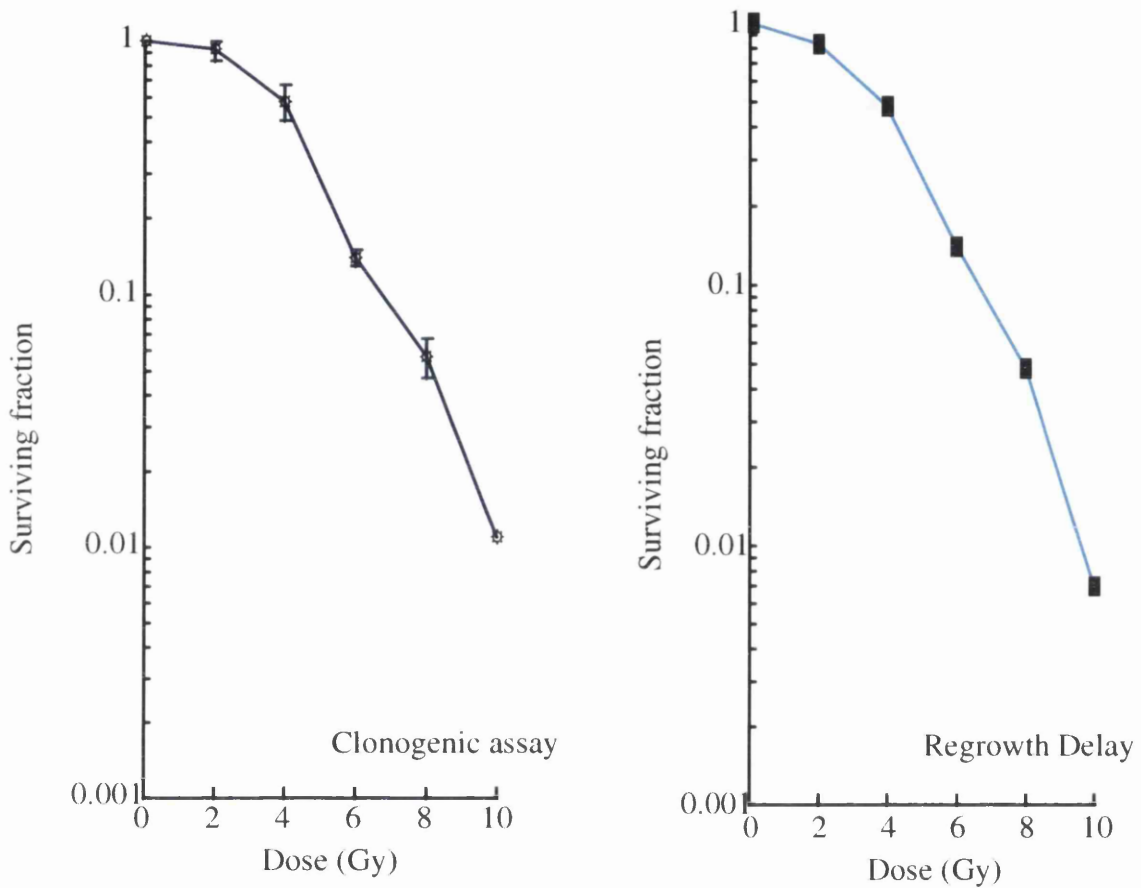


**Figure 6.4** Surviving fraction of UVW spheroids obtained from regrowth delay (filled squares) and clonogenic assay methods (spiked circles).

## 6.5 Discussion

In these experiments, we assessed the effect of external beam radiation on UVW monolayers and spheroids in order to establish the radiosensitivity of this cell line by a standard technique which allows comparison with other cell lines and to provide a basis for comparison with the surviving fraction obtained after radionuclide treatment, as described in later chapters.

Survival curves for spheroids were determined by two independent methods: growth delay and clonogenic assay. The first of these techniques is potentially subject to inaccuracy because it requires the subjective identification of the exponential part of the growth curves for curve fitting. The clonogenic assay is regarded as the most reliable method of determining cell survival, but is still dependent on the assumption that the number of colonies formed after dissociation and sampling is an accurate measure of the number of surviving cells in the spheroids. The fact that both techniques yielded similar results at all doses provides a high degree of confidence that errors were small.

Fertil and Malaise, (1981) and Deacon et al. (1985) suggested that intrinsic radiosensitivity of tumour cells measured by the surviving fraction at 2Gy ( $SF_2$ ), could play a critical role in tumour response to radiation treatment. However, Taghian et al. (1993) documented that the parameter  $SF_2$  is useful to discriminate between the sensitivity of different grades or types of histology *in vitro* but is not a predictor of the clinical outcome on an individual basis for malignant glioma. According to the categories of clinical radioresponsiveness illustrated by Deacon et al. (1984), glioma was placed in category E with an average  $SF_2$  value of 0.52 which was consistent with the  $SF_2$  value of 0.55 for monolayer cells and 0.83-0.9 for

spheroids constructed from UVW cells. These results were also in agreement with the results gained by Allalunis-Turner et al. (1990), who reported a wide range of intrinsic radiation sensitivity in different glioma cell lines, the most radiosensitive having an SF<sub>2</sub> of 0.15 and the most radioresistant having an SF<sub>2</sub> of 0.93.

Spheroids are more resistant to killing by ionizing radiation than monolayers. The increase in radiation resistance was confined largely to the shoulder of the radiation survival curve, implicating differences in cellular capacity to sustain and repair damage (Hinz and Dertinger, 1983). If at the time of irradiation the cells are out of the cell cycle and in a nonproliferative state, cells can be induced into proliferation at any time after the irradiation. If there is a time delay, repair of potentially lethal damage (PLD) is likely to occur. This process stops when the cells are induced into cycle, by induction of proliferation to form colonies. Recovery from PLD of noncycling cells in 9L rat gliosarcoma spheroids and monolayers was described by Rodriguez et al. (1988). They showed that spheroid cells were more resistant than monolayer cells and concluded that difference in time to recruit cells into the cell cycle, is responsible for this difference in radioresistance. The results obtained in this study are consistent with this interpretation.

## **Chapter 7**

### **Flow cytometric cell cycle analysis**

<b>7.1 Non-radioactive IUdR uptake studies</b>	136
7.1.1 Aims	136
<b>7.2 Introduction</b>	136
<b>7.3 Methods and materials</b>	138
7.3.1. Effect of IUdR concentration on incorporation in monolayer cells	138
7.3.2. Effect of IUdR concentration in spheroids	138
7.3.3 The effect of incubation time on IUdR uptake in monolayer cell cultures	139
7.3.4 The effect of spheroid size and incubation time on IUdR uptake	139
7.3.5 Statistical analysis	139
<b>7.4 Results</b>	140
7.4.1 IUdR concentration for monolayer studies	140
7.4.2 IUdR concentration for spheroid studies	140
7.4.3 IUdR uptake in monolayer cell cultures	141
7.4.4 The effect of spheroid size and incubation time on IUdR uptake	142
<b>7.5 Discussion</b>	147

## **Non-radioactive IUdR uptake studies**

### **7.1.1 Aims**

The aim of this set of experiments was to determine the suitable concentration of IUdR which was necessary for *in vitro* experiments as a basis for determination of the uptake of IUdR in cultured cells and spheroids by DNA analysis. We further wished to investigate the effect of incubation time on IUdR uptake in different cell cultures.

## **7.2 Introduction**

Knowledge of proliferation in human tumours can provide valuable information which may be used prognostically or diagnostically to select appropriate treatment scheduling. Cell kinetics studies have helped to elucidate the growth characteristics of various types of human brain tumours and to predict their biological malignancy (Hoshino and Wilson, 1979). Traditional methods to measure cell kinetics have involved the use of radioactive precursors of DNA, in particular tritiated thymidine, and autoradiography to visualize the incorporation of radionuclides into cells (Mayer and Connor, 1977; Kury and Carter 1965). However autoradiographic studies may require several months to complete and therefore the results are of limited value in supplementing treatment in individual patients. For this reason and because of the radiation hazard associated with  $^3\text{H}$ -thymidine, it has never become popular for measuring cell kinetics (Tannock, 1978).

An alternative technique uses flow cytometry to study the incorporation of bromodeoxyuridine (BUdR) relative to DNA content measured by propidium iodide (PI). Like thymidine and IUdR, BUdR is incorporated into DNA during S phase. Anti-BUdR antibody can be used

to measure the proportion of dividing cells. Advantages of flow cytometry over tritium autoradiography include speed, quantitative power, and ability to make several measurements simultaneously. Several studies have used flow cytometric techniques in the assessment of proliferative activity in brain tumours after the incorporation of IUdR or BUdR (Nishizaki et al., 1989; Assietti et al., 1990; Perez et al., 1995).

The flow cytometric technique has been adapted in the present study to measure the uptake of IUdR by UVW glioma cells under different conditions. The essence of the procedure is to label with IUdR by incubation *in vitro*. After fixation of the cells in ethanol, they are stained using a monoclonal antibody against IUdR that can be bound to a second antibody conjugated with FITC (fluorescein isothiocyanate). The cells are then counterstained with PI to measure the DNA content and analysed on the flow cytometer for red (DNA) and green (IUdR) fluorescence. The relative movement of the IUdR-labelled cells through the cell cycle was not measured in these experiments; the red fluorescence was used only to count the total number of cells and allow the calculation of the IUdR labelling index. Because of background fluorescence due to cellular debris, the technique should allow the estimation of proportions of cells in cell cycle phases with errors of approximately 10% (Dean et al., 1982; Haag et al., 1987).

## **7.3 Materials and methods**

### **7.3.1. Effect of IUdR concentration on incorporation in monolayer cells**

The uptake of IUdR was studied to measure the suitable concentration required for flow cytometric analysis. 5-iodo-2'-deoxyuridine (Sigma, Poole, Dorset) was dissolved in medium to prepare IUdR solutions ranging in concentration from 10nM to 100 $\mu$ M. The solutions were sterilised by filtration using 0.22 $\mu$ m mesh Millipore filters (Millipore, Molsheim, France). Monolayer cells in exponential phase were incubated with IUdR solutions after equilibrating with 5% CO<sub>2</sub>. The cells were incubated for one doubling time (44 hours) at 37°C. They were fixed and labelled with anti-BUdR antibody and PI according to the protocol described in section 4.5. The IUdR labelling index was calculated by expressing the number of nuclei incorporating IUdR as a percentage of all PI-labelled nuclei.

### **7.3.2. Effect of IUdR concentration on incorporation in spheroids**

The uptake of IUdR was studied using two different ranges of size of spheroid (300-400 $\mu$ m and 700-1000 $\mu$ m diameter). The flow cytometric procedure was as described for monolayer cells. Spheroids were cultured according to the protocol described in section 4.4. Spheroids were transferred from spinner flasks into 25cm<sup>2</sup> flasks coated with 1% (w/v) agar. After equilibrating with 5% CO<sub>2</sub>, the spheroids were incubated with different concentrations of IUdR for one doubling time (52 hours for UVW spheroids) at 37°C. Spheroids were washed several times in PBS and then disaggregated by treatment with 0.5 ml of PBS containing 0.25% trypsin and 1mM EDTA for 10 minutes at 37°C. Microscopic examination confirmed that the cell preparation was free from clumps. Labelling and counting was the same as for

monolayer cells.

### 7.3.3 The effect of incubation time on IUdR uptake in monolayer cell cultures

To find the effect of incubation time on IUdR uptake in monolayer cell cultures, cells in exponential and confluent cultures were incubated with 10 $\mu$ M of non-radiolabelled IUdR for one to three doubling times (44 to 132 hours). After washing several times with PBS, the cells were trypsinized and fixed by 70% (v/v) ice cold ethanol. The cells were labelled with anti-BUdR antibody according to the protocol described in section 4.5.

### 7.3.4 The effect of spheroid size and incubation time on IUdR uptake

Uptake of IUdR was studied using different sizes of spheroid (100-200 $\mu$ m and 700-1000 $\mu$ m diameter) and different incubation times to find the effect of incubation time on IUdR uptake in small and large spheroids by flow cytometry. Spheroids were transferred from spinner flasks to 25cm<sup>2</sup> flasks coated with 1% (v/v) agar. After equilibrating with 5% CO<sub>2</sub>, the spheroids were incubated with 100 $\mu$ M of cold IUdR for one to four volume doubling times (52 to 208 hours) at 37°C. The protocols for fixing and labelling were as described above.

### 7.3.5 Statistical analysis

The relationship between the IUdR labelling index and incubation time for each mode of cell culture was analysed by linear regression. The labelling indices after incubation for two or more doubling times were also compared on a pairwise basis with the labelling index after

one doubling time using Dunnett's test (Dunnett, 1955). Student's t test was used to compare labelling indices for different culture modes (exponentially-growing versus plateau phase monolayers and small versus large spheroids). In all cases a p value of less than 0.05 was considered significant.

## **7.4 Results**

### 7.4.1 IUdR concentration for monolayer studies

Figure 7.1 shows the percentage of labelled cells over the range of IUdR concentrations from 10nM to 100 $\mu$ M. A constant, maximum percentage of labelled cells was obtained at concentrations of 1 $\mu$ M or higher, and it was decided to use 10 $\mu$ M IUdR in the experiments which were designed to evaluate the effect of incubation time on labelling index. IUdR concentrations less than 0.1 $\mu$ M resulted in complete absence of staining with anti-BUdR antibodies.

### 7.4.2 IUdR concentration for spheroid studies

This study was undertaken to determine the amount of uptake of cold IUdR required for flow cytometry experiments with UVW multicellular spheroids. The incorporation of IUdR was studied after incubating for one doubling time over a range of IUdR concentration between 10nM to 100 $\mu$ M. Two sizes of spheroid (300-400 $\mu$ m and 700-1000 $\mu$ m diameter) were selected to examine the size-related effect of proliferative heterogeneity on IUdR uptake. The relationship between concentration of IUdR and incorporation is shown in Figure 7.2. In contrast to the results for monolayer cells, IUdR labelling did not reach a clearly defined

maximum for either of the size ranges of spheroids. However, the apparent labelling index at an IUdR concentration of 100 $\mu$ M was sufficiently high to be accurately determined. Also a concentration of 100 $\mu$ M was similar to the maximum levels occurring clinically. Therefore, it was decided to use this concentration for the experiments on the effect of incubation time. There was essentially no staining with anti-BUdR antibodies in spheroids for IUdR concentrations less than 0.1 $\mu$ M.

#### 7.4.3 IUdR uptake in monolayer cultures

The effect of proliferative heterogeneity on IUdR uptake was studied in exponential phase cells (low level heterogeneity) and confluent cells (higher level of heterogeneity). Cells were incubated with 10 $\mu$ M of IUdR for one to three doubling times. Figure 7.3 shows the IUdR labelling index in monolayer cells in exponential and plateau phases.

The labelling index for exponentially-growing cells remained constant ( $r=0.00$ ) and high (mean 97%) over the range of incubation times. In the case of confluent cells the labelling index increased with increasing incubation time ( $r=0.94$ ,  $p<0.001$ ), ranging from a mean of 61.5% (SE $\pm$ 1.7%) after one doubling time to 84.8% (SE $\pm$ 1.9%) after three doubling times. The linear regression equation relating labelling index (LI) and incubation time (T) in units of doubling times was  $LI = 50.1 + 11.5 T$ . Pairwise comparison of the groups showed that the labelling index after two and three doubling times was significantly higher than after one doubling time ( $p<0.05$ , Dunnett's test).

#### 7.4.4 The effect of spheroid size and incubation time on IUdR uptake

The relationship between the IUdR labelling index and incubation time is shown in Figure 7.4. The incorporation of IUdR into small spheroids (100-200 $\mu$ m) increased with increasing incubation time ( $r=0.77$ ,  $p<0.001$ ). The labelling index ranged from a mean of 76.5% (SE $\pm$ 1.9%) after one doubling time to 88.5% (SE $\pm$ 1.0%) after four doubling times. The linear regression equation relating labelling index (LI) and incubation time (T) in units of doubling times was  $LI = 72.8 + 4.0 T$ . Pairwise comparison of the groups showed that the labelling index after three and four doubling times was significantly higher than after one doubling time ( $p<0.05$ , Dunnett's test).

The labelling index for large spheroids (700-1000 $\mu$ m) also increased with increasing incubation time ( $r=0.82$ ,  $p<0.001$ ), but was significantly lower than for small spheroids for all incubation times ( $p<0.005$ , Student's t test). It ranged from a mean of 29% (SE $\pm$ 2.3%) after one doubling time to 51% (SE $\pm$ 4.3%) after four doubling times. The linear regression equation relating labelling index (LI) and incubation time (T) for large spheroids was  $LI = 21.5 + 7.8 T$ . Pairwise comparison of the groups again showed that the labelling index after three and four doubling times was significantly higher than after one doubling time ( $p<0.05$ , Dunnett's test).

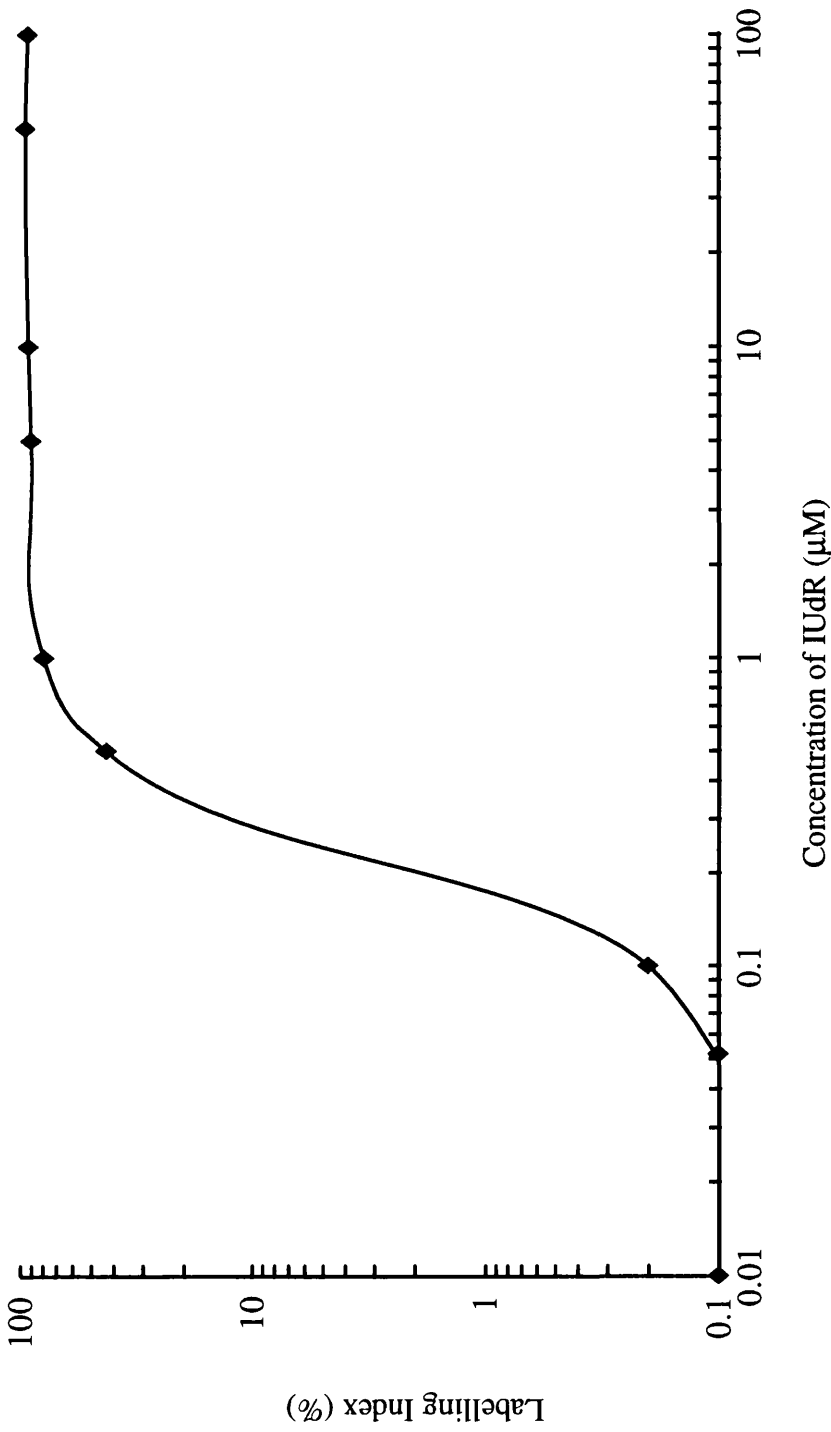


**Figure 7.1** Concentration dependence of IUdR uptake in exponentially growing UVW cells after incubation with a range of concentrations of IUdR (0.01-100µM).

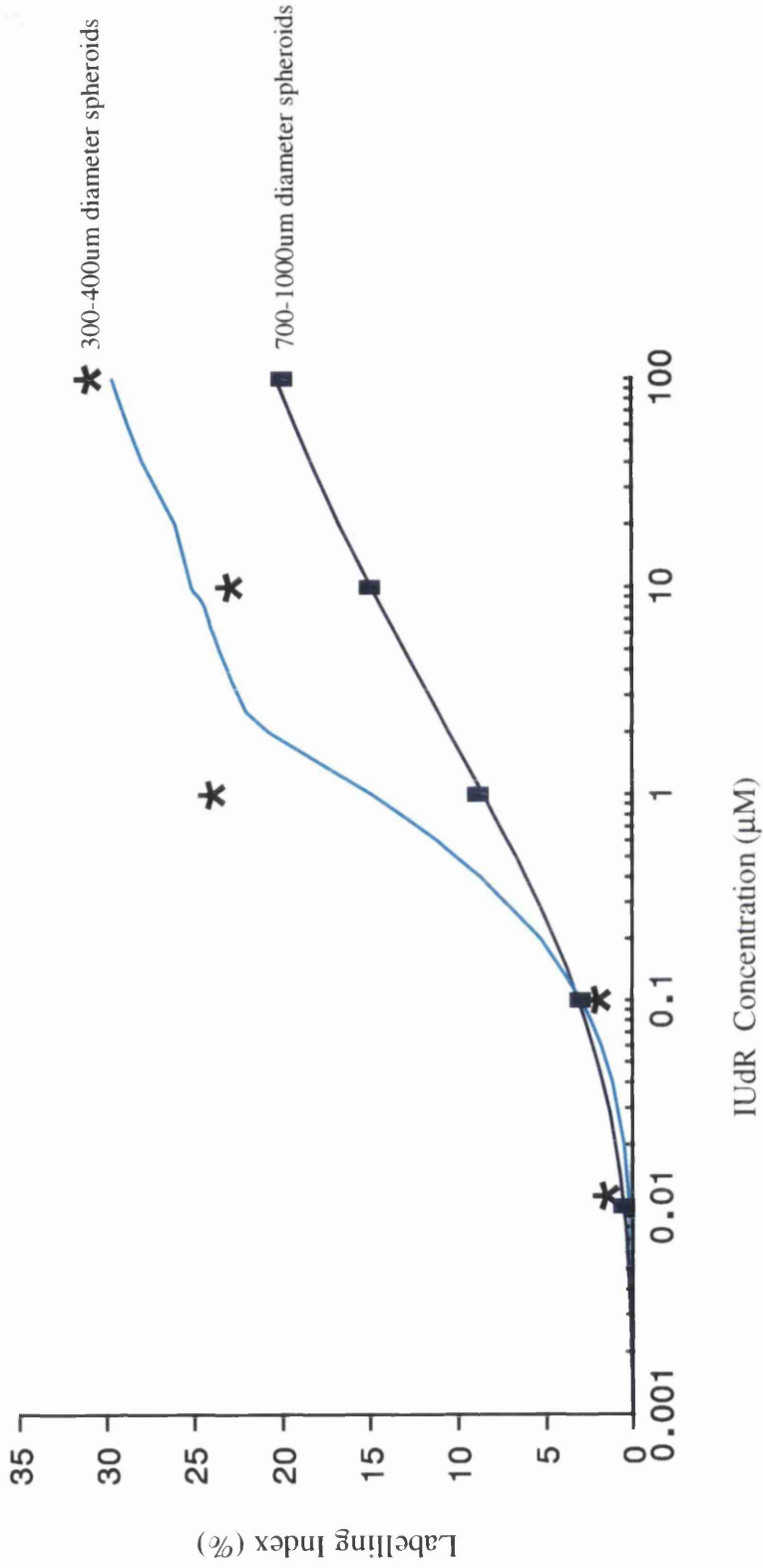


**Figure 7.2** Concentration dependence of IUdR uptake in spheroids of different size. IUdR exposure was for one volume doubling time in each case.

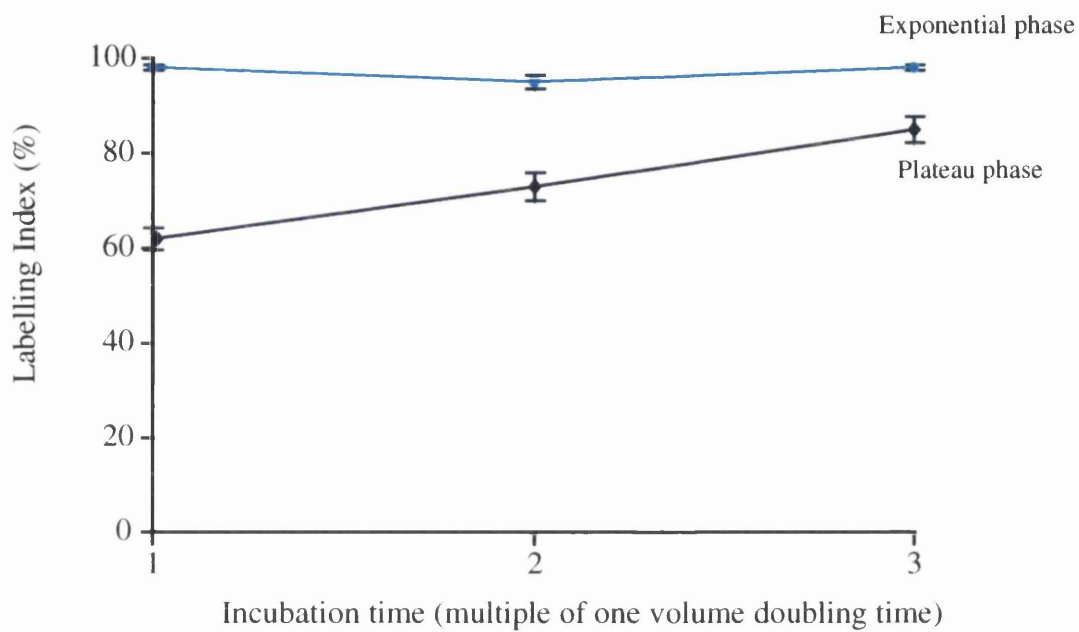


**Figure 7.3** Comparison between labelling index studied by flow cytometry of monolayers cells in exponential phase and plateau phase after one to three doubling times incubation. Bars show the means ( $\pm$  SEM ) of three separate experiments.

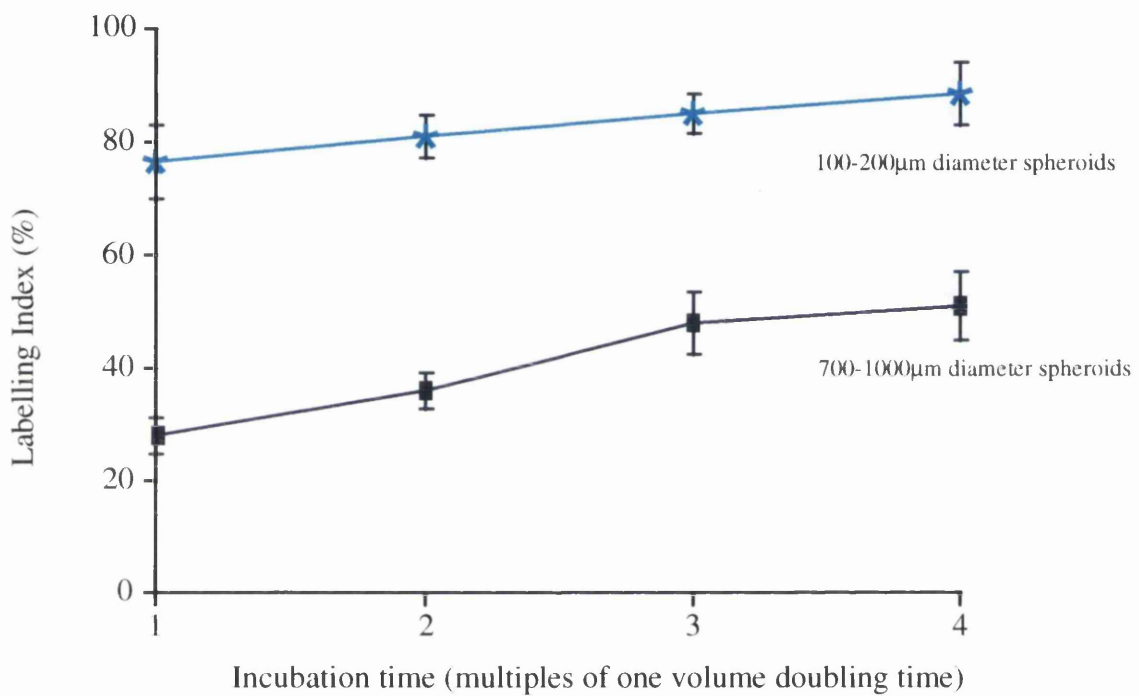


**Figure 7.4** Labelling indices of small and large spheroids after one to four volume doubling times incubation with 100µM of non-radiolabelled IUdR. Bars show the mean ( $\pm$  SEM ) of three separate experiments.

## 7.5 Discussion

The main purpose of these experiments was to investigate differences in uptake of IUdR for different modes of cell culture, and to determine the effect of prolonging the incubation time on overcoming any limitation on uptake imposed by proliferative heterogeneity. The results demonstrate that because of the insensitivity of antibody detection, it was necessary to determine the suitable concentration of non-radiolabelled IUdR required for measurement of the labelling index in different types of culture (monolayers and spheroids).

As shown in Figure 7.1, the IUdR labelling index in exponentially-growing monolayers achieved a maximum value of 97% at concentrations greater than  $1\mu\text{M}$ . By contrast, the labelling index in spheroids (Figure 7.2) continued to increase with IUdR concentration at least up to  $100\mu\text{M}$ . The reason for this difference is unclear. Possibly many cells in spheroids incorporate such a small proportion of the available IUdR that it falls below the threshold of detection by flow cytometry except at the highest concentration. It is possible that a higher labelling index would have been achieved by further increasing the concentration of IUdR. However, the purpose of these experiments was to find a suitable concentration for studying the effect of varying the incubation time, rather than the concentration yielding the maximum labelling index, and it was felt that  $100\mu\text{M}$  satisfied this purpose while remaining within a clinically realistic range.

IUdR is incorporated in DNA only during S-phase. Therefore a proportion of cells in which the cycle time exceeds the duration of incubation with IUdR would be expected to remain unlabelled with IUdR. In exponentially growing monolayers, the IUdR labelling indices were

unaffected by prolonged exposure to the drug (Figure 7.3). This suggests that few cells had a longer cycle time than the average, and hence that there is little heterogeneity in the duration of the cell cycle in monolayers.

Monolayers in plateau phase growth consist of cycling cells and cells in  $G_0$ . This *in vitro* model is intermediate in complexity between exponentially growing monolayers and spheroids, which contain proliferating cells, necrotic cells,  $G_0$  cells and cells which are poorly oxygenated and nutrient-deprived. The effect of increasing incubation time (one to three doubling times) on monolayers in plateau phase of growth was an increase in the percentage of labelled cells from 62 to 85% (Figure 7.3). This is probably due to cells in  $G_0$  phase reentering the proliferative cycle.

Whereas in monolayer culture more than 95% of exponentially growing cells and 62 percent of plateau phase cells were labelled with IUdR after one doubling time (Figure 7.3), the labelling index in the small spheroids (100-200 $\mu\text{m}$ ) was approximately 76% and for large spheroids (700-1000 $\mu\text{m}$ ) 28% after one volume doubling time incubation (Figure 7.4). The results of the study in which IUdR concentration was varied confirm that there is an inverse relationship between the proportion of cycling cells and spheroid diameter. The percentage of cells labelled by IUdR after 52 hours incubation was higher for small spheroids (300-400 $\mu\text{m}$ ) at concentrations of 10 $\mu\text{M}$  and 100 $\mu\text{M}$  than for large spheroids (700-1000 $\mu\text{m}$ ) (Figure 7.2). As spheroids increase in size, the peripheral, well nourished cells continue to divide but the interior cells, lacking nutrients, often exit the cell cycle and enter  $G_0$  or non-proliferating state (Olive and Durand, 1994). Therefore, it is expected that large spheroids will accumulate less IUdR due to the lower percentage of cells in S phase of the growth

cycle.

Increasing the period of incubation with IUdR from one to four volume doubling times increased the proportion of cells that incorporated IUdR in small and large sizes of spheroids. This probably resulted from IUdR incorporation into cells which are proliferating less rapidly; for example cells existing in the hypoxic and nutrient deprived regions of large spheroids.

Hence, relative to monolayer culture, UVW cells growing as spheroids manifest a reduction in division rate among cycling cells as well as a reduction in the proportion of cells in cycle. The reduction in proliferative activity may be due to several factors, such as accumulation of metabolic waste products and decreased availability of oxygen and nutrients in the interior of spheroids (Olive and Durand, 1994).

IUdR targeted radiotherapy will be successful only if it results in the sterilisation of all tumour cells. Therefore, strategies must be designed to overcome the limitations imposed by proliferative heterogeneity, the presence of  $G_0$  cells and cells cycling very slowly. Such variation in proliferation was observed in the spheroid model. These experiments clearly illustrated that increased time of incubation with IUdR allows the maximum number of potentially cycling cells to incorporate IUdR.

One of the disadvantages of flow cytometry, as applied clinically, is the requirement for disaggregation of tissue into single cell suspensions and the corresponding loss of ability to relate kinetic parameters to tissue architecture. The effects of spheroid size and incubation time on labelling index, measured by autoradiography, is described in chapter 8.

## **Chapter 8**

### **Incorporation of radiolabelled IUdR in glioma cells grown as monolayers and spheroids**

<b>8.1 Aims</b>	151
<b>8.2 Introduction</b>	151
<b>8.3 Methods and materials</b>	153
8.3.1 Spheroid growth and size determination	153
8.3.2 Uptake of [ <sup>125</sup> I]IUdR by UVW monolayer	153
8.3.3 Uptake of [ <sup>125</sup> I]IUdR by UVW spheroids	153
8.3.4 Ki67 staining	154
8.3.5 Autoradiography	155
8.3.6 Measurement of IUdR and Ki67 labelling indices	155
<b>8.4 Results</b>	157
<b>8.5 Discussion</b>	167

## 8.1 Aims

To examine the influence of proliferative heterogeneity and incubation time on cellular incorporation of [ $^{125}\text{I}$ ]IUdR.

## 8.2 Introduction

Although glioma does not metastasise to distant sites, it undergoes diffuse local spread and total surgical resection with a generous margin of adjacent normal tissue is rarely feasible. As discussed in Chapter 1, glioma is resistant to most cytotoxic drugs and, while some benefit has been reported with radiation treatment (Leibel et al., 1994), external beam radiotherapy is limited by normal tissue tolerance.

An alternative possibility is the therapeutic use of DNA-targeted Auger electron emitters such as  $^{123}\text{I}$  or  $^{125}\text{I}$ , bound to IUdR. Compared with non-radiolabelled cytotoxic drugs which are also thought to operate through interaction with DNA, radioiodinated IUdR may be, molecule for molecule, between 1000 and 100,000 times more potent (Humm and Charlton, 1989). The effectiveness of locoregional administration of this agent has been demonstrated in rodent models of gliosarcoma (Kassis, 1994), meningeal carcinoma (Kassis and Adelstein, 1996) and ovarian ascites (Baranowska-Kortylewicz et al., 1991). As few cells are proliferating in normal brain tissue, treatment with a proliferation-specific agent with high cytotoxic potency should be therapeutically beneficial.

Since IUdR is incorporated into the DNA only of those cells in S-phase, a major limitation to the efficacy of the radiopharmaceutical will be the presence of non-dividing cells in the targeted tumour. It is important that the effect of proliferative heterogeneity on IUdR

targeted therapy should be evaluated because theoretical calculation suggests that this could be the dominant factor in the efficacy of treatment (O'Donoghue and Wheldon, 1996). Multicellular tumour spheroids as previously described in section 2.4, are a well-established model of prevascular microtumours that provide a means of studying the intratumour distribution of therapeutic agents and of determining the effect of alternative schedules of administration on cellular incorporation.

In this chapter, an autoradiographic technique using [ $^{125}\text{I}$ ]IUdR is described as a means of studying IUdR incorporation at different times and depths within multicellular glioma spheroids of a range of sizes. Cellular uptake of IUdR was compared with labelling for the proliferation marker Ki67. These investigations have suggested strategies to overcome the incomplete sterilisation of tumour cells which would result from the administration of a single dose of IUdR incorporating an Auger electron emitter.

### **8.3 Materials and methods**

Cells were cultured as monolayers and as spheroids as described in section 4.1 and 4.4.

#### 8.3.1 Spheroid growth and size determination

Spheroid growth rate and size was determined as described in section 5.2.3.

#### 8.3.2 Uptake of [<sup>125</sup>I]IUdR by UVW monolayers

UVW cell monolayers in exponential growth were incubated in chamber slides with 0.06MBq/ml of no-carrier-added [<sup>125</sup>I]IUdR for 44 hours (the doubling time for exponentially growing cells). [<sup>125</sup>I]IUdR was prepared according to the method described in section 4.7.

After washing several times with PBS to remove unbound radioactivity, cells were fixed with 50% (v/v) methanol / 50% (v/v) acetone. Slides were then subjected to Ki67 labelling and autoradiography as described below.

#### 8.3.3 Uptake of [<sup>125</sup>I]IUdR by UVW spheroids

Cell aggregates of approximately 100 µm diameter, were transferred to spinner flasks containing 150 ml of medium. The contents of the vessels were equilibrated with a mixture of 5% CO<sub>2</sub> and 95% air for 3 min. The flasks were sealed and placed on a magnetic stirrer platform in a hot room at 37°C. Half of the medium was changed 3 times

per week. After 2-6 weeks of growth, spheroids of 150 $\mu$ m to 1000 $\mu$ m diameter were transferred from the spinner flask into 50 ml tubes, each containing 10 ml of medium with 0.06 MBq/ml of [<sup>125</sup>I]IUdR. Each tube contained 10-20 spheroids, depending on size.

After equilibration with 5% CO<sub>2</sub> the tubes were placed on a roller shaker (Luckham, Ltd, Sussex) and incubated at 37°C for either 52 or 104 hours, i.e. one or two multiples of the initial volume doubling time calculated as described in section 5.2.3. The spheroids were then washed several times in culture medium until no further soluble radioactivity could be eluted. They were embedded in mounting medium on cork discs, and frozen by cooling in liquid nitrogen. The time between the end of the incubation period and freezing was 120 min. Sections (5 $\mu$ m) were cut in a cryostat (Bright) at -20°C and thawed onto silanised slides. After drying at room temperature, the sections were stored desiccated at -20°C.

#### 8.3.4 Ki67 staining

Ki67 is a nuclear antigen expressed during the G<sub>1</sub>, S, G<sub>2</sub> and M phases of the cell cycle, but absent in the G<sub>0</sub> phase. Immunocytochemical staining for Ki67 was used to evaluate the growth fraction in monolayers and different size of spheroids.

The Ki67 antigen was labelled in spheroid sections and monolayers by a conventional 3-step streptavidin-biotin-peroxidase system. Sections were removed from storage, warmed to room temperature, and fixed in 1% (v/v) formaldehyde in PBS. After 3 x 10 min. washes in PBS, non-specific binding was blocked with PBS containing 25% (v/v) swine serum and 25% (v/v) human serum for 10 min. This was replaced by the primary

antibody (Dako, Ltd, UK) or non-immune rabbit immunoglobulins as a negative control, both diluted in PBS containing 10% (v/v) of each blocking serum. After one hour the primary antibody was washed off with 3 changes of PBS over 15 min., and the sections were incubated for 30 min with a 1:400 dilution of the secondary antibody, biotinylated swine anti-rabbit immunoglobulins (Dako, Ltd, UK), in the same diluent (initial concentrations are given in section 4.10). After 3 washes in PBS over 15 min., the sections were incubated with the streptavidin-biotin-peroxidase complex diluted in PBS for 30 min. After further washes in PBS, the peroxidase signal was developed with a 10 min. incubation in 0.05% (v/v) diaminobenzidine tetrahydrochloride containing 0.01% H<sub>2</sub>O<sub>2</sub> (v/v) in PBS.

#### 8.3.5 Autoradiography

Following Ki67 staining, slides were dipped in a 1:1 dilution of Kodak NTB-2 emulsion (Kodak, IBI Limited, England) in distilled water at 43°C. After drying, sections were exposed in light-proof desiccating boxes for 92 hours. Sections were developed in 1:1 dilution of Kodak D19 developer at 10°C for 4 min. After a brief wash in distilled water, the emulsion was fixed in Kodafix (Kodak, IBI Limited, England) for 5 min. The slides were washed and counterstained with haematoxylin before dehydration through graded ethanols before being mounted in DPX synthetic resin mountant (BDH Laboratory Supplies).

### 8.3.6 Measurement of IUdR and Ki67 labelling indices

Slides were examined using an Olympus BH<sub>2</sub> microscope and an Imaging Research MCID image analysis system. All measurements were performed in equatorial sections of spheroids, which were identified by examination of serial sections and selecting the section in which the apparent diameter was at a maximum. The diameter of each spheroid was estimated by taking the mean of the maximum and the perpendicular to the maximum diameter in the equatorial section. Only spheroids in which these orthogonal diameters differed by less than 10% were included in the analysis.

UVW glioma spheroids with a diameter  $\geq 300\mu\text{m}$  invariably showed a central core characterised by a complete absence of Ki67 and IUdR labelling, surrounded by an outer shell containing proliferating cells (Figure 2a), whereas those with a diameter of less than 250 microns had no quiescent core (Figure 2b). The diameter of the quiescent core, if present, was measured in an equatorial section in the same manner as the spheroid diameter.

A single observer classed cells as either labelled or unlabelled for IUdR and Ki67. Cells were deemed to be positive for IUdR labelling if there were 10 or more silver grains overlying the nucleus. IUdR and Ki67 labelling indices were measured by counting the number of labelled nuclei and expressing this as a percentage of the total number of nuclei in predefined regions of the spheroid sections. Both IUdR and Ki67 labelling indices were calculated for either the whole section (in the absence of a quiescent core) or the whole proliferating rim of tissue (in the presence of a core). We refer to these values as “total” labelling indices. Additionally, regional IUdR labelling indices were calculated for concentric tissue layers, consisting of an outer layer extending from the

surface of the spheroid to a depth of 25µm, a middle layer extending from 25µm to 50µm, and an inner layer extending from 50µm to 75µm from the surface. In the small number of sections in which the thickness of the proliferating rim was less than 75µm, the inner layer extended from 50µm to the edge of the quiescent core.

Differences between IUdR labelling indices for the two periods of incubation, and differences between Ki67 and IUdR labelling indices, were assessed by Student's unpaired t test and paired t test respectively.

#### 8.4 Results

UVW glioma monolayers in exponential growth showed a Ki67 labelling index of 93% ±0.65% (SE) and an IUdR labelling index of 91% ±1.29% (SE) (mean of 8 slide chambers). Figure 8.3.2 shows the total IUdR labelling index in spheroids after incubation for 52 and 104 hours, and the corresponding Ki67 index, as a function of spheroid diameter. All labelling indices decreased with increasing spheroid diameter. For spheroids of less than 300 µm diameter, there was no significant difference between the IUdR labelling indices for 52 and 104 hours incubation, whereas for larger spheroids the longer incubation time increased labelling. The Ki67 labelling index was greater than both IUdR labelling indices for all sizes of spheroids.

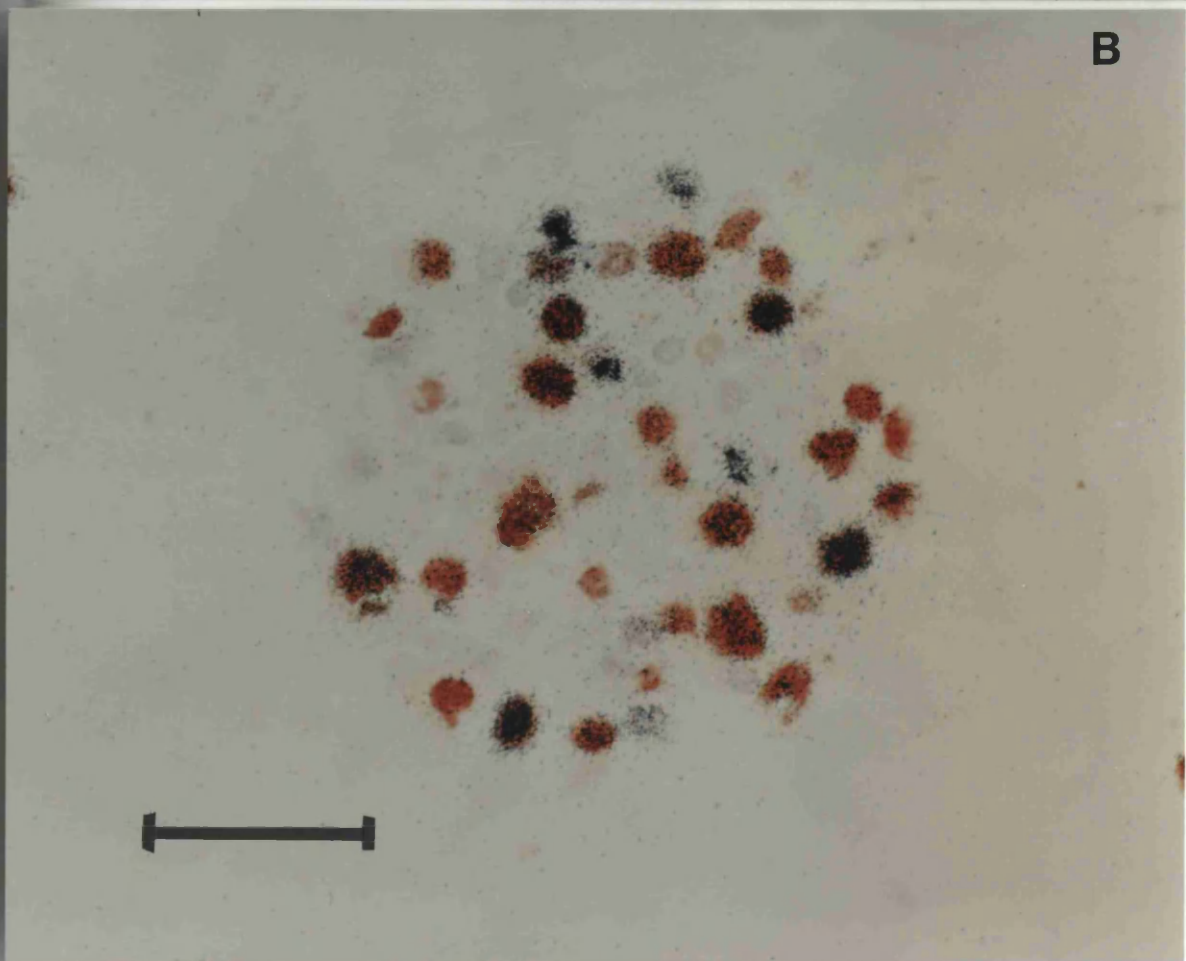
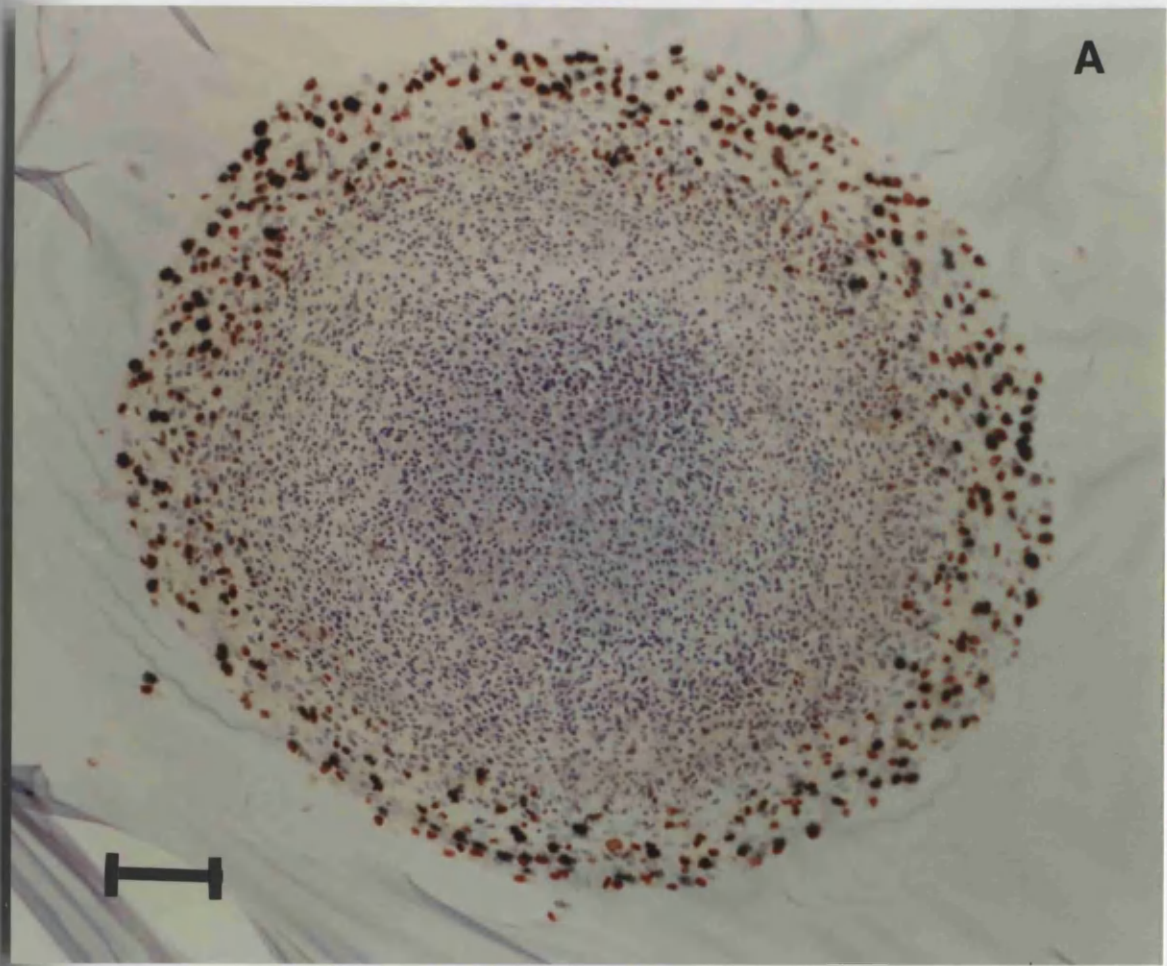
There were strong correlations between the Ki67 and IUdR labelling indices for both 52 and 104 hour incubations ( $r=0.95$ ,  $p<0.001$  and  $r=0.86$ ,  $p<0.001$  respectively) as shown in Figure 8.3.3. For the shorter period of incubation the relationship was  $LI_{IUdR} = 1.09 \times LI_{Ki67} - 21$ , and for the longer period  $LI_{IUdR} = 1.08 \times LI_{Ki67} - 12$ .

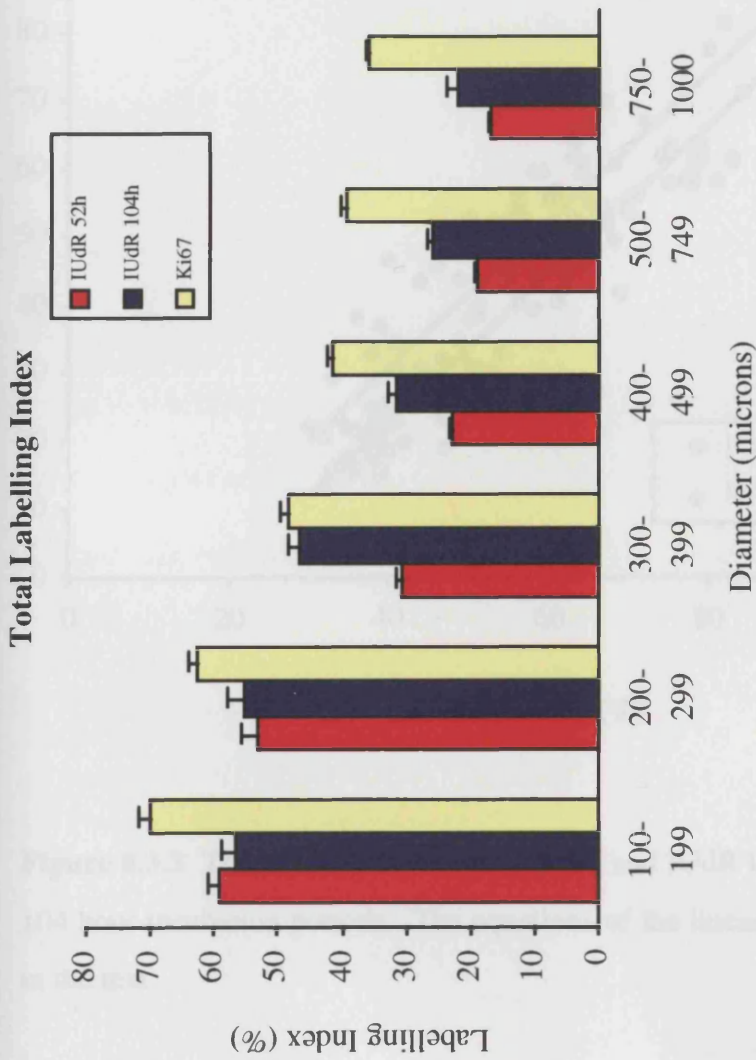
Figure 8.3.4 shows the IUdR labelling indices in each of the three 25 $\mu$ m layers as a function of spheroid diameter. The results can be summarised qualitatively as follows:

- a) For any given spheroid diameter, the labelling index decreased with increasing depth within the spheroids.
- b) The reduction in the labelling indices with increasing spheroid diameter occurred in all layers, but was more marked at depths greater than 25 $\mu$ m (middle and inner layers) than in the outer layer.
- c) The effect of increasing the IUdR incubation time was greatest in the middle and inner layers of 300-400  $\mu$ m diameter spheroids, where a doubling in the number of labelled cells was observed.

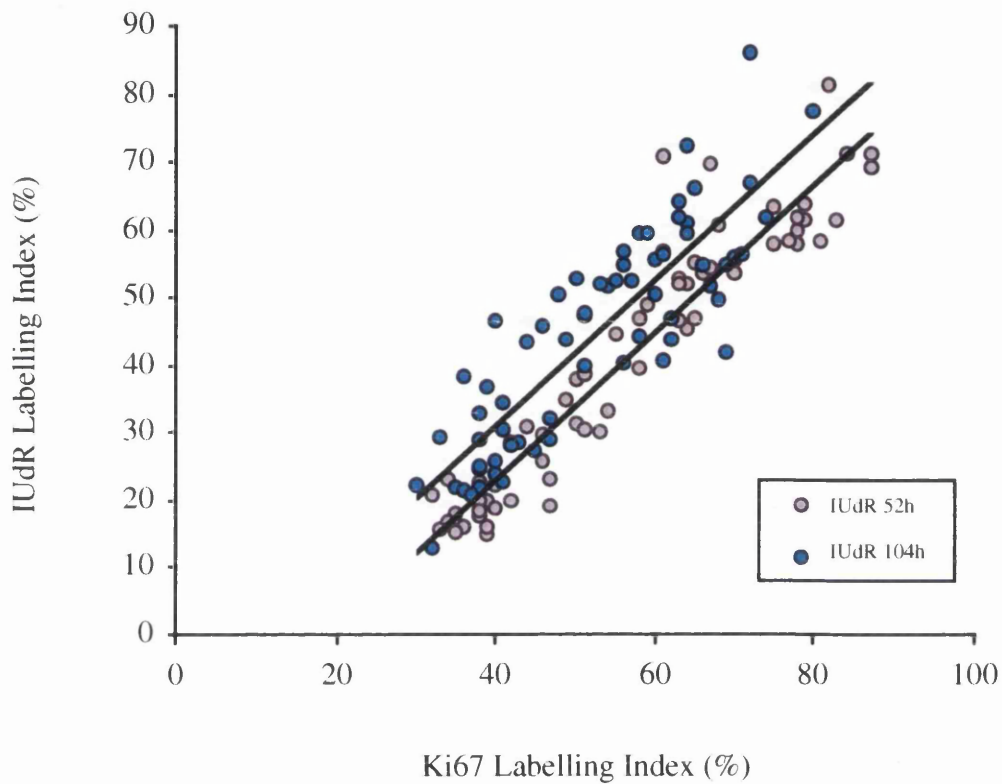
Even the highest regional IUdR labelling index (60-70%), achieved in the outer layer of small (<300  $\mu$ m)spheroids was substantially lower than the index achieved in monolayers.

Figure 8.3.1. Sections of (a) 1000  $\mu\text{m}$  diameter and (b) 250  $\mu\text{m}$  diameter spheroids, showing cells labelled with both Ki67 (brown stain) and IUdR (black grains) or with Ki67 alone, and unlabelled cells (haematoxylin counterstain). Scale bar = 100  $\mu\text{m}$ .





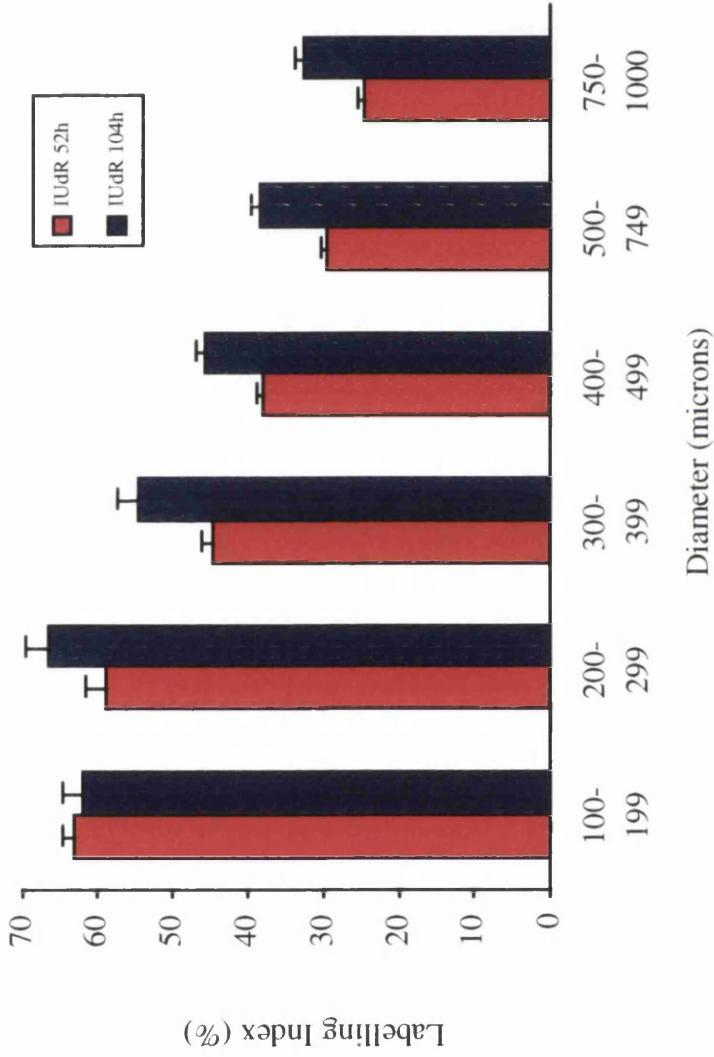
**Figure 8.3.2** Total Ki67 and IUDR (52 and 104 hours incubation) labelling indices in the viable rim of spheroids as a function of spheroid diameter. Bars show the mean and SEM for at least 6 spheroids in each size group for each period of incubation. There was a significant difference between the two IUDR labelling indices for each of the four largest size groups ( $p < 0.01$ , unpaired t test), but not for the two smallest groups ( $p > 0.05$ ). The Ki67 labelling index was significantly higher than both IUDR indices for all size groups ( $p \leq 0.01$ , paired t test), with the exception of 300-399 $\mu$ m diameter spheroids incubated with IUDR for 104 hours ( $p > 0.05$ ).



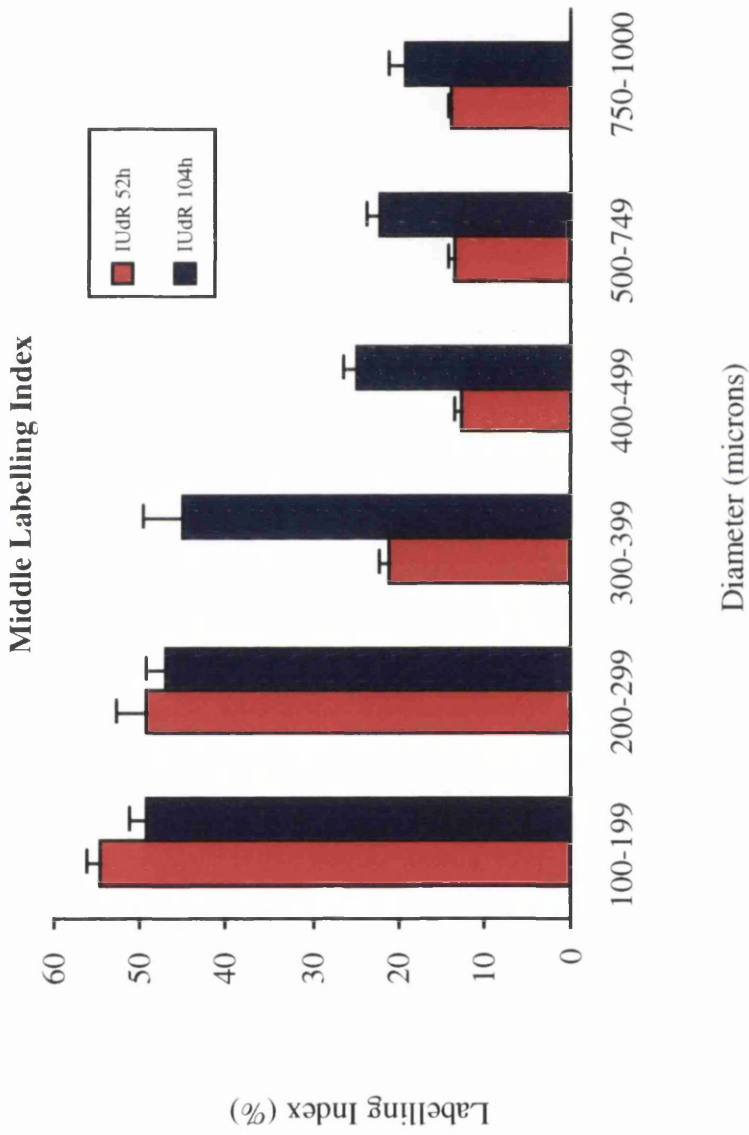
**Figure 8.3.3** The relationship between Ki67 and IUdR labelling indices for 52 and 104 hour incubation periods. The equations of the linear regression lines are given in the text.

Figure 8.3.4. Regional IUdR labelling indices for 52 and 104 hours incubation as a function of spheroid diameter in (a) outer, (b) middle and (c) inner 25 $\mu$ m cell layers. For the outer and middle layers, the two labelling indices were significantly different for each of the four largest size groups ( $p < 0.05$ , unpaired t test). For the inner layer, the difference was significant only for the size groups 300-399 $\mu$ m and 400-499 $\mu$ m ( $p \leq 0.01$ ).

Outer Labelling Index



**Figure 8.3.4 (a)** IUDR Labelling indices for the outer region of the tumour spheroids after 52 and 104 hours incubation as a function of spheroid diameter.



**Figure 8.3.4 (b)** IUDR Labelling indices for the middle region of the tumour spheroids after 52 and 104 hours incubation as a function of spheroid diameter.

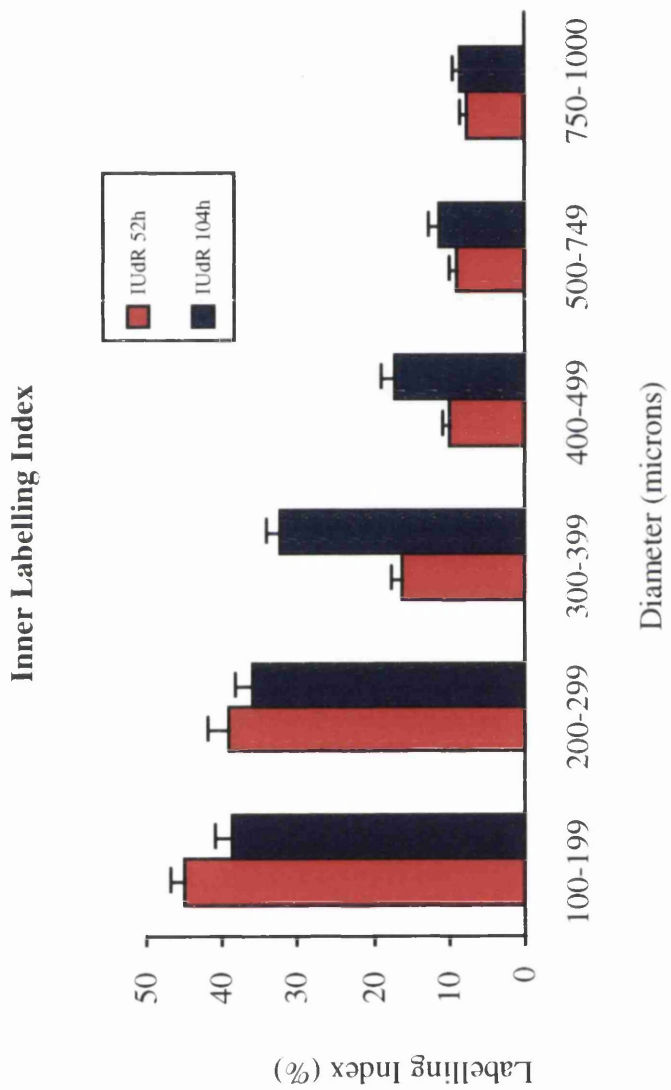


**Figure 8.3.4 (c)** IUDR Labelling indices for the inner region of the tumour spheroids after 52 and 104 hours incubation as a function of spheroid diameter.

## 8.5 Discussion

The purpose of this study was to assess the limitations to IUdR-targeted Auger electron therapy for glioma imposed by heterogeneity of cellular proliferation. The model chosen for this investigation was the human glioma cell line UVW cultured as multicellular spheroids. The growth characteristics of spheroids are similar to those of solid tumour nodules: composed of dividing cells close to the capillaries, adjacent non-proliferating cells and more distant necrotic regions (Carlsson and Nederman, 1989).

As has been observed for other cell lines (Wheldon et al., 1985; Olea et al., 1992), UVW glioma spheroids initially grew exponentially but then underwent a progressive reduction in growth rate, and this pattern showed a good fit to a Gompertzian equation as was shown in section 5.2.3. The spheroids developed a well-defined core in which Ki67 and IUdR labelling was completely absent, which was observed when they reached a diameter of 250-300 microns. In spheroids of numerous other cell types, it has been reported that central necrosis occurs at a distance of 50-300 microns from the periphery, depending on cell type and substrate concentrations in the media (Sutherland, 1988). Experiments in which cell layers were stripped progressively from spheroids suggest that the necrotic region is surrounded by cells with little or no proliferative activity and clonogenic capacity (Freyer and Sutherland, 1980). Although it is uncertain whether the core of large UVW spheroids contained cells that were necrotic, irreversibly damaged, merely quiescent or a combination of all of these, the fact that proliferation is confined to a superficial rim of cells is consistent with findings in other spheroid models.

The rim of proliferating tissue represented a decreasing proportion of total spheroid volume with increasing spheroid diameter, which partially accounts for the decreasing gradient of the spheroid growth curve. Other factors that may contribute to limitation of growth include reduced rates of cell division and increased cell death. It has recently been shown that a 3-dimensional cellular growth configuration is characterised by an enhanced tendency to apoptosis relative to monolayer cell culture (Rak et al., 1995). The relative contributions of these factors are of great importance to the potential efficacy and optimal mode of administration of cycle-specific therapy.

The results of the present study indicate that, in this model, there is an inverse relationship between the number of cycling cells, as assessed by Ki67 labelling, and spheroid diameter. Whereas in monolayer culture more than 90% of exponentially growing cells stained positively with Ki67, the growth fraction in the smallest spheroids studied was approximately 70% and this fraction decreased progressively with increasing spheroid size. For the largest spheroids, only 40 per cent of cells in the proliferating rim were cycling.

Ki67 labelling provides information about the proportion of cells in cycle, irrespective of phase, at the time of fixation, whereas IUdR is incorporated in DNA only during S-phase. Hence a proportion of any cells in which the cycle time exceeds the duration of incubation with IUdR would be expected to remain unlabelled with IUdR while still expressing the Ki67 antigen. In exponentially-growing monolayers, the IUdR and Ki67 labelling indices were essentially equal after incubation with IUdR for one doubling time. This suggests that few cells had a longer cycle time than the average, and hence that there is little heterogeneity in the duration of the cell cycle in monolayers.

IUdR labelling indices in spheroids after incubation for 52 hours (the doubling time of the initial monoexponential growth phase) were significantly lower than the corresponding Ki67 labelled fraction. This suggests that, of the cycling fraction of cells, a considerable proportion had a cycle time longer than 52 hours. Hence, relative to monolayer culture, UVW cells growing as spheroids manifest a reduction in division rate among cycling cells as well as a reduction in the proportion of cells in cycle. In addition, the present study demonstrates that IUdR incorporation is further reduced at depth within the proliferating region of spheroids relative to the superficial cell layers. Similar findings for radiolabelled thymidine incorporation were reported for spheroids derived from human breast carcinoma cell line MCF-7 (Olea et al., 1992). The reduction in proliferative activity with depth, and the complete absence of proliferation within the central core, may be due to several factors, including decreased availability of oxygen and nutrients, and accumulation of metabolic waste products, growth-inhibitory agents and hydrogen ions (Groebe & Mueller-Klieser, 1996).

Another factor that could, in principle, affect the spatial and temporal variation in labelling index is the rate at which IUdR penetrates the interior of spheroids. Thymidine, of which IUdR is an analogue, diffuses readily through cell membranes and has been shown to penetrate spheroids to a depth of 300  $\mu\text{m}$  within 1 min (Nederman et al., 1988). Another halogenated thymidine analogue, BUdR (bromodeoxyuridine), penetrated 390  $\mu\text{m}$  from the surface of human glioma fragments after 1 hour and achieved a maximum penetration of 0.8 mm (Morimura et al., 1991). It is therefore unlikely that limited penetration of IUdR was a significant factor in the present study in which we observed a gradient in labelling index within 75  $\mu\text{m}$  of the surface of spheroids after a minimum incubation period of 52 hours.

Increasing the period of incubation with IUdR from 52 to 104 hours increased the proportion of cells that incorporated IUdR in most size classes, although the IUdR labelling index remained lower than the corresponding index for Ki67. It is therefore likely that a higher uptake of IUdR could be achieved by further prolongation of the incubation time. This is particularly true for the treatment of cells which are proliferating less rapidly as exemplified by cells existing in the hypoxic and nutrient deprived regions of large spheroids.

The success of curative targeting strategies is governed by the ability to sterilise all clonogens. Therefore, therapeutic regimes must be designed to overcome the limitations imposed by proliferative heterogeneity, including the presence of viable tumour cells which are temporarily out of cycle or cycling very slowly. Such conditions were apparent using this spheroid model, in which substantial variation in proliferative fraction was observed. This study clearly demonstrates that increased time of incubation with IUdR partially overcomes this obstacle. The optimal benefit from radioiodinated IUdR therapy is likely to be obtained by prolonged exposure to the drug so that the maximum number of potentially cycling cells will incorporate the Auger emitter. Possible modes of delivery include multiple injection, slow release from biodegradable polymer implants (Whately et al., 1995) and continuous infusion via osmotic pumps. However, it is possible that practical limitations to the duration of therapy will preclude the targeting of every potential clonogen by IUdR therapy alone. Consequently, modification to this promising therapeutic approach must be considered, such as the use of radiohalogen conjugates with longer range emissions which may eradicate adjacent, untargeted cells by crossfire irradiation.

Theoretical considerations of proliferative heterogeneity imply that benefit may be obtained from use of both short-range and long-range emitters (e.g.  $^{123}\text{I}$  and  $^{131}\text{I}$ ) with external beam irradiation (O'Donoghue and Wheldon, 1996). The optimal strategy will depend on the magnitude and nature of the proliferative heterogeneity in the target tumour. The comparative cytotoxicity of short-range and long-range radionuclide conjugates of deoxyuridine is discussed in chapter 9.

## **Chapter 9**

**Differential cytotoxicity of alternative radioiodoanalogues of IUdR to human glioma cells in monolayer or spheroid cultures**

<b>9.1 Aims</b>	174
<b>9.2 Introduction</b>	174
<b>9.3 Materials and methods</b>	176
9.3.1 Synthesis of radiolabelled IUdR	176
9.3.2 Clonogenic assay	176
9.3.3 Incorporation of IUdR into DNA	176
9.3.4 Converting external activity to number of molecules	176
9.3.5 Statistical analysis	177
<b>9.4 Results</b>	177
9.4.1 Clonogenic Assay	177
9.4.1.1 UVW monolayer cells in exponential phase	177
9.4.1.2 UVW monolayer cells in plateau phase	178
9.4.1.3 UVW spheroids	179
9.4.2 Comparison of survival and labelling index	181
9.4.3 Incorporation of IUdR into DNA	182
<b>9.5 Discussion</b>	189

**9.1 Aims:** To compare the therapeutic potential of IUdR labelled with different radioisotopes ( $^{123}\text{I}$ ,  $^{125}\text{I}$  and  $^{131}\text{I}$ ) using glioma cells cultured as monolayers in exponential or plateau phase of growth and as spheroids.

## 9.2 Introduction

$^{123}\text{I}$  and  $^{125}\text{I}$  decay to emit highly radiotoxic Auger electrons whose effective range, in terms of DNA damage, is a few nanometers (Martin and Haseltine., 1981). In order to kill cells, these radionuclides must be incorporated into DNA (Kassis et al., 1987a) or be closely associated with it (Schwartz et al., 1996). Therefore IUdR, conjugated to radioiodine, has great potential as a radiotherapeutic agent which is capable of selectively targeting dividing cells. This cycle-specific treatment strategy is especially attractive for the elimination of malignant glioma cells because, when administered intracranially, IUdR should be toxic to the tumour but have no adverse effect on normal, quiescent tissue of the central nervous system (Kassis et al., 1990).

Several *in vitro* studies have demonstrated the exquisite toxicity of  $^{123}\text{I}$ - and  $^{125}\text{I}$ -iodinated IUdR to dividing cells (Hofer and Smith, 1975; Makrigiorgos et al., 1989; Schneiderman and Schneiderman, 1996) and the effectiveness of locoregional administration of this agent has been shown in rodent models of gliosarcoma (Kassis, 1994), meningeal carcinoma (Kassis and Adelstein, 1996) and ovarian ascites (Baranowska-Kortylewicz et al., 1991). Recently, the incorporation of IUdR in a range of human tumours has been reported (Mariani et al., 1996a; Kassis et al., 1996; Mariani et al., 1996b; Macapinlac et al., 1996; Daghighian et al., 1996).

A well-recognised limitation of treatment with IUdR labelled with Auger electron emitting radionuclides is the existence of a subpopulation of malignant cells which is not in the DNA synthetic phase of the cell cycle during the time of exposure to IUdR. Cells that fail to incorporate the IUdR into DNA will not be exposed to significant amounts of the highly localised energy deposition of Auger electrons. Possible means of overcoming this limitation include the use of prolonged or repeated exposures, and the use of other treatment modalities in combination with Auger electron therapy. One potential complementary therapeutic agent is the  $\beta$ -emitter [ $^{131}\text{I}$ ]IUdR. Although less cytotoxic to the targeted proliferation cells than [ $^{123}\text{I}$ ]IUdR or [ $^{125}\text{I}$ ]IUdR (Hofer and Hugues, 1971; Chan et al., 1976), the relatively long range of beta electrons results in the irradiation of neighbouring non-proliferating cells by the cross-fire or bystander effect (Wheldon and O'Donoghue 1997).

None of these investigations has directly addressed the limitation to efficacy of IUdR-targeted Auger electron therapy imposed by proliferative heterogeneity. Conventional *in vitro* cell monolayers do not exhibit the heterogeneity associated with solid tumours *in vivo*, but in the latter the study of cycle-specific effects is complicated by the separate issues of ensuring the delivery of the agent to all malignant cells and quantifying their exposure to it. An alternative model system is provided by tumour spheroids. The non-uniform uptake of IUdR by multi-cellular tumour spheroids and how this may be partially overcome by prolonged incubation has been described in Chapters 7 and 8. This chapter describes the limitation on cell killing by DNA-targeted Auger electron radiotherapy in spheroids resulting from proliferative heterogeneity, and evaluates the use of [ $^{131}\text{I}$ ]IUdR as a complementary or alternative treatment.

### **9.3 Materials and methods**

#### 9.3.1 Synthesis of radiolabelled IUdR

Radioiodinated (no-carrier-added) IUdR was prepared according to the method described in section 4.7.

#### 9.3.2 Clonogenic assay

The effect of radioiodinated IUdR was determined upon the clonogenicity of UVW cell cultures treated in exponential growth phase, in plateau growth phase and growing as multicellular spheroids as described in section 4.8.

#### 9.3.3 Incorporation of IUdR into DNA

Monolayer cells in exponential phase were incubated with a range of concentrations of [<sup>125</sup>I]IUdR (1.0 kBq/ml to 100 kBq/ml) for one doubling time (44 hours) at 37°C. Incorporation of [<sup>125</sup>I]IUdR into DNA was determined according to the procedure described in section 4.9.

#### 9.3.4 Converting radioactivity to number of radioactive atoms

The number of molecules of each radioisotope that produce a given quantity of radioactivity was calculated using the equations:

$$t_{1/2} = \ln 2 / \lambda$$

where  $t_{1/2}$  is the radioactive half life in seconds and  $\lambda$  is the decay constant, and

$$A = \lambda N$$

where A is the radioactivity in Bequerels and N is the number of molecules.

### 9.3.5 Statistical analysis

Cell survival for the three radiopharmaceuticals at a given concentration of radioactivity was compared using one-way analysis of variance together with Tukey's method for pairwise comparisons between groups, which corrects significance levels for multiple simultaneous comparisons. Statistical significance was assessed at the 5% level.

## **9.4 Results**

### 9.4.1 Clonogenic Assay

#### 9.4.1.1 UVW monolayer cells in exponential phase

The survival fraction of cells in exponential growth is plotted as a function of initial radioactive concentration in the medium for [<sup>125</sup>I]IUdR, [<sup>123</sup>I]IUdR and [<sup>131</sup>I]IUdR in Figure 9.1. The survival curves could be approximated by a monoexponential function of concentration (survival fraction =  $\exp[-C/C_{37}]$ , where C represents concentration of radioactivity in the medium) but may not be directly comparable with  $D_0$  expressed in absorbed dose units, as in conventional survival curves.  $C_{37}$  is a constant equal to the concentration at 37% clonogenic survival). The slope ( $1/C_{37}$ ) and  $C_{37}$  for each survival curve, derived from the fitted monoexponential function, are given in Table 9.1. In terms of concentration of radioactivity, [<sup>125</sup>I]IUdR was the most potent and [<sup>131</sup>I]IUdR the least potent of the three agents.

Radioisotope	Slope (ml/ kBq)	C <sub>37</sub> (kBq/ ml)
[ <sup>125</sup> I]IUdR	-0.423±0.018	2.36
[ <sup>123</sup> I]IUdR	-0.102±0.004	9.75
[ <sup>131</sup> I]IUdR	-0.053±0.006	18.9

**Table 9.1** Slope ( $\pm$ SE) and C<sub>37</sub> of survival curve of UVW monolayer cells in exponential growth incubated with radiolabelled IUdR for 44 hours.

Non-radioactive IUdR at a concentration of 1.2 nM, which is equivalent to the maximum molar concentration of radiolabelled IUdR employed in this study, was found to have no effect on cell survival as determined by the clonogenic assay. Incubation of UVW monolayer cells in Na<sup>125</sup>I or Na<sup>131</sup>I at a concentration of 100kBq/ml also did not result in any measurable change in survival (Figure 9.2).

#### 9.4.1.2 UVW monolayer cells in plateau phase

Figure 9.3 shows the survival fraction of monolayer cells in plateau phase following incubation with [<sup>125</sup>I]IUdR, [<sup>123</sup>I]IUdR, and [<sup>131</sup>I]IUdR. The survival curves consisted of two parts: an initial steep portion in which survival was dependent on concentration, and

a region where survival was effectively constant for all concentrations of radioactivity above a certain level. The Auger emitters [ $^{123}\text{I}$ ]IUdR and [ $^{125}\text{I}$ ]IUdR were more effective than [ $^{131}\text{I}$ ]IUdR over the whole range of concentrations, although only the differences between [ $^{123}\text{I}$ ]IUdR and [ $^{131}\text{I}$ ]IUdR at 5, 10 and 20 kBq/ml were statistically significant ( $p < 0.05$ ). [ $^{123}\text{I}$ ]IUdR appeared to be more effective than [ $^{125}\text{I}$ ]IUdR over the concentration range 5-40 kBq/ml, but the difference was not statistically significant at any concentration ( $p > 0.05$ ). A maximum of approximately 60% of cells were killed by [ $^{123}\text{I}$ ]IUdR and [ $^{125}\text{I}$ ]IUdR and 40% by [ $^{131}\text{I}$ ]IUdR.

#### 9.4.1.3 UVW spheroids

Figure 9.4 shows the survival curves of spheroids after incubation with [ $^{125}\text{I}$ ], [ $^{123}\text{I}$ ] and [ $^{131}\text{I}$ ]IUdR. Like the curves for plateau-phase monolayer cells, survival curves showed a dose-dependent region at low concentrations of all three radiopharmaceuticals, and a dose-independent region for high concentrations of [ $^{125}\text{I}$ ]IUdR and [ $^{123}\text{I}$ ]IUdR. However, at concentrations greater than 40 kBq/ml, the survival curve for [ $^{131}\text{I}$ ]IUdR continued to decline with a reduced gradient.

Both [ $^{125}\text{I}$ ]IUdR and [ $^{123}\text{I}$ ]IUdR were significantly more effective than [ $^{131}\text{I}$ ]IUdR at doses up to and including 20 kBq/ml ( $p < 0.05$ ). However, in contrast to the results for monolayers, the survival curve for [ $^{131}\text{I}$ ]IUdR crossed the curves for [ $^{125}\text{I}$ ]IUdR and [ $^{123}\text{I}$ ]IUdR, resulting in lower survival for [ $^{131}\text{I}$ ]IUdR than for the other radiopharmaceuticals at concentrations of 40 kBq/ml and above. This difference was statistically significant at 100 kBq/ml ( $p < 0.05$ ).

$[^{125}\text{I}]\text{IUdR}$  was more effective than  $[^{123}\text{I}]\text{IUdR}$  over the whole concentration range, and this was statistically significant at concentrations of 1, 20 and 100 kBq/ml ( $p < 0.05$ ). The initial slopes of the three survival curves were similar to those for exponentially growing monolayers (Table 9.2)

Figure 9.5 shows the survival curve of spheroids after incubation with  $[^{125}\text{I}]\text{IUdR}$  for 52 and 104 hours. Like the curve for spheroid cells after incubation with  $[^{125}\text{I}]\text{IUdR}$  for 52 hours, 104 hours survival curves showed a dose-dependent region at low concentrations and a dose-independent region for high concentrations of  $[^{125}\text{I}]\text{IUdR}$ . However, there was no significant difference in survival fraction at any concentration after 52 and 104 hours incubation.

Radioisotope	Initial slope (ml/kBq)
$[^{125}\text{I}]\text{IUdR}$	$-0.616 \pm 0.090$
$[^{123}\text{I}]\text{IUdR}$	$-0.096 \pm 0.009$
$[^{131}\text{I}]\text{IUdR}$	$-0.043 \pm 0.002$

**Table 9.2** Slope ( $\pm$ SEM) of the initial portion of the survival curves of the UVW spheroids incubated with radiolabelled IUdR for 52 hours.

#### 9.4.2 Comparison of survival and labelling index

The percentage of cells labelled by IUdR in the different conditions of culture as measured by flow cytometry or autoradiography, are compared with the percentage of cells killed by the three radiopharmaceuticals in Table 9.3. The percentage of cells killed by [<sup>125</sup>I]IUdR at the maximum concentration studied, as determined by the clonogenic assay, was of a similar magnitude to the labelling index as determined by flow cytometry for the corresponding conditions of culture. There was also good agreement between the labelling index and the percentage of monolayer cells killed by [<sup>123</sup>I]IUdR, although this radiopharmaceutical was somewhat less effective in spheroids than the flow cytometric labelling index would predict. [<sup>131</sup>I]IUdR killed a smaller percentage of cells in monolayer growth and a higher percentage in spheroids than were labelled with IUdR according to the flow cytometric measurements.

Culture phase	Labelling index (%) by flow cytometry	Labelling index (%) by auto-radiography	Maximum % cells killed <sup>125</sup> I	Maximum % cells killed <sup>123</sup> I	Maximum % cells killed <sup>131</sup> I
Exponential monolayer	97±1	91±1	98±1	96±1	91±1
Plateau monolayer	62±2	ND*	60±2	56±16	41±12
Spheroids	76±7	59.2±1.7	72±1	55±4	87±1

**Table 9.3** Comparison between labelling index studied by flow cytometry, autoradiography and cell killing by clonogenic assay (mean±SEM) at the maximum concentrations studied.

\* ND= Not determined

#### 9.4.3 Incorporation of IUdR into DNA

The uptake of [<sup>125</sup>I]IUdR into DNA was linearly related to the concentration of the agent in the medium over the range studied (Table 9.4).

Concentration of activity (kBq/ml)	DNA-associated activity per cell (mBq)
1.0	0.50±0.01
10	5.2±0.4
100	55.6±1.65

**Table 9.4** Uptake of [<sup>125</sup>I]IUdR into UVW cells in exponential monolayer growth (mean±SEM) for different concentrations of the radiopharmaceutical in the medium.

	<sup>125</sup> I	<sup>123</sup> I	<sup>131</sup> I
44 hour incubation (monolayer cultures)	1.00	0.26	0.91
52 hour incubation (spheroid culture)	1.00	0.21	0.90

**Table 9.5** Number of decays per cell for <sup>123</sup>I and <sup>131</sup>I relative to <sup>125</sup>I, integrated over incubation periods of 44 and 52 hours, given equal initial concentrations of radioactivity (in the form of radioiodinated IUdR) in the medium, calculated according to the formula derived by Makrigiorgos et al. (1989).

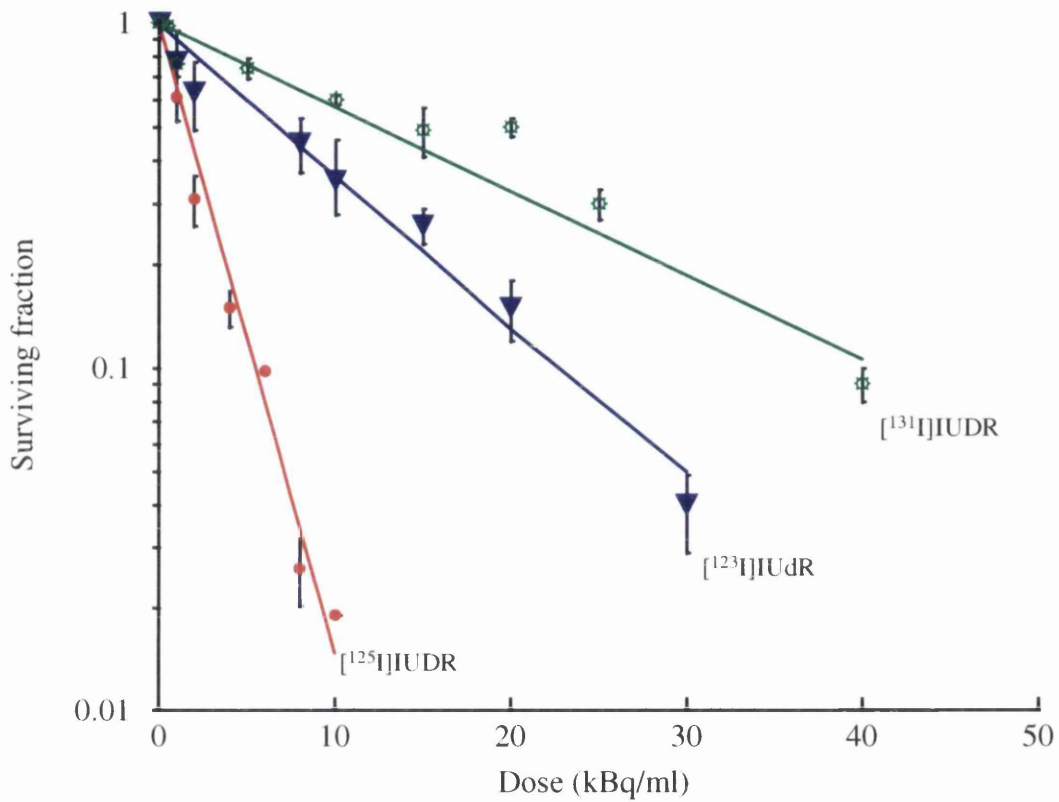


**Figure 9.1** Surviving fraction of UVW monolayer cells in exponential growth phase after incubation with [<sup>125</sup>I] IUDR , [<sup>123</sup>I] IUDR and [<sup>131</sup>I]IUDR. Each point represents the mean  $\pm$ SEM of three experiments.

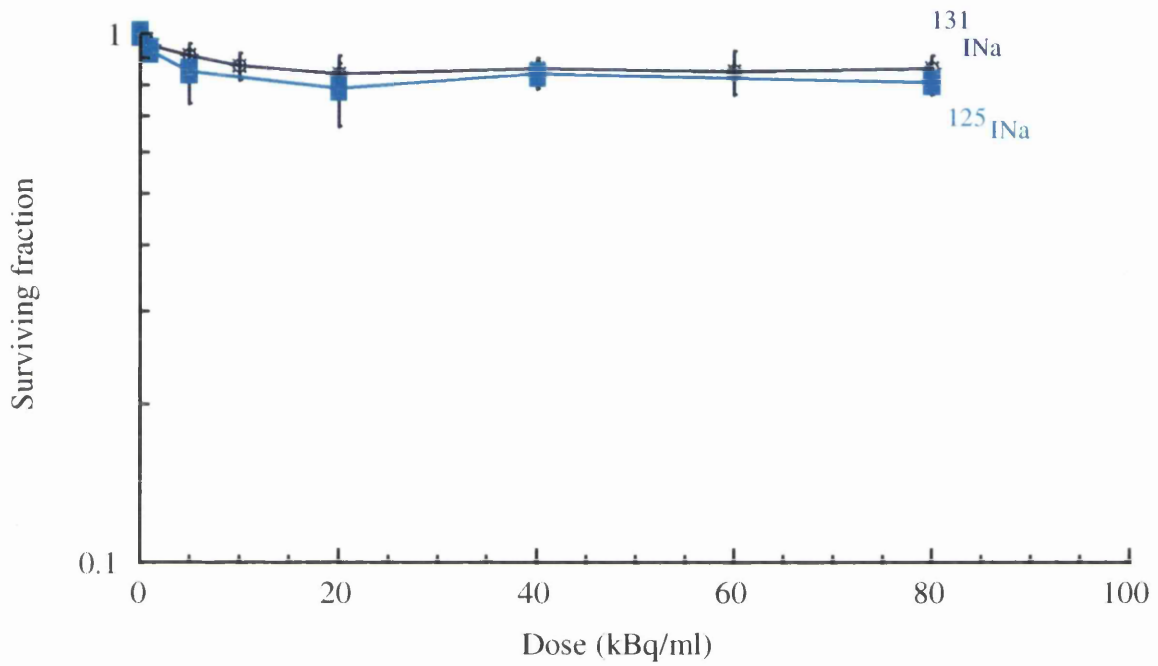


**Figure 9.2** Surviving fraction of UVW monolayer cells in exponential growth phase after incubation with Na[<sup>125</sup>I] and Na[<sup>131</sup>I]. Each point represent the mean  $\pm$ SEM of three experiments.

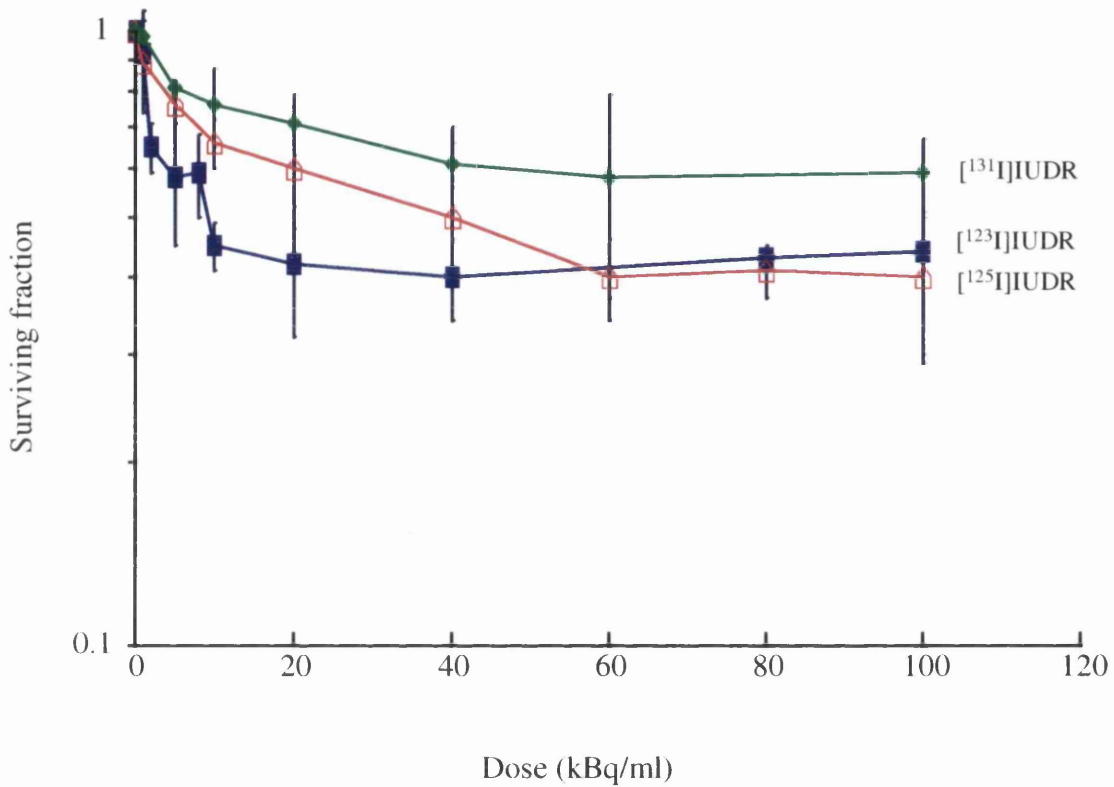


**Figure 9.3** Surviving fraction of UVW monolayer cells in plateau growth phase after incubation with [<sup>125</sup>I] IUDR , [<sup>123</sup>I] IUDR and [<sup>131</sup>I]IUDR. Each point presents the mean  $\pm$ SEM of three experiment

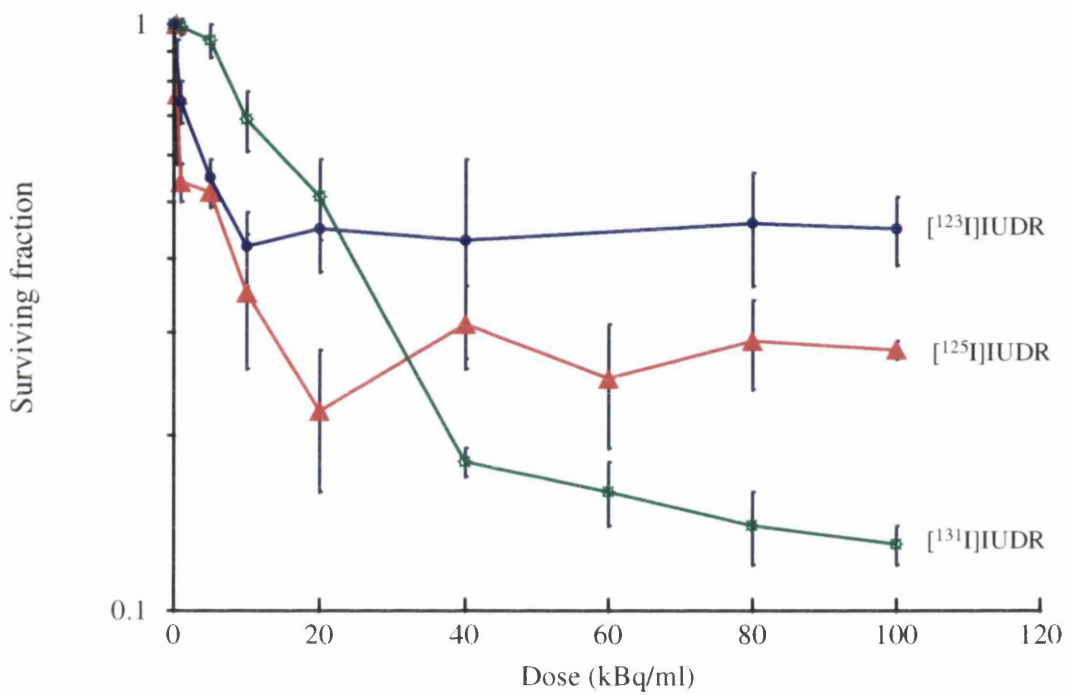


**Figure 9.4** Surviving fraction of UVW spheroids after incubation with  $[^{125}\text{I}]$ IUdR,  $[^{123}\text{I}]$  IUdR and  $[^{131}\text{I}]$ IUdR. Each point represents the mean  $\pm$ SEM of three experiments.

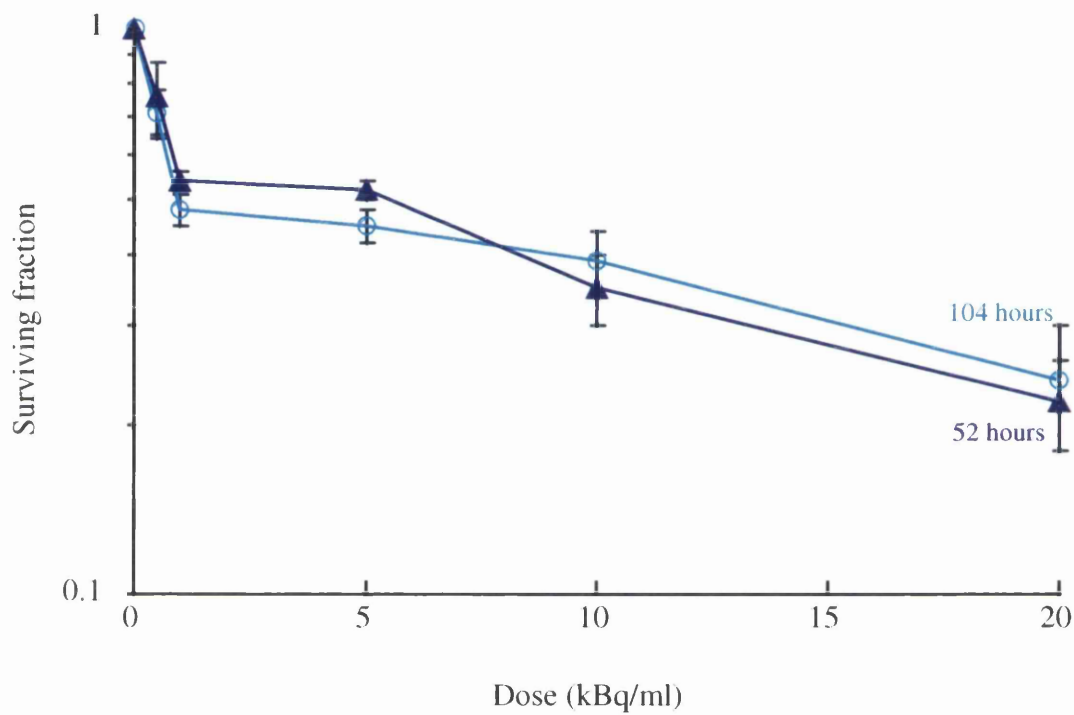


**Figure 9.5** Surviving fraction of spheroids after 52 and 104 hours incubation with  $[^{125}\text{I}]\text{IUdR}$ . Each point represents the mean  $\pm$ SEM of three experiments.

## 9.5 Discussion

The local administration of  $^{125}\text{I}$ - or  $^{123}\text{I}$ -labelled IUdR for DNA-targeted therapy of glioma, is a potential means for the selective eradication of residual malignant cells following surgical resection. However, due to the extremely short range of the Auger electrons emitted by  $^{125}\text{I}$  or  $^{123}\text{I}$ , only those tumour cells which are engaged in DNA synthesis during the time of exposure to the radiopharmaceutical will be sterilised. Accordingly, strategies must be devised which are capable of overcoming the limitations imposed by proliferative heterogeneity (Neshastehriz et al., 1997). In this study, we have assessed the relative efficacies of three radioiodoconjugates of deoxyuridine: two ultra-short range Auger electron emitters ( $^{125}\text{I}$  and  $^{123}\text{I}$ ) and one long-range  $\beta$ -emitter ( $^{131}\text{I}$ ).

The results of the toxicity studies have been expressed in terms of the initial concentration of radioactivity in the culture medium, rather than the number of radioactive decays per cell from DNA-incorporated IUdR. The justification for this approach is that the initial concentration is directly measured and is a readily-understood variable in a clinical context. The number of decays per cell is important for microdosimetry calculations, but this was not the aim of this study. Furthermore, it is clear from the autoradiographic studies of IUdR incorporation in spheroids (Chapter 8), that the incorporated radioactivity is highly variable from cell to cell in this mode of culture, which reduces the utility of an average value for quantitative microdosimetric purposes. However, to estimate the relative number of decays per cell for the three radioisotopes for the purpose of comparison with other studies, the formula derived by Makrigiorgos et al. (1989), may be used:

$$\text{Cumulative number of decays per cell} = kC_0[1-(1+\lambda T)e^{-\lambda T}]/\lambda^2$$

where  $k$  is a constant representing the rate of uptake of radioactivity into cells relative to the concentration in the medium,  $C_0$  is the initial concentration of extracellular radioactivity,  $\lambda$  is the physical decay constant for the radionuclide in question, and  $T$  is the incubation period. This formula assumes that the rate of incorporation of IUdR is proportional to concentration and is linear with time over the incubation period. It does not include decays after the end of incubation. Table 9.5 shows the relative number of decays for the three radioisotopes according to this formula for incubation periods of 44 and 52 hours, given equal initial concentrations of radioactivity in the medium.

In exponentially-growing UVW monolayers, incorporation of [ $^{125}\text{I}$ ]IUdR was directly proportional to extracellular concentration, which is consistent with the findings of other authors (Kassis et al., 1987b; Makrigiorgos et al., 1989). All three agents yielded exponential survival curves with no evidence of a shoulder. For [ $^{125}\text{I}$ ]IUdR and [ $^{123}\text{I}$ ]IUdR this is also consistent with previous studies (Kassis et al., 1987b; Makrigiorgos et al., 1989; Schneiderman and Schneiderman, 1996), although [ $^{131}\text{I}$ ]IUdR has been reported to produce a curve with a shoulder in other cell lines (Hofer and Hughes, 1971; Chan et al., 1976). This may reflect differences in the efficacy of DNA repair mechanisms in different cell lines and under different experimental conditions.

The initial concentration of radioactivity required to achieve a given level of cell kill was approximately four times greater for  $^{123}\text{I}$  than  $^{125}\text{I}$ . However, the cumulative number of radioactive decays per cell for DNA-incorporated IUdR, as estimated by applying the decay correction factor of 0.26 (Table 9.5), was approximately equal for the two Auger electron emitters. In Chinese hamster V79 lung fibroblasts, Makrigiorgos et al. (1989)

observed a twofold difference in cytotoxic efficacy (on the basis of decays per cell), in favour of [ $^{125}\text{I}$ ]IUdR for the same two radioiodinated drugs. It is again possible that the different result in the present study is related to differences in the cell lines, incubation periods and other experimental variables.

The radioactive concentration required to reduce cellular survival to 37% was eight times larger for  $^{131}\text{I}$  than for  $^{125}\text{I}$  in exponentially growing monolayers. This is comparable with the elevenfold difference in effectiveness for these agents previously reported in L1210 lymphoid leukaemia cells (Hofer and Hughes, 1971) and Chinese hamster V79 lung fibroblasts (Chan et al., 1976). The superiority of  $^{125}\text{I}$  and  $^{123}\text{I}$  relative to  $^{131}\text{I}$  for the treatment of rapidly-proliferating single cells is due to the short range of the Auger electrons and their efficient absorption in the nuclei of single cells.

Using Tables 9.1 and 9.4, the estimated decay-corrected activity per cell corresponding to a 37% survival level ( $C_{37}$ ) was 1.3, 5.4 and 10.4 mBq/cell for [ $^{125}\text{I}$ ]IUdR, [ $^{123}\text{I}$ ]IUdR and [ $^{131}\text{I}$ ]IUdR respectively. The number of IUdR molecules that would be incorporated through the salvage pathway into DNA, calculated by using the equations described in section 9.3.4 from  $C_{37}$ , were 9785, 371 and 10448 molecules per cell for [ $^{125}\text{I}$ ]IUdR, [ $^{123}\text{I}$ ]IUdR and [ $^{131}\text{I}$ ]IUdR respectively. This may be compared with the values of 3915 and 356 molecules per cell for [ $^{125}\text{I}$ ]IUdR and [ $^{123}\text{I}$ ]IUdR in Chinese hamster ovary (CHO) cells obtained by Schneiderman and Schneiderman (1996). No saturation was observed in the cytotoxicity of the three agents in rapidly-proliferating monolayer cells, and it was possible to achieve a cell kill of greater than 90% by administration of a sufficiently high dose of radiopharmaceutical. This is in agreement with the BrdU labelling index as determined by flow cytometry and autoradiography described in Chapters 7 and 8

respectively which indicates that almost all cells in these conditions are in cycle and capable of incorporating the agent during DNA synthesis. However, under more clinically realistic conditions of tumour cell growth, the situation is more complex: a proportion of cells may be out of cycle or not actively involved in DNA synthesis during the period of exposure to IUdR, and this would be expected to limit the efficacy of DNA-targeted Auger electron emitters. The results in plateau phase monolayers and in spheroids support this prediction.

As was previously discussed, monolayers in plateau phase growth consist of cycling cells and cells in  $G_0$ . This *in vitro* model is intermediate in complexity between exponentially-growing monolayers (composed almost entirely of dividing cells) and spheroids, which contain proliferating cells, necrotic cells,  $G_0$  cells and cells which are poorly oxygenated and nutrient-deprived. In the treatment of confluent UVW monolayers in plateau phase of growth, the effectiveness of all three radioiodoanalogues of IUdR was attenuated by the presence of non-cycling cells. The percentage of cells killed increased with the concentration of each agent up to a maximum of approximately 60% in the case of the Auger electron emitter conjugates, and 40% in the case of [ $^{131}\text{I}$ ]IUdR. The cell kill for the more potent agents corresponded closely with the labelling index determined by flow cytometry, supporting the concept of the lethality of DNA incorporation of Auger electron emitters.

In the spheroid model, both [ $^{125}\text{I}$ ]IUdR and [ $^{123}\text{I}$ ]IUdR showed a strongly dose-dependent effect at low concentrations, but their cytotoxicity reached a maximum of approximately

55-70%, and did not further increase at activity concentrations greater than 40 kBq/ml. This confirms that only a proportion of cells in this growth model are vulnerable to sterilisation by Auger electrons. There was a small but statistically significant difference in clonogenic survival between spheroids exposed to high concentrations (>40 kBq/ml) of [<sup>125</sup>I]IUdR and [<sup>123</sup>I]IUdR. Even allowing for the expected fivefold difference in the number of decays per cell (Table 9.5), [<sup>125</sup>I]IUdR at an extracellular concentration of 20 kBq/ml was more effective than [<sup>123</sup>I]IUdR at 100 kBq/ml. Hence, the difference in survival is difficult to explain if it is assumed that all cells that incorporate a significant fraction of the available activity for either agent at the highest concentration are killed. Closer agreement was observed between the labelling index as measured by flow cytometry and autoradiography in spheroids and the proportion of cells killed by [<sup>125</sup>I]IUdR than by [<sup>123</sup>I]IUdR, suggesting that some factor may be limiting the cytotoxic effect of the latter agent in this model.

In contrast to the Auger emitters, [<sup>131</sup>I]IUdR was progressively more toxic at increasing doses in the spheroid model. This is consistent with microdosimetric expectations: whereas most of the decay energy of <sup>131</sup>I incorporated in monolayers is dissipated above and below the plane of the cells,  $\beta$ -radiation cross-fire is effective in cellular aggregates. Hence, in addition to DNA-synthesising cells, adjacent non-cycling cells suffer the effects of  $\beta$ -decay energy. The fact that the steepest part of the survival curve for [<sup>131</sup>I]IUdR occurred at low concentrations, suggests that its cytotoxic effect on cycling cells outweighs its effect on non-cycling cells within the range of concentrations studied, although it is likely that higher concentrations of [<sup>131</sup>I]IUdR would prove more effective in killing non-cycling cells within spheroids.

It is clear that there are major differences in the shape of survival curves for cells in spheroid culture following exposure to the different forms of radioiodinated IUdR and to external beam irradiation (Chapter 6). These differences are broadly in accordance with the expected effect of the different types of radiation involved. Although spheroids were more resistant than monolayers to external beam treatment, the survival curves in both cases had a classical linear-quadratic form, and there was no evidence of a lower limit to cell survival at increasing doses. By contrast, the response of spheroid cells to radioiodinated IUdR was sharply differentiated both from that of monolayers exposed to the same agent and from that of spheroids subjected to gamma irradiation. The Auger electron emitters [<sup>125</sup>I]IUdR and [<sup>123</sup>I]IUdR, as expected, were capable of sterilising only the cells undergoing DNA synthesis during the period of incubation, while the [<sup>131</sup>I]IUdR survival curve at high concentrations showed a decline consistent with a cross-fire effect which was absent from the curves for [<sup>125</sup>I]IUdR and [<sup>123</sup>I]IUdR.

The absorbed fraction of decay energy of <sup>131</sup>I (0.11 g Gy/MBq/h), uniformly distributed in tissue spheres of 100µm diameter, has been calculated to be approximately 10% (O'Donoghue et al., 1995). If the average rate of uptake of IUdR by cells in spheroids were the same as in monolayers (Table 9.4), and assuming a cellular density of 5×10<sup>8</sup> cells per gram, the cross-fire radiation dose to spheroids during incubation with [<sup>131</sup>I]IUdR at a concentration of 100 kBq/ml would be approximately 8 Gy. This gives a surviving fraction of 0.13 (see Figure 9.4). The true average rate of uptake of IUdR by cells in spheroids would be substantially smaller in spheroids than in monolayers because of the presence of non-cycling and slowly-cycling cells, and, because of the highly non-uniform distribution of radioactivity, the radiation dose to individual cells is likely to vary

considerably. Also, the radiation from  $^{131}\text{I}$  is given at low dose rate over one volume doubling time (52 hours) incubation. For comparison the external beam radiation dose to achieve a surviving fraction of 0.13 in UVW spheroids is approximately 6 Gy (see Figure 6.4). Therefore, the calculation dose from [ $^{131}\text{I}$ ]IUdR is in reasonable agreement with the external beam studies.

No significant difference was observed in the survival fraction of spheroids after one or two volume doubling times incubation with [ $^{125}\text{I}$ ]IUdR. This is consistent with the result obtained by autoradiography for the small size of spheroids described in Chapter 8. The labelling index as measured by flow cytometry over an extended range of incubation times showed a small enhancement, which would correspond to a predicted difference in survival fraction of approximately 4% in the present experiment. This small difference is within the confidence limits of the results of this study. The effects of prolonging the incubation time on the labelling index in different sizes of spheroid suggests that a limited increase in cell killing by [ $^{125}\text{I}$ ]IUdR or [ $^{123}\text{I}$ ]IUdR could be achieved by extending the period of exposure, particularly for larger spheroids (Chapters 7 and 8). However, the small gradients of the labelling index versus time curves suggests that 100% sterilisation of cells in spheroid culture is not realistically achievable by Auger electron emitters alone.

It is possible that the maximal therapeutic benefit may be derived from the use of 'cocktails' of radioiodoconjugates of IUdR including both Auger electrons to kill cycling cells and the  $\beta$ -emitter  $^{131}\text{I}$ , at sufficiently high activity, to eliminate untargeted cells by cross fire. Nevertheless, the optimum agent or combination of agents for targeted

radiotherapy of gliomas *in vivo* depends on several factors in addition to those addressed in this study. These include whether the number of molecules of the radiopharmaceutical that can be incorporated into tumour cells is a limiting factor, rather than the quantity of radioactivity. The former would favour the use of  $^{123}\text{I}$  rather than  $^{125}\text{I}$  since, in terms of the number of atoms incorporated per cell to induce a given reduction in clonogenic survival, it was many times more effective. By contrast, at equal activities, the longer-lived radioisotope,  $^{125}\text{I}$ , was superior. Other factors that would influence the choice of radioactive atom include the uptake of radiopharmaceutical by critical normal organs as well as rates of deiodination and escape from the intracranial space to the circulation. The short half life of  $^{123}\text{I}$  is a further advantage in this respect. The effects of some of these variables is currently being investigated by researchers in the Department of Radiation Oncology using an *in vivo* glioma model system.

## **Chapter 10**

### **Conclusions and future work**

## Conclusions

Malignant glioma account for approximately 40% of all central nervous system malignancies. These are essentially localized neoplastic tumours that have to date defied most treatments and despite improved techniques, surgery has been shown to be unlikely to prolong patient survival. Unfortunately the tumour is also resistant to most cytotoxic drugs and while some benefit has been reported with radiation treatment, external beam radiotherapy is limited by normal tissue intolerance.

Due to fundamental problems such as limitation of current diagnostic techniques, localisation of malignant glioma and difficulty of total removal or effective sterilization of the tumour, the prognosis for patients has not improved greatly in the last 15 years. This low median survival of patients, motivates the search for alternative diagnostic procedures and treatment modalities that will allow selective killing of glioma cells.

In this study, human glioma continuous cell lines have provided useful models for the study of the *in vitro* behaviour of human malignant glioma. *In vivo* human gliomas exhibit heterogeneity of cell type, cell cycle status and irregular vascularisation. It is vital that these factors be taken into account when establishing a model system to investigate effective cell kill. One such tool, tumour spheroids, represent a useful *in vitro* model for the study of heterogeneity with respect to the effects of cytotoxic drugs and targeted radiotherapy on gliomas. Spheroids exhibit a histological structure similar to that of solid tumours. This holds for the distribution of vital and necrotic areas, and for the histologic appearance. It is a general finding that the degree of structural and functional differentiation in the primary tumour may be retained in spheroids rather than in conventional monolayer cultures. We therefore employed spheroids derived from glioma cell lines to evaluate the effect of

proliferative heterogeneity of tumour cells on the therapeutic potential of the cycle-specific agent, radiolabelled IUdR.

The human glioma cell lines originally analyzed in this study were UVW, SB18 and U251. They exhibited a heterogeneous range of phenotypic characteristics. The UVW cell line was regarded as the most satisfactory *in vitro* model because of its capability to grow as very large and regularly shaped spheroids. The latter characteristic was essential for our study of the effect of targeted radiotherapy on proliferative heterogeneity, which increases with spheroid size. This cell line was highly aneuploid and contained populations of cells which were sub tetraploid (74 chromosomes per genome).

We wished to determine the radiosensitivity of this cell line under different conditions of culture for comparison with the response to IUdR targeted radiotherapy. The effect of external beam irradiation on UVW cells was assessed in both monolayer and spheroid culture. The results indicated that UVW was a highly radioresistant cell line in both monolayer and spheroid cultures, with SF<sub>2</sub> values of 0.55 and 0.83-0.93 (obtained from clonogenic assay and growth delay) respectively, which placed this cell line at the resistant end of the radiosensitivity spectrum of cell lines.

Biologically targeted radiotherapy entails the preferential delivery of radiation to malignant cells by means of tumour-seeking delivery vehicles to which radionuclides can be conjugated. Once such vehicle, iodo-2'-deoxyuridine (IUdR), is a low-molecular-weight thymidine analogue that diffuses readily within tissues. When radiolabelled with an Auger electron emitter (e.g., <sup>123</sup>I or <sup>125</sup>I), it is highly toxic when incorporated into DNA. Since the majority of the cells within the CNS are nondividing, they do not incorporate IUdR into their DNA, allowing the agent to be taken up selectively by dividing malignant cells

(Halperin et al.,1988).

Heterogeneous uptake of radiolabelled IUdR in glioma which are comprised of cells in different stages of the cell cycle, can lead to under dosing of untargeted cells if there is insufficient cross-fire irradiation from targeted dividing cells. This problem will be minimal when the bound radionuclide is a long range  $\beta$ -emitter such as  $^{131}\text{I}$  but the dosage to surrounding normal tissue may be substantial. Conversely, strategies based upon the incorporation of ultra short range Auger electron emitters should reduce damage to adjacent organs but may fail to sterilise all tumour clonogens if cellular uptake is not completely uniform.

In order to assess the IUdR labelling index, we used non-radiolabelled IUdR, detected by anti-BUdR/IUdR monoclonal antibody in conjunction with flow cytometry. The uptake of non-radiolabelled IUdR was examined by studying different sizes of UVW human glioma spheroids and monolayer cell cultures in exponential and plateau phases, to assess the effect of proliferative heterogeneity. Whereas in monolayer culture more than 95% of exponentially growing cells and 62% of plateau phase cells were labelled with IUdR after one doubling time, the labelling index in the small spheroids (100-200 $\mu\text{m}$ ) was approximately 76% and for large spheroids (700-1000 $\mu\text{m}$ ) was 28% after one volume doubling time incubation (52 hours). The results of the study in which IUdR concentration was varied, confirm that there is an inverse relationship between the proportion of cycling cells and spheroid diameter. The percentage of cells labelled by IUdR after one volume doubling time incubation was higher for small spheroids (300-400 $\mu\text{m}$ ) at concentrations of 10 $\mu\text{M}$  and 100 $\mu\text{M}$  than for large spheroids (700-1000 $\mu\text{m}$ ).

Increasing the period of incubation with IUdR from one to four volume doubling times increased the proportion of cells that incorporated IUdR in small and large sizes of spheroids.

We analysed the labelling index in different sized spheroids by flow cytometry, however one of the disadvantages of this procedure is the requirement for disaggregation of tissue into single cell suspensions. This results in the loss of ability to relate kinetic parameters to tissue architecture. We therefore studied the effect of spheroid size and incubation time on labelling index by autoradiographic assessment. This represent the proliferative state of cells in a glioma *in vivo*.

Autoradiographic identification of labelled cells indicated that nuclear incorporation of [<sup>125</sup>I]IUdR decreased markedly with increasing size of spheroid. IUdR incorporation was maximal in the surface layer of cells and decreased with depth within the spheroids.

Radiopharmaceutical uptake corresponded closely to the regions of cell cycling as indicated by staining for the nuclear antigen Ki67. The uptake of drug was enhanced by increasing the duration of incubation from 52 hours to 104 hours. These observations suggest that significant sparing of non-cycling malignant cells would result from treatment delivered as a single injection of radiolabelled IUdR. To achieve maximal therapeutic effect, it is hypothesised that IUdR should be administered in multiple doses by multiple injections, by slow release from biodegradable implants, or by slow-pump delivery.

In previous studies, we observed that IUdR uptake decreased with increasing heterogeneity in proliferative activity of tumour cells. To overcome this treatment problem, we compared the toxicities of three radioiodoanalogues of IUdR, [<sup>123</sup>I]IUdR, [<sup>125</sup>I]IUdR and [<sup>131</sup>I]IUdR -

to the human glioma cell line UVW, cultured as monolayers in exponential and plateau phase of growth and as multicellular spheroids using a clonogenic end point. Monolayers treated in exponential growth phase were most efficiently sterilised by [ $^{125}\text{I}$ ]IUdR (concentration resulting in 37% survival ( $C_{37}$ ) = 2.36 kBq/ml), while [ $^{123}\text{I}$ ]IUdR and [ $^{131}\text{I}$ ]IUdR were less effective eradicators of clonogens ( $C_{37}$  = 9.75 and 18.9 kBq/ml respectively). Plateau phase monolayer cultures were marginally more susceptible to treatment with [ $^{123}\text{I}$ ]IUdR and [ $^{125}\text{I}$ ]IUdR (40% clonogenic survival) than [ $^{131}\text{I}$ ]IUdR (60% clonogenic survival). In cells derived from glioma spheroids, both [ $^{125}\text{I}$ ]IUdR and [ $^{123}\text{I}$ ]IUdR were again more effective than [ $^{131}\text{I}$ ]IUdR at concentration up to and including 20 kBq/ml. However, the survival curve for [ $^{131}\text{I}$ ]IUdR crossed the curves for the other agents, resulting in lower survival for [ $^{131}\text{I}$ ]IUdR than [ $^{123}\text{I}$ ]IUdR and [ $^{125}\text{I}$ ]IUdR at concentrations of 40 kBq/ml and higher. The clonogenic survival values at 100 kBq/ml were 13%, 45% and 28% respectively. It was concluded that IUdR incorporating the Auger electron emitters  $^{123}\text{I}$  and  $^{125}\text{I}$ , killed only cells which were in S phase during the period of incubation with radiopharmaceutical, whereas the superior toxicity to clonogenic cells in spheroids of [ $^{131}\text{I}$ ]IUdR at higher concentration was due to cross-fire  $\beta$ -irradiation. These findings suggest that [ $^{131}\text{I}$ ]IUdR or combinations of [ $^{131}\text{I}$ ]IUdR and [ $^{125}\text{I}$ ]IUdR or [ $^{123}\text{I}$ ]IUdR may be more effective than Auger electron emitters alone for the treatment of residual glioma.

## Future work

1) In chapter 9 we developed radiobiological analyses of DNA-targeted radiotherapy using ultra-short-range Auger electron emitters such as  $^{123}\text{I}$ ,  $^{125}\text{I}$  and  $\beta$ -emitting radionuclides such as  $^{131}\text{I}$  conjugated to IUdR. There are several important findings from this study, including the predicted superiority of  $^{125}\text{I}$  which has to be targeted to DNA in order to achieve optimal cell kill and the cross fire effect of  $^{131}\text{I}$  on non-dividing cells. The results obtained strongly favour a combined modality approach to Auger electron therapy together with  $\beta$ -emitting radionuclides such as  $^{131}\text{I}$ . The optimal proportion of each radioisotope in such cocktails remain to be established.

2) Recently, high specific activity 5- $^{211}\text{At}$ -astato-2'-deoxyuridine ( $^{211}\text{At}$ AUdR) has been synthesised and has been shown, like IUdR, to be readily incorporated into cellular DNA. However,  $^{211}\text{At}$ AUdR may be 100 times more toxic to clonogenic cells *in vitro* than  $^{125}\text{I}$  or  $^{123}\text{I}$ [IUdR] (Vaidyanathan et al., 1996).  $^{211}\text{At}$  emits high LET  $\alpha$  particles whose range is equivalent to a few cell diameters. These characteristics suggest that  $^{211}\text{At}$ AUdR could be superior to Auger electron emitters both in terms of tumour cell kill and homogeneity of dose distribution. However, the use of  $^{211}\text{At}$ -astatinated radiopharmaceuticals presents formidable difficulties in relation to logistics and radiation protection. The strategies in which the problems associated with the use of this radiopharmaceutical might be minimized and the possibilities of maximal therapeutic benefit by use of 'cocktails' of radioiodoconjugates of IUdR including both Auger electrons to kill cycling cells and the  $\alpha$ -emitter  $^{211}\text{At}$ AUdR to eliminate untargeted cells by cross fire must be explored.

3) The limitation of conventional radiotherapy lies in the fact that it is not tumour specific. Targeted radiotherapy seeks to improve biological specificity by conjugation of radioisotopes to tumour-seeking agents. However, there are few tumour types for which sufficiently selective agents exist and the therapeutic advantage is generally modest (Wheldon, 1994). An alternative strategy would be tumour-specific radiosensitisation to confer biological specificity on radiotherapy, whilst preserving its physical advantages of 'steerability' and dosimetric precision. Recent developments in molecular radiobiology and the availability of viral delivery vectors have raised the possibility that gene therapy methodology could be developed as a radiosensitising modality (McBride and Dougherty, 1995; Kim et al., 1995). Weichselbaum et al. (1994), have described the combination of gene therapy and radiation therapy as providing a new paradigm for cancer treatment.

Cell sterilisation by ionising radiation remains incompletely understood at the molecular level. Double strand breaks in DNA are certainly implicated but more complex lesions may be involved. Some genes have been identified and sequenced whose expression appears to have radioprotective effect such as the superoxide dismutase gene (Suresh et al., 1994), the Ataxia telangiectasia (AT) gene (Dahlberg and Little, 1995) and the Ku gene (Ross et al., 1995). The recent sequencing of the AT gene by Savitsky (1995), creates the possibility of radiosensitisation by gene inhibition. If gene inhibition could be made tumour selective, this could significantly improve the therapeutic ratio in radiotherapy. Inhibition could be accomplished by transfecting an 'anti-protector gene' in the form of an anti-sense RNA, a gene repressor protein or an inactivator of the protein product of the protector gene. The anti-protector gene might be selectively expressed in tumour cells using an engineered viral construct as a delivery vehicle under control of a promoter which is selectively active in tumour cells or in the tissue from which the tumour is derived. The exploration of such novel approaches is a task for future.

## References

- Adelstein, S. J. (1993). The Auger process: A therapeutic promise? *Am. J. Roentgen.* 160, 707-713.
- Agosti, R. M., Leuthold, M., Gullick, W. J., Yasargil, M. G., Wiestler, O. D. (1992). Expression of the epidermal growth factor receptor in astrocytic tumours is specifically associated with glioblastoma multiform. *Virchows Arch A Pathol Anat Histopathol.* 420, 321-325.
- Allalunis-Turner, M. J., Zia, P. K., Barron, G. M., Mirzayan, R., Day, R. S. 3rd. (1995). Radiation-induced DNA damage and repair in cells of the radiosensitive human malignant glioma cell line. *Radiat Res.* 144, 288-293.
- Allalunis-Turner, M. J., Pearcey, R., Urtasun, R. (1990). Inherent radiosensitivity testing of human tumour biopsy specimens. 38<sup>th</sup> Annual Meeting of the Radiation Research Society, New Orleans, Louisiana, April 7-12, Abstract Cn-1. p 67.
- Allegranza, A., Girlando, S., Arrigoni, G. L., Veronesi, S., Mauri, F. A., Gambacorta, M., Pollo, B., Dallapalma, P., et al. (1991). Proliferating cell nuclear antigen expression in central nervous system neoplasms. *Virch. Arch. Pathol. Ana. Histopathol.* 419, 417-423.
- Andersson, A., Capala, J., Carlsson, J. (1992). Effects of EGF-dextran-tyrosine <sup>131</sup>I conjugates on the clonogenic survival of cultured glioma cells. *J. Neur Oncol.* 14, 213-223.
- Assietti, R., Butti, G., Magrassi, L., Danova, M., Riccardi, A., Gaetani, P. (1990). Cell-kinetic characteristics of human brain tumours. *Oncology.* 47, 344-351.
- Baranowska-Kortylewicz, J., Helseth, L. D., Lai, J., Schneiderman, M. H., Schneiderman, G. S., Dalrymple, G. V. (1994). Radiolabelling kit generator for 5-radiohalogenated uridines. *J. Labelled Comp. Radiopharmaceutical.* 34, 513-521.
- Baranowska-Kortylewicz, J., Makrigiorgos, G. M., Van Den Abbeele, A. D., Berman, R. M., Adelstein, S. J., Kassis, A. I. (1991). 5[<sup>123</sup>I]iodo-2'-deoxyuridine in the radiotherapy of an early ascites tumour model. *Int. J. Radiat. Oncol. Biol. Phys.* 21, 1541-1551.
- Baranowska-Kortylewicz, J., Kinsey, B. M., Layne, W. W. and Kassis, A. I. (1988). Iododemercuration; a simple synthesis of 5 (<sup>123/125/127</sup>I)Iodo-2'-deoxyuridine, *Appl. Radiat. Isot.* 39, 335-341.
- Bardies, M., Thedrez, P., Gestin, J.F., Marcille, B.M., Guerreau, D., Faivre-Chauvet, A., Mahe, M., Sai-Maurel, C., Chatel, J.F. (1992). Use of multi-cell spheroids of ovarian carcinoma as an intraperitoneal radioimmunotherapy model: uptake, retention kinetics and dosimetric evaluation. *Int. J. Cancer.* 50, 984-991.
- Battermann, J. J. (1980). Fast neutron therapy for advanced brain tumours. *Int. J. Radiat. Oncol. Biol. Phys.* 6, 333-335.

- Bello, M. J., Vaqueroz, J., Decampos, J. M., Kusak, M. E., Sarasa, J. L., Saezcastresana, J., Pestana, A., Rey, J. A. (1994). Molecular analysis of chromosome-1 abnormalities in human gliomas reveals frequent loss of 1p in oligodendrioglial tumours. *Int. J. Cancer*. 57, 172-175.
- Bennet, A. H. and Godlee, R. J. (1884). Excision of a tumour from the brain. *Lancet*. 2, 1090.
- Bender, H., Takahashi, H., Adachi, K., Belser, P., Liang, S., Prewett, M., Schrappe, M., Sutter, A. et al. (1992). Immunotherapy of human glioma xenograft with unlabelled <sup>131</sup>I-, or <sup>125</sup>I-labelled monoclonal antibody 425 to epidermal growth factor receptor. *Cancer Res*. 52, 121-126.
- Bernstein, M., Laperrirer, N., Leung, P. McKenzie, S. (1990). Interstitial brachytherapy for malignant brain tumours: Preliminary results. *Neurosurgery*. 26, 371-380.
- Biard, D. S. F., Martin, M., Le Rhun, Y., Duthu, A., Lefaix, J. L., May, E., May, P. (1994). Concomitant p53 gene mutation and increased radiosensitivity in rat lung embryo epithelial cells during neoplastic development. *Cancer Res*. 54, 3361-3364.
- Bigner, S. H., Burger, P. C., Wong, A J. Werner, M. H., Hamilton, S. R., Mulbaire, L. H., et al. (1988). Gene amplification in malignant human gliomas: clinical and histopathologic aspects. *J. Neuropathol. Exp. Neurol*. 47, 191-205.
- Bigner, S. H., Mark, J., Burger, P. C., Mahaley, K. S., Bullard, D. E., Muhlbaier, L. H., Bigner, D. D. (1988). Specific chromosomal abnormalities in malignant human gliomas. *Cancer Res*. 88, 405- 411.
- Bigner, S. H., Mark, J., Buliard, D. F., Nahaley, M. S. Jr., Bigner, D. D. (1986). Chromosomal evolution in malignant human gliomas start with specific and usually numerical deviations. *Cancer Genet Cytogenet*. 22, 121-135.
- Bigner, D. D., Bigner, S. H., Ponten, J., Westermarck, B. Nahaley, N. S., Ruoslahti, E., Herschman, H., Eng L.F., Wikstrand, C. J. (1981). Heterogeneity of genotypic and phenotypic characteristics of fifteen permanent cell lines derived from human gliomas. *J. Neuropathol. Exp. Neurol*. 40, 201-229.
- Bignami, A., Eng. L., Dahi, D., Uyeda, C. (1972). Localization of the glial fibrillary acidic protein in astrocytes by immunofluorescence. *Brain Res*. 43, 429-435.
- Bhuyan, B. K., Fraser, T. J., Day, K. J. (1977). Cell proliferation kinetics and drug sensitivity of exponential and stationary phase populations of cultured L1210 cells. *Cancer Res*. 37, 1057-1063.
- Bleehen, N. M. (1980). The Cambridge glioma trial of misonidazole and radiation therapy with associated pharmacokinetic studies. *Cancer Clin. Trials*. 3, 267-273.
- Bleehen, N. M. (1983). MRC study of misonidazole and radiotherapy for high grade astrocytomas (Abstr.) Proceedings II. Meeting of ESTRO, Bordeaux, France, p 21.

- Bleehen, N. M. and Stenning, S. P. (1991). A Medical Research Council trial of two radiotherapy doses in the treatment of grade 3 and 4 astrocytoma. *Br. J. Cancer.* 64, 769-774.
- Bloom, H. J. G., Bradley, N. J., Davies, A. J. S., Richardson, S. G. (1986). An experimental study of xenografted human gliomas. In: "Biology of Brain Tumour", editors: Walker, M. D. and Thomas, D. G. T., Martinus Nijhoff, Boston, pp 415-421.
- Boring, C. C., Squires, T. S., Tong, T., Montgomery, S. (1994). Cancer statistics, 1994. *Cancer J. Clin.* 44, 7-26.
- Bouchard, J. (1966). Radiation therapy of tumours and diseases of the nervous system. Philadelphia, PA: Lea and Febinger.
- Brachman, D. G., Beckett, M., Graves, D., Haraf, D., Vokes, E., Weichselbaum, R. R. (1993). p53 mutation does not correlate with radiosensitivity in 24 head-and-neck cancer cell lines. *Cancer Res.* 53, 3667-3669.
- Brady, L. W., Markoe, M. A., Woo, D. V., Rakover, M. A., Koprowski, H., Steplewski, Z., Peyster, R. G. (1990). Iodine <sup>125</sup> labelled anti-epidermal growth factor receptor-425 in the treatment of malignant astrocytomas. A pilot study. *J Neurosurg Sci.* 34, 243-249.
- Bravo, R. and MacDonald-Bravo, H. (1984). Induction of the nuclear protein cycling in the quiescent mouse 3T3 cells stimulated by serum and growth factors: correlation with DNA synthesis. *EMBO J.* 3, 3177-3181.
- Brem, H., Piantadosi, S., Burger, P. C., Walker, M., Secker, R., Vick, N. A., Black, K., Sisti, N., Brem, G., Mohr, G. et al. (1995). Placebo controlled trial of safety and efficacy of intra-operative controlled delivery by biodegradable polymers of chemotherapy for recurrent gliomas. *Lancet.* 345, 1008-1012.
- Bresnik, E. and Thompson, U. B. (1965). Properties of deoxythymidine kinase partially purified from animal tumours. *J. Biol. Chem.* 240, 3967-3974.
- Buchsbaun, D. J. (1995). Experimental approaches to increase radiolabelled antibody localization in tumours. *Cancer Res.* 55 (23Suppl), 5729s-5732s.
- Burger, P. C., Shibata, T., Kleihus, P. (1986). The use of the monoclonal antibody Ki67 in the identification of proliferating cells: application to surgical neuropathology. *Am. J. Surg. Pathol.* 10, 611-617.
- Burki, H. J., Roots, R., Feinendegen, L. E., Bond, V. P. (1973). Inactivation of mammalian cells after disintegrations of <sup>3</sup>H or <sup>125</sup>I in cell DNA at -196°C. *Int. J. Radiat. Biol.* 24, 363-375.
- Capala, J. and Carlsson, J. (1991). Influence of chloroquine and lidocaine on retention and cytotoxic effect of <sup>131</sup>I-EGF: Studies on cultured glioma cells. *Int. J. Radiat. Biol.* 60, 497-510.
- Carlsson, J. and Nederman, T. (1989). Tumour spheroid technology in cancer therapy research. *Eur. J. Cancer Clin. Oncol.* 25, 1127-1133.

- Carlsson, J., Daniel-Szolgay, E., Frykholm, G., Glimelius, B., Hedin, A., Larsson, B. (1989). Homogeneous penetration but heterogeneous binding of antibodies to carcinoembryonic antigen in human-colon carcinoma HT-29 spheroids. *Cancer Immunology Immunotherapy* 30, 269-276.
- Chan, P. C., Lisco, E., Lisco, H., Adelstein, S. J. (1976). The radiotoxicity of iodine-125 in mammalian cells. A comparative study on cell survival and cytogenetic responses to <sup>125</sup>IUdR, <sup>131</sup>IUdR, and <sup>3</sup>HTdR. *Radiat. Res.* 67, 332-343.
- Chang, C. H. (1977). Hyperbaric oxygen and radiation therapy in the management of glioblastoma. *Natl. Cancer Inst. Monogr.* 46, 57-76.
- Chun, M., McKeough, P., Wu, A. Kasdon, D., Heros, D., Chang, H. (1989). Interstitial iridium-192 implantation for malignant brain tumours. *Br. J. Radiol.* 62, 158-162.
- Chung, R., Whaley, J., Kley, N., Anderson, K., Louis, D., Menon, A., Hettlich, C., Freiman, R., Hedley-Whyte, E. T., Martuza, R., Jenkins, R., Yandell, D., Seizinger, B. R. (1991). Tp53 gene mutations and 17p deletions in human astrocytomas. *Genes Chromosome Cancer.* 3, 323-331.
- Clifton, K. H., Szybalskiw, Heidelberger, C., Gollin, F. F., Ansfield, F. J., Vermund H. (1963). Incorporation of <sup>125</sup>I-labelled iododeoxyuridine into the deoxyribonucleic of murine and human tissues following therapeutic doses. *Cancer Res.* 23, 1715-1722.
- Cocchia, D., Michetti, F., Donato, R. (1981). Immunochemical and immunocytochemical localization of S-100 antigen in normal human skin. *Nature.* (London). 294, 85-87.
- Codd, M. B. and Kurland, L. .T. (1985) Descriptive epidemiology of primary intracranial neoplasms. *Prog. Exp. Tumor. Res.* 29, 1-11.
- Collins, V. P.(1983). Cultured human glial and glioma cells. *Int. Rev. Exp. Pathol.* 24, 135-202.
- Cooper, G. (1991). 'Oncogenes'. Jones and Bartlett Publishers: Boston, p179.
- Courtenay, V. D. and Mills, J. (1978). An in vitro colony assay for human tumours grown in immune-suppressed mice and treated In vivo with cytotoxic agents. *Br. J. Cancer.* 37, 261-268.
- Courtenay, V. D. (1976). A soft agar colony assay for Lewis lung tumour and B16 melanoma taken directly from the mouse. *Br. J. Cancer.* 34, 39-45.
- Daghighian, F., Humm, J. L., Macapinlac, H. A., Zhang, J., Izzo, J., Finn, R., Kemeny, N., Larson, M. (1996). Pharmacokinetics and dosimetry of iodine-125-IUdR in the treatment of colorectal cancer metastatic to liver. *J. Nucl. Med.* 37 (Suppl), 29S-32S.

- Dahlberg, W. K. and Little, J. B. (1995). Response of dermal fibroblast cultures from patients with unusually severe responses to radiotherapy and from ataxia telangiectasia heterozygotes to fractionated radiation. *Clinical Cancer Res.* 1, 785-790.
- Dean, P. N., Gray, J. W., Dolbeare, F. A. (1982). The analysis and interpretation of DNA distributions measured by flow cytometry. *Cytometry.* 3188-3195.
- Deacon, J. M., Wilson, P. A., Peckham, M. J. (1985). The radiobiology of human neuroblastoma. *Radiother. Oncol.* 3, 201-209.
- Deacon, J., Peckham, M. J., Steel, G. G. (1984). The radioresponsiveness of human tumours and the initial slope of the survival curve. *Radiother. Oncol.* 2, 317-323.
- Desmeules, M., Middelsen, T., Mao, Y. (1992). Increasing incidence of primary malignant brain tumours: influence of diagnostic methods. *J. Natl. Cancer Inst.* 84, 442-445.
- Deutsch, M., Green, S. B., Strike, T. A., Burger, P. C., Robertson, J. T., Selker, R. G., Shapiro, W. R., Mealey, J., Ransohoff, J. et al. (1989). Results of randomized trial comparing BCNU plus radiotherapy, streptozotocin plus radiotherapy, BCNU plus hyperfractionated radiotherapy, and BCNU following misonidazole plus radiotherapy in the post-operative treatment of malignant glioma. *Int. J. Radiat. Oncol. Biol. Phys.* 16, 1389-1396.
- Diserens, A. C., deTribolet, N., Martin-Achard, A., Gaide, A. C., Schnegg, J. F., Carrel, S. (1981). Characterization of an established human malignant glioma cell line: LN-18. *Acta. Neuropathol.(Berl).* 53, 21-28.
- Donato, R. (1991). Perspective in S-100 protein biology. *Cell Calcium.* 12, 713-726.
- Dressler, L. G., Bartow, M. B., Bartow, S. A. (1989). DNA flow cytometry in solid tumours: practical aspects and clinical applications. *Sem. Diagnostic Pathol.* 6, 55-82.
- Duffy, P., Huang, Y. Y., Rapport, M. (1982). The relationship of glial fibrillary acidic protein to the shape, motility, and differentiation of human astrocytoma cells. *Exp. Cell Res.* 58, 393-400.
- Dunnett, C. W. (1955). A multiple comparison procedure for comparing several treatments with a control. *J. Am. Statist. Asso.* 50, 1096-1121.

- Durand, R. E. (1990). Multicell spheroids as a model for cell kinetics studies. *Cell Tissue Kinet.* 23, 141-159.
- Eidinoff, M. L., Cheong, L., Rich, M. A. (1959). Incorporation of unnatural pyrimidine basis into deoxyribonucleic acid of mammalian cells. *Science.* 129, 1550-1551.
- Ekstrand, A. J., Sugawa, N., James, C. D., Collins, V. P. (1992). Amplified and rearranged epidermal growth factor receptor genes in human glioblastoma reveal deletions of sequences encoding portions of the N-and/or C-terminal tails. *Proc. Natl. Acad. Sci. U S A.* 89, 4309-4313.
- Elkind, M. M. and Whitmore, G. F. (1976). *The radiobiology of cultured mammalian cells.* Gordon and Breach, New York. pp 351-353.
- Elvidge, A., Penfield, W., Cone, W. (1937). The glioma of central nervous system. A study of two hundred and ten verified cases. *Res. Publ. Assos. Nerv. Ment. Dis.* 16, 107-181.
- Enoch, T. and Norbury, C. (1995). Cellular responses to DNA damage: cell-cycle checkpoints, apoptosis and the roles of *p53* and ATM. Elsevier Science, Amsterdam. pp 426-430.
- Ewing, J. (1921). The structure of nerve tissue tumours with reference to radium therapy. *J. Nerv. Ment. Dis.* 53, 130-131.
- Fertil, B. and Malaise, E. P. (1981). Inherent cellular radio-sensitivity as a basic concept for human tumour radiotherapy. *Int. J. Radiat. Oncol. Biol. Phys.* 7, 621-629.
- Feun, L. G., Savaraj, N., Landy, H. J. (1994). Drug resistance in brain tumours. *J. Neuro. Oncol.* 20, 165-176.
- Feychting, M. and Ahlbom, A. (1992). Magnetic fields and cancer in people residing near Swedish high voltage power lines. Karolinska Institute, Stockholm.
- Figge, C., Reifeberger, G., Vogeley, K. T., Messing, M., Roosen, N., Wechsler, W. (1992). Immunohistochemical demonstration of proliferating cell nuclear antigen in glioblastomas: pronounced heterogeneity and lack of prognostic significance. *J. Cancer Res. Clin. Oncol.* 118, 289-295.

- Fine, H. A. (1994). The basis for current treatment recommendation for malignant gliomas. *J. Neuro. Oncol.* 20, 111-120.
- Flickinger, J. C., Loeffler, J. S., Larson, D. A. (1994). Stereotactic radiosurgery for intracranial malignancies. *Oncology.* 8, 81-86.
- Florell, R. C., MacDonald, D. R., Irish, W. D., Berstein, M., Leibel, S. A., Gutin, P. H., Cairncross, J. G. (1992). Selection bias, survival and brachytherapy for glioma. *J. Neurosurg.* 76, 179-183.
- Folkman, J. and Moscona, A. (1978). Role of cell shape in growth control. *Nature.* 288, 551-556.
- Fowler, J. F. (1990). Radiobiological aspects of low dose rates in radioimmunotherapy. *Int. J. Radiat. Oncol. Biol. Phys.* 18, 1261-1269.
- Frame, M. C., Freshney, R. I., Vaughan, P. F. T., Graham, D. I., Shaw, R. (1984). Interrelationship between differentiation and malignancy associated properties in glioma. *Br. J. Cancer.* 49, 269-280.
- Frankle, R. H., Bayona, W., Koslow, M., Newcomb, E. W. (1992). p53 mutation in human malignant gliomas: comparison of loss of heterozygosity with mutation frequency. *Cancer Res.* 52, 1427-1433.
- Freeman, C. R., Krischer, J., Sanford, R. A., Burger, P.C., Cohen, N., Norris, D. (1988). Hyperfractionated radiotherapy in brain stem tumors: results of a paediatric oncology group study. *Int. J. Radiat. Oncol. Biol. Phys.* 15, 311-318.
- Freshney, R. I. (1984). Effects of glucocorticoids on glioma cells in culture. *Exp. Cell Biol.* 52, 286-292.
- Freshney, R. I. (1980). Tissue culture of glioma of the brain. In: *Brain tumours: scientific basis, clinical investigation and current therapy*, Thomas, D.G.T. and Graham, D.I., Butterworths, London, pp 21-50.
- Freyer, J. P. and Sutherland, R. M. (1980). Selective dissociation and characterization of cells from different regions of multicell tumour spheroids. *Cancer Res.* 40, 3956-3965.

- Fults, D., Petrnio, J., Noblett, BD., Pedone, CA. (1992a). Chromosome 11p15 deletions in human malignant astrocytomas and primitive neuroectodermal tumours. *Genomics*. 12, 57-66.
- Fults, D., Brockmeyer, D., Tullous, M. W., Pedone, C. A., Cawthon, R. M. (1992b) . p53 mutation and loss of heterozygosity on chromosomes 17 and 10 during human astrocytoma progression. *Cancer Res*. 52, 674-679.
- Garrett, C., Wataya, Y., Santi, D. V. (1979). Thymidylate synthetase: catalysis of dehalogenation of 5-bromo-and 5-iodo-2'-deoxyuridylate. *Biochemistry*. 18, 2798-2804.
- Gati, S., Bergstrom, M., Muhr, C., Carlsson, J. (1994). Leukotriene and 5-Lipoxygenase inhibitor induced variations in thymidine uptake in a human glioma cell line cultured as monolayers or as multicellular spheroids. *Anticancer Res*. 14, 453-460.
- Gaynor, R., Irie, R., Norton, D., Herschman, H. R. (1980). S100 protein is present in cultured human malignant melanomas. *Nature*. (London). 286, 400-401.
- Gaze, M. N., Mairs, R. J., Boyack, S. M., Wheldon, T. E., Barrett, A. (1992). <sup>131</sup>I metaiodobenzylguanidine therapy in neuroblastoma spheroids of different sizes. *Br. J. Cancer*. 66, 1048-1052.
- Gelb, A. B., Kamel, O. W., Lebrun, D. P., Warnke, R. A. (1992). Estimation of tumour growth fractions in archival formalin-fixed, paraffin-embedded tissues using two anti-PCNA/Cycling monoclonal antibodies. *Am. J. Pathol*. 141, 1453-1458.
- Giles, G. G. and Gonzales, M. F. (1995). Epidemiology of brain tumours and factors in prognosis. In: *Brain tumours*. Churchill Livingstone. Tokyo. pp 47-67.
- Gerdes, J., Lemke, H., Baisch, H., Wacker, H. H., Schwab, U., Stein, H. (1984). Cell cycle analysis of a cell proliferation-associated human nuclear antigen defined by the monoclonal antibody Ki-67. *J. Immunol*. 133, 1710-1715.
- Gerdes, J., Li, L., Schlueter, C., Duchrow, M., Wohlenberg, C., Gerlach, C., Stahmer Kloth, S., Brandt, E., Flad, H. D. (1991). Immunobiochemical and molecular biologic characterization of the cell proliferation-associated nuclear antigen that is defined by monoclonal antibody Ki-67. *Am. J. Pathol*. 138, 867-873.

- Goldenberg, D. M.(1993). Monoclonal antibodies in cancer detection and therapy. *Am. J. Med.* 94, 297-312.
- Gonzalez, D., Menten, J., Bosch, D. A., Vanderschueren, E., Troost, D., Mulshof, M. C. C. M., Bernier, J. (1994). Accelerated radiotherapy in glioblastoma multiforme: a dose searching prospective study. *Radiat. Oncol.* 32, 98-105.
- Grant, R., Collie, D., Counsell, C. (1996). The incidence of cerebral glioma in the working population: a forgotten cancer. *Br. J. Cancer.* 73, 252-254.
- Grinspan, J. B., Stern, J., Franceschini, B., Yasuda, T., Pleasure, D. (1994). Protein growth factors as potential therapies for central nervous demyelinating disorders. *Ann Neuro.* 36 Suppl, S 140-142.
- Groebe, K. and Muller-Klieser, W. (1996). On the relation between size of necrosis and diameter of tumour spheroids. *Int. J. Radiat. Oncol. Biol. Phys.* 34, 395-401.
- Gronvik, C., Capala, J., Carlsson, J. (1996). The non-variation in radiosensitivity of different proliferative states of human glioma cells. *Anticancer Res.* 16, 25-31.
- Grover, A., Oshima, R. G., Adamson, E. D. (1983). Epithelial layer formation in differentiating aggregates of F9 embryonal carcinoma cells. *J. Cell. Biol.* 96, 1960-1969.
- Gupa, N., Rohini, V., Haas-Kogan, D. A., Israel, M. A., Deen, D. F., Morgan, W. F. (1996). Cytogenic damage and the radiation-induced G<sub>1</sub>-phase checkpoint. *Radiat. Res.* 145, 289-298.
- Gutin, P. H., Prados, M. D., Philips, T. L. Wara, W. N., Larson, D. A., Leibel, S. A., Sneed, P. K., Levin, V. A. et al. (1991). External irradiation followed by an interstitial high activity iodine-125 implant "boost" in the initial treatment of malignant gliomas: NCOG study 6G-82-2. *Int. Radiat. Oncol. Biol. Phys.* 21, 601-606.
- Haag, D., Feichter, G., Goerttler, K., Kaufmann, M. (1987). Influence of systematic errors on the evaluation of the S phase portions from DNA distribution of solid tumours as shown for 328 breast carcinomas. *Cytometry.* 8, 377-385.
- Hagen, U. (1990). Molecular radiation biology: future aspects. *Radiat. Environ. Biophys.* 29, 315-322.

- Halperin, E. C., Bugar, P. C., Bullard, D. E. (1988). The fallacy of the localized supratentorial malignant glioma, *Int. J. Radiat. Oncol. Biol. Phys.* 15, 505-509
- Hall, P. A. and Levison, D. A. (1990). Assessment of cell proliferation in histological material. *J. Clin. Pathol.* 43, 184-192.
- Hartwell, L. H. and Weinert, T. A. (1989). Checkpoints: controls that ensure the order of cell-cycle events. *Science.* 246, 629-634.
- Hayashi. Y., Yamashita, J., Yamaguchi, K. (1991). Timing and role of *p53* gene mutation in the recurrence of glioma. *Biochem. Biophys. Res. Commun.* 180, 1145-1150.
- Heldin, C. H, Wasteson, A., Westermark, B. (1980). Growth of normal human glial cells in defined medium containing platelet-derived growth factor. *Proc. Natl. Acad. Sci. USA*, 77, 6611-6615.
- Hess, C. F., Schaaf, J. C., Kortmann, R. D., Schabet, M., Bamberg, M. (1994). Malignant glioma: patterns of failure following individually tailored limited volume irradiation. *Radiother. Oncol.* 30, 146-149.
- Hinz, G. and Dertinger, H. (1983). Increased radioresistance of cells in cultured multicell spheroids. II. Kinetic and cytogenetic studies. *Radiat. Envir. Biophys.* 21, 255-264.
- Hill, B. T.(1985). Methodologies for *in vitro* growth of human 'solid' tumours and their applications. In *Brain tumors biopathology and therapy*, Gerosa, M. A., Rosenblum, M. L. and Tridente, G., pp 13-13.
- Holtfreter, J. (1944). A study on the mechanics of gastrulation. *J. Exp. Zool.* 95, 171-212.
- Hofer, K. G. (1980). Radiation biology and the potential therapeutic applications of the radionuclides. *Bull. Cancer.* 67, 343-353.
- Hofer, K. G. and Hughes, W. L. (1971). Radiotoxicity of intranuclear tritium, <sup>125</sup>I and <sup>131</sup>I. *Radiat. Res.* 47, 94-109.

- Hofer, K. G. and Smith, J. M. (1975). Radiotoxicity of intracellular  $^{67}\text{Ga}$ ,  $^{125}\text{I}$  and  $^3\text{H}$  nuclear versus cytoplasmic radiation effects in murine L1210 leukaemia. *Int. J. Radiat. Biol.* 28, 225-241.
- Holley, R. W., Armour, R., Baldwin, J. H. (1978). Density-dependent regulation of growth of BSC-1 cells in cell culture: Growth inhibitors formed by the cells. *Proc. Nat. Acad. Sci. USA.* 75, 1864-1866.
- Hoshino, T. and Wilson, C. B. (1979). Cell kinetic analyses of human malignant brain tumours (gliomas). *Cancer.* 44, 956-962.
- Hoshino, T., Ito, S., Asai, A., Shibuya, M., Prados, M. D., Dodson, B. A. (1992). Cell kinetic analysis of human brain tumours by in situ double labelling with bromodeoxyuridine and iododeoxyuridine. *Int. J. Cancer.* 50, 1-5.
- Hoshino, T., Prados, M. D., Wilson, C. B., Cho, K. G., Lee, K. S., Davis, R. L. (1989). Prognostic implications of the bromodeoxyuridine labelling index of human gliomas. *J. Neurosurg.* 71, 335-341.
- Humm, J. L. and Charlton, D. E. (1989). A new calculational method to assess the therapeutic potential of Auger electron emission. *Int. J. Radiat. Oncol. Biol. Phys.* 17, 351-360.
- Humm, J. L. (1986). Dosimetric aspects of radiolabelled antibodies for tumour therapy. *J. Nucl. Med.* 9, 1490-1496.
- Humphrey, P. A., Wong, A. J., Vogelstein, B., Zalutsky, M. R., Fuller, G. N., Archer, G. E., Friedman, H. S., Kwara, M. M., Bigner, S. H., Bigner, D. D. (1990). Antisynthetic peptide antibody reacting at the fusion junction of deletion-mutant epidermal growth factor receptors in human glioblastomas. *Proc. Natl. Acad. Sci. USA.* 87, 4207-4211.
- Hurt, M. R., Mossay, J., Donovan-Peluso, M., Locker, J. (1992). Amplification of epidermal growth factor receptor gene in gliomas: histopathology and prognosis. *J. Neuropathol. Exp. Neurol.* 51, 84-90.
- Inch, W. R., McCredie, J. A., Sutherland, R. M. (1970). Growth of nodular carcinomas in rodents compared with multi-cell spheroids in tissue culture. *Growth.* 34, 271-282.

Jain, R. K. (1991). Haemodynamic and transport barriers to the treatment of solid tumours. *Int. J. Radiat. Biol.* 60, 85-100.

James, C. D., Carlbom, E., Dumanski, J. P., Hausen, M., Nordenskjold, M. D., Collins, V. P. (1988). Clonal genomic alterations in gliomas malignancy stages. *Cancer. Res.* 48, 5546-5551.

Jeffers, G. J., Fuller, T. C., Cosimi, A. B., Russell, P. S., Winn, H. J., Colvin, R. B. (1986). Monoclonal antibody therapy: anti-idiotypic and non-idiotypic antibodies to OKT3 arise despite intense immunosuppression. *Transplantation.* 41, 572-578.

Jeremic, B., Grujicic, D., Antunovic, V., Ljubodarg, D., Stojanovic, M., Shibamoto, Y. (1994). Hyperfractionated radiation therapy (HFX RT) followed by multiagent chemotherapy (CHT) in patients with malignant glioma: a phase II study. *Int. J. Radiat. Oncol. Biol. Phys.* 30, 1179-1185.

Jaskulski, D., Gatti, G., Travali, S., Calabrett, A. B., Baserg, A. R. (1988). Regulation of proliferating cell nuclear antigen cycling and thymidine kinase mRNA levels by growth factors. *J. Biol. Chem.* 263, 1175-1179.

Kallman, R. F. (1988). Reoxygenation and repopulation in irradiated tumours. *Front. Radiat. Ther. Oncol.* 22, 30-49.

Kalofonos, H. P., Pawlikowska, T. R., Hemingway, A., Courtenaylucky, N., Dhokia, B., Snook, D., Sivolapenko, G. B., Hooker, G. R., et al. (1989). Antibody guided diagnosis and therapy of brain gliomas using radiolabelled monoclonal antibodies against epidermal growth factor receptor and placental alkaline phosphatase. *J. Nucl. Med.* 30, 1636-1645.

Kassis, A. I. and Adelstein, S. J. (1996). Preclinical animal studies with radiolabelled IUdR. *J. Nucl. Med.* 37, 343-352.

Kassis, A. I., Tume, S. S., Wen, P. Y. C., Baranowska-Kortylewicz, J., Van den Abeele, A. D., Zimmerman, R. E., Carvalho, P. A., et al. (1996). Intratumoural administration of 5-[<sup>125</sup>I]iodo-2'-deoxyuridine in a patient with a brain tumour. *J. Nucl. Med.* 37(Suppl), 19S-22S.

Kassis, A. I. (1994). Toxicity and therapeutic effects of low-energy electrons. *Nucl. Instrum. Meth. Phys. Res. [B]*, 87, 279-284.

Kassis, A. I., Guptill, W. E., Taube, R. A., Adelstein, S. J. (1991). Radiotoxicity of 5-<sup>[125I]</sup>iodo-2'-deoxyuridine in mammalian cells following treatment with 5-fluoro-2'-deoxyuridine. *J. Nucl. Biol. Med.* 35, 167-173.

Kassis, A. I., Annick D., Vanden, Abbeele, Patrick, Y.C., Wen, Baranowska-Kortylewicz, J. (1990). Specific uptake of the Auger electron-emitting thymidine analog.5-<sup>[123I/125I]</sup>Iodo-2'-deoxyuridine in rat brain tumours: Diagnostic and therapeutic implications in humans. *Cancer Res.* 50, 5199-5203.

Kassis, A. I., Fayad, F., Kinsey, B. M., Sastry, K. S. R., Adelstein, S. J. (1989). Radiotoxicity of an I-125-labelled DNA intercalator in mammalian cells. *Radiat. Res.* 118, 283-294.

Kassis, A. I., Fayad, F., Kinsey, B.M., Sastry, K. S. R., Taub, R. A. and Adelstein, S.J. (1987a). Radio toxicity of <sup>125</sup>I in mammalian cells. *Radiat. Res.* 111, 305-318.

Kassis, A. I., Sastry, K. S. R., Adelstein, S. J. (1987b). Kinetics of uptake, retention of <sup>125</sup>IUdR in mammalian cells: implications of localized energy deposition by Auger processes. *Radiat. Res.* 109, 78-89.

Kawamoto, K., Herz, F., Wolley, R. C., Hirano, A., Kazikawa, U., Koss, L.G.(1979). Flow cytometric analysis of the DNA distribution in human brain tumours. *Acta Neuropathol.* 46, 39-51.

Kellerer, A., M. and Rossi, H. H. (1972). The theory of dual radiation action. *Curr. Top. Radiat. Res.* 8, 85-158.

Kennedy, P., Watkins, B., Thomas, D., & Nobel, M. (1987). Antigenic expression by cells derived from human gliomas does not correlate with morphological classification. *Neuropathol.Appl.Neurobiol.* 3, 327-347.

Kim, J. H., Kim, S. H., Kolosvary, A., Brown, S. L., Kim, O. B., Freytag, S. O. (1995). Selective enhancement of radiation response of herpes simplex virus thymidine kinase transduced 9L gliosarcoma cells *in vitro* and *in vivo*. *Int. J. Radiat. Oncol. Biol. Phys.* 33, 861-868.

Kinsella, T., Dobson, P., Fornace, A. (1988). Enhancement of X-ray-induced DNA strand breaks (SB) following unifilar substitution with iododeoxyuridine (IDURD). *Proc. Amer. Asso. Cancer Res.* 29, 498.

- Kleihues, P., Burger, P. C., Scheithauer, B. W. (1993). The new WHO classification of brain tumours. *Brain pathol.* 3, 255-268.
- Kohler, G. and Milstein, C. (1975). Continuous culture of fused cells secreting antibody of predefined specificity. *Nature.* 256, 495-496.
- Kornblitch, P. L., Walker, M. D., Cassady, J. R. (1987). *Neurologic Oncology.* Philadelphia, PA: Lippincott Co.
- Kramer, S., Southard, M. E., Mansfield, C. M. (1972). Radiation effect and tolerance of the central nervous system. *Front. Radiat. Ther. Oncol.* 6, 332-345.
- Kramer, S. (1975). Editorial. Brain tumours: where have we been? where are we going? *Sem. Oncol.* 2, 3-4.
- Kreth, F. W., Warnke, P. C., Scheremet, R., Ostertag, C., B. (1993). Surgical resection and radiation therapy in the treatment of glioblastoma multiforme. *J. Neurosurg.* 78, 762-766.
- Kuerbitz, S.J., Plunkett, B.S., Walsh, W.V., Kastan, M.B. (1992). Wild type *p53* in a cell cycle checkpoint determination following irradiation. *Proc. Natl. Acad. Sci. U S A.* 89, 7491-7495.
- Kury, G. and Carter, H. W. (1965). Autoradiographic study of human nervous system tumours. *Arch. Pathol.* 80, 38-42.
- Kuzel, T. M. and Rosen, S. T. (1994). Antibodies in the treatment of human cancer. *Curr. Opin. Oncol.* 6, 622-626.
- Kwock, C. S., Crivici, A., MacGregor, W. D., Unger, M. W. (1989). Optimization of radio immunotherapy using human malignant melanoma multicell spheroids as a model. *Cancer Res.* 49, 3276-3281.
- Kyritsis, A. P. and Levin, V. A. (1992). Chemotherapeutic approaches to the treatment of malignant gliomas. *Adv. Oncol.* 8, 9-13.
- Laerum, O. D., Steinsvag, S., Bjerkvig, R. (1985). Cell and tissue culture of the central nervous system: recent developments and current applications. *Acta. Neurol. Scand.* 72, 529-549.

Laerum, O. D., Bigner, D. D., Rajewski, M. F. (1978). *Biology of brain tumours*, International Union Against Cancer. Geneva.

Lane, D. P. (1992). p53 guardian of the genome. *Nature*. 358, 15-16.

Laird, P.W., Zijderveld, A., Linders, K., Rudnicki, M. A., Jaenisch, R., Berns, A. (1991). Simplified mammalian DNA isolation procedure. *Nucleic Acids Res.* 19, 4293.

Langmuir, V. K., McGann, J. K., Buchegger, F., Sutherland, R.M. (1991). The effect of antigen concentration, antibody valency and size, and tumour architecture on antibody-binding in multicell spheroids. *Nucl. Med. Biol.* 18, 753-764.

Langmuir, V. K., Mendonca, H. L., Woo, D. V. (1992a). Comparison between two monoclonal antibodies that bind to the same antigen but have differing affinities: uptake kinetics and <sup>125</sup>I-antibody therapy efficacy in multicell spheroids. *Cancer Res.* 52, 4728-4734.

Langmuir, V. K., Medonca, H. L., Vanderheyden, J. L., Su, F. M. (1992b). Comparison of the efficacy of Re-186-labelled and I-131-labelled antibody in multicell spheroids. *Int. J. Radiat. Oncol. Biol. Phys.* 24, 127-132.

Langmuir, V. K. and Mendonca, H. L. (1992). The combined use of <sup>131</sup>I-labelled antibody and the hypoxic cytotoxin SR 4233 *in vitro* and *in vivo*. *Radiat. Res.* 132, 351-358.

Laramore, G. E., Griffin, T. W., Gerdes, A. J., Parker, R. G. (1978). Fast neutron and mixed (neutron-photon) beam teletherapy for grade III and IV astrocytomas. *Cancer.* 42, 96-103.

Larson, D. A., Flickinger, J. C., Loeffler, J. S. (1993). Stereotactic radiosurgery: Techniques and results. *Princ Pract Oncol Updates.* 7, 1-13.

Larson, D. A., Flickinger, J. C., Loeffler, J. S. (1993). The radiobiology of radiosurgery. *Int. J. Radiat. Oncol. Biol. Phys.* 25, 557-561.

Lee, J. M. and Bernstein, A. (1993). p53 mutations increase resistance to ionizing radiation. *Proc. nat. Acad. Sci.* 90, 5742-5746.

Leenstra, S., Bijlsma, E. K., Troost, D., Oosting, J., Westerveld, A., Bosch, D. A., Hulsebos, T. J. (1994). Allele loss on chromosomes 10 and 17p and epidermal growth factor receptor gene amplification in human malignant astrocytoma related to prognosis. *Br. J. Cancer.* 70, 684-689.

Leibel, S. A., Scott, C. B., Loeffler, J. S. (1994). Contemporary approaches to the treatment of malignant gliomas with radiation therapy. *Semin. Oncol.* 21, 198-219.

Leibel, S. A., Gutin, P. H., Wara, W. M., Silver, P. S., Larson, D. A., Edwards, M. S. B., Lamb, S. A., Ham, B., et al. (1989). Survival and quality of life after interstitial implantation of removable high-activity iodine-125 sources for the treatment of patients with recurrent malignant gliomas. *Int. J. Radiat. Oncol. Biol. Phys.* 17, 1129-1139.

Leksell, L. (1951). The stereotactic method and radiosurgery of the brain. *Acta Chir. Scand.* 102, 316-319.

Levin, V. A., Silver, P., Hannigan, J., Wara, W. M., Gutin, P. H., Davis, R. L., Wilson, C. B. (1990). Superiority of post-radiotherapy adjuvant chemotherapy with CCNU, procarbazine and vincristin (PCV) over BCNU for anaplastic gliomas. *Int. J. Radiat. Oncol. Biol. Phys.* 18, 321-324.

Levin, V. A., Sheline, G. E., Gutin, P. H. (1989). Neoplasms of the central nervous system. In: *Cancer. principles and practice of oncology*, 3rd Edition. De Vita, V.T. Jr., Hellman, S., Rosenberg, S. A: J. B. Lippincott, Philadelphia. pp 1557-1579.

Levin, V. A. (1985). Chemotherapy of primary brain tumours. *Neurol. Clin.* 3, 855-866.

Lewis, I. J., Lashford, L. S., Fieldings, S., Flower, M. A., Ackery, D., Kemshead, J. T. (1991). A phase I/II study of <sup>131</sup>I-mIBG in chemoresistant neuroblastoma. In: *Advances in neuroblastoma research*. Evans, A.E. D'Angio, G. J. Kundson, A. G. and Seeger, R.C. Eds. Wiley-Liss, New York. pp 463-470.

Lindstorm, A. and Carlsson, J. (1993). Penetration and binding of epidermal growth factor-dextran conjugates in spheroids of human glioma origin. *Cancer Biother.* 8, 145-158.

Louis, D. N., Edgerton, S., Thor, A. D., Hedley-Whyte, E. T. (1991). Proliferating cell nuclear antigen and Ki-67 immunohistochemistry in brain tumours: a comparative study: *Acta Neuropathol.* 81, 675-679.

MacDonald, D. R. (1994). Low-grade gliomas, mixed gliomas and oligodendrogliomas. *Semin. Oncol.* 21, 236-248.

MacDonald, C. M., Freshney, R. I., Hart, E., Graham, D. I. (1985). Selective control of human glioma cell proliferation by specific cell interaction. *Exp. Cell. Biol.* 53, 130-137.

Macapinlac, H. A., Kemeny, N., Daghighian, F., Finn, R., Zhang, J., Humm, J. L., Squire O, Larson, S. M. (1996). Pilot clinical trial of 5-[<sup>125</sup>I]iodo-2'-deoxyuridine in the treatment of colorectal cancer metastatic to the liver. *J. Nucl. Med.* 37 (Suppl), 25S-29S.

Mahaley, M. S., Mettlin, C., Natarajan, N., Laws, Jr., Peace, B. B. (1989). National survey of patterns of care for brain tumour patients. *J. Neurosurg.* 71, 826-836.

Mairs, R. J., Angerson, W., Gaze, M. N. Murray, T., Babich, J. W., Reid, R., McSherry, C. (1991). The distribution of alternative agents for targeted radiotherapy within human neuroblastoma spheroids. *Br. J. Cancer.* 63, 404-409.

Mairs, R. J. and Wheldon, T. E. (1995). Experimental tumour therapy with targeted radionuclides in multicellular tumour spheroids. *Tenth International Congress of Radiation Research.* 2, 819-826.

Makrigiorgos, G .M., Berman, M., Baranowska-Kortylewicz, J., Bump, E., Humm, J. L., Adelstein, S. J., Kassis, A. I. (1992). DNA damage produced in V79 cells by DNA incorporated <sup>123</sup>I-a comparison with <sup>125</sup>I. *Radiat. Res.* 129, 309-314.

Makrigiorgos, G .M., Kassis, A. I., Baranowska-Kortylewicz, J., McElvany, K. D., Welch, M. J., Sastry, K. S. R., Adelstein, S. J. (1989). Radio toxicity of 5-[<sup>123</sup>I]Iodo-2'-deoxyuridine in V79 cells: a comparison with 5-[<sup>125</sup>I]Iodo-2'-deoxyuridine *Radiat. Res.* 118, 532-544.

Manuelidis, E. E. (1969). Experiments with tissue culture and heterologous transplantation of tumours. *Ann. N. Y. Acad. Sci.* 159, 409.

Martin, R. F. and Haseltine, W. A. (1981). Range of radiochemical damage to DNA with decay of iodine-125. *Science.* 213, 896-898.

Mariani, G., Cei, A., Collechi, P., Baranowska-Kortylewicz, J., Van den Abbeele, A. D., Di Luca, L., Di Stefano, R., Viacava, P., Ferdeghini, E. M., Di Sacco, S., et al. (1993). Tumour targeting *in vivo* and metabolic fate of 5-[iodine-125]iodo-2'-deoxyuridine following intratumoural injection in patients with colorectal cancer. *J. Nucl. Med.* 34, 1175-83.

Mariani, G., Collechi, P., Baldassarri, P., Diluca, L., Buralli, S., Fontanini, G., Baranowska-Kortylewicz, J., Adelstein, S. J., Kassis, A. I. (1996a). Tumour uptake and mitotic activity pattern of 5-[<sup>125</sup>I]iodo-2'-deoxyuridine after intravesical infusion in patients with bladder cancer. *J. Nucl. Med.* 37 (Suppl), 16S-19S.

Maraiani, G., Di Sacco, S., Volterrani, D., Di Luca, L., Buralli, S., Di Stefana, R., Baranowska-Kortylewicz, J., Bonara, D., et al. (1996b). Tumour targeting by intra-arterial infusion of 5-[<sup>123</sup>I]iodo-2'-deoxyuridine in patients with liver metastases from colorectal cancer. *J. Nucl. Med.* 37 (Suppl), 22S-25S.

Maruno, M., Kovach, J. S., Kelly, P. J., Yanagihara, T. (1991). Transforming growth factor- $\alpha$  epidermal growth factor receptor, and proliferating potential in benign and malignant gliomas. *J. Neurosurg.* 75, 97-102.

Masuda, K., Aramaki, R., Takaki, T., Wakisaka, S. (1983). Possible explanation of radioresistance of glioblastoma in situ. *Int. J. Radiat. Oncol. Biol. Phys.* 9, 255-258.

Maunoury, R. (1977). Establishment and characterization of 5 human cell lines derived from a series of 50 primary intracranial tumours. *Acta. Neuropath.* 39, 33-41.

Mayer, J. S. and Connor, R. E. (1977). *In vitro* labelling of solid tissues with tritiated thymidine for autoradiographic detection of S-phase nuclei. *Stain Technol.* 52, 185.

McBride, W. H. and Dougherty, G. J. (1995). Radiotherapy for genes that cause cancer. *Nature Med.* 1, 1215-1517.

McIlwrath, A. J., Vasey, P. A., Ross, G. M., Brown, C. (1994). Cell cycle arrests and radiosensitivity of human tumour cell lines: dependence on wild-type p53 for radiosensitivity. *Cancer Res.* 54, 3718-3722.

Merry, S., Kaye, S. B., Freshney, R. I. (1984). Cross-resistance to cytotoxic drugs in human glioma cell lines in culture. *Br. J. Cancer.* 50, 831-835.

- Millar, B. and Jinks, S. (1985). Studies on the relationship between the radiation resistance and glutathione content of human and rodent cells after treatment with dexamethasone *in vitro*. *Int. J. Radiat. Biol.* 47, 539-552.
- Miller, E. M., Fowler, J. F., Kinsella, T. J. (1992). Linear quadratic analysis of radiosensitization by halogenated pyrimidines. 1. Radiosensitization of human colon cancer-cells by iododeoxyuridine. *Radiat. Res.* 131, 81-89.
- Morantz, R. A. (1995). Low grade astrocytomas. In: *Brain tumours*. Churchill Livingstone. pp 433-448.
- Morimura, T., Kitz, K., Stein, H., Budka, H. (1991). Determination of proliferative activities in human brain tumour specimens: a comparison of three methods. *J. Neurooncol.* 10, 1-11.
- Morris, N. R. and Cramer, J. W. (1966). DNA synthesis by mammalian cells inhibited in culture by 5-iodo-2'-deoxyuridylate. *Mol. Pharmacol.* 2, 1-9.
- Moscona, A. (1961). Rotation-mediated histogenic aggregation of dissociated cells. *Exp. Cell. Res.* 22, 455-475.
- Moulder, J. E. and Rockwell, S. (1987). Tumour hypoxia: its impact on cancer therapy. *Cancer Metast. Rev.* 5, 313-341.
- Moyes, J. S. E., Babich, J. W., Carter, R., Meller, S. T., Agrawal, M., McElwain, T. J. (1989). A quantitative study of meta-iodo-benzylguanidine (mIBG) uptake in children with neuroblastoma: correlation with tumour histopathology. *J. Nucl. Med.* 30, 474-480.
- Moynihan, T. J. and Grossman, S. A. (1994). The role of chemotherapy in the treatment of primary tumours of the central nervous system. *Cancer Invest.* 12, 88-97.
- Muir, C. S., Storm, H. H., Polendak, A. (1994). Brain and other nervous system tumours. *Cancer Surv.* 19/20, 369-392.
- Munzenrider, J. E., Crowell, C: Charged particles. In: *Radiation oncology: biology and technology*. Mauch, P. M., Loeffler, J. S. (1994). W B Saunders. Philadelphia, pp 34-55.

- Nederman, T., Carlsson, J., Kuoppa, K. (1988). Penetration of substances into tumour tissue. Model studies using saccharides, thymidine and thymidine-5'-triphosphate in cellular spheroids. *Cancer Chemother. Pharmacol.* 22, 21-25.
- Neshastehriz, A., Angerson, W. J., Reeves, J. R., Smith, G., Rampling, R., Mairs, R. J. (1997). Incorporation of iododeoxyuridine in multicellular spheroids: implications for DNA-targeted radiotherapy using Auger electron emitters. *Br. J. Cancer.* 75, 493-499.
- Nishizaki, T., Orita, T., Furutani, Y., Ikeyama, Y., Aoki, H., Sasaki, K. (1989). Flow-cytometric DNA analysis and immunohistochemical measurement of Ki67 and BUdR labelling indices in human brain tumours. *J. Neurosurg.* 70, 379-384.
- Nordentoft, S. (1922). On roentgen-ray treatment of brain tumours. *U-gesk f. Laeger.* 84, 73-79.
- O'Donoghue, J.A., Wheldon, T.E. (1996). Targeted radiotherapy using Auger electron emitters. *Phys. Med. Biol.* 41, 1973-1979.
- O'Donoghue, J.A., Bardis, M., Wheldone, T. E. (1995). Relationships between tumour size and curability for uniformly targeted therapy with beta-emitting radionuclides. *J. Nucl. Med.* 36, 1902-1909.
- Ohgaki, H., Eibl, R. H., Schwab, M., Reichel, M. B., Mariani, L., Gehring, M., Petersen, I. et al. (1993). Mutations of the p53 tumour suppressor gene in neoplasms of the human nervous system. *Mol. Carcinog.* 8, 74-80.
- Ohgaki, H., Eibl, R. H., Wiestler, O. D., Yasargil, M. G., Newcomb, E. W., Kleihues, P. (1991). p53 mutations in non-astrocytic human brain tumours. *Cancer Res.* 51, 6202-6205.
- Olea, N., Villalobos, M., Ruiz de Almodovar, J.M., Pedraza, V. (1992). MCF-7 breast cancer cells grown as multicellular spheroids in vitro: effect of 17 $\beta$ -estradiol. *Int. J. Cancer,* 50, 112-117.
- Olive, P. L., Durand, R. E. (1994). Drug and radiation resistance in spheroids: cell contact and kinetics. *Cancer Metast. Rev.* 13, 121-138.
- Olive, P. L., Leonard, J. C., Durand, R. E. (1982). Development of tetraploidy in V79 spheroids. *In vitro.* 18, 708-714.

- Onda, K., Davis, R. L., Shibuya, M., Wilson, C. B., Hoshino, T. (1994). Correlation between the bromodeoxyuridine labelling index and the MIB-1 and Ki67 proliferating cell indices in cerebral gliomas. *Cancer*. 74, 1921-1926.
- Ozanne, B. W., Richards, C. S., Hendler, F. J., Burns, D., Gustersen, B. (1986). Over-expression of the EGF receptor is a hall-mark of squamous cell carcinomas. *J. Pathol.* 149, 9-14.
- Painter, R. B., Young, B. R., Burki, H. J. (1974). Nonrepairable strand breaks induced by 125I incorporated into mammalian DNA. *Proc. Natl. Acad. Sci. USA*. 71, 4836-4838.
- Papanastassiou, V., Pizer, B. L., Coakham, H. B., Bullimore, J., Zanarini, T., Kemshead, J. T. (1993). Treatment of recurrent and cystic malignant gliomas by a single intracavity injection of 131I monoclonal antibody: feasibility pharmacokinetics and dosimetry. *Br. J. Cancer*. 67, 144-151.
- Paulus, W. and Peiffer, J. (1989). Intratumoural histologic heterogeneity of gliomas- a quantitative study. *Cancer*. 64, 442-447.
- Peacock, J. H., Cassoni, A. M., McMillan, T. J., Steel, G.G. (1988). Radiosensitive human tumour cell lines may not be recovery deficient. *Int. J. Radiat. Biol.* 54, 945-953.
- Peacock, J. H., Eady, J. J., Edwards, S., Holmes, A., McMillan, T. J., Steel, G. G. (1989). Initial damage or repair as the major determinant of cellular radiosensitivity? *Int. J. Radiat. Biol.* 56, 543-547.
- Perez, L. A., Dombkowski, D., Efirid, J., Preffer, F., Suit, H. D. (1995). Cell proliferation kinetics in human tumour xenografts measured with iododeoxyuridine labelling index and flow cytometry: A study of heterogeneity and comparison between different methods of calculation and other proliferation measurements. *Cancer Res*. 55, 392-398.
- Pertuiset, B., Dougherty, D., Cromeyer, C., Hoshino, T., Berger, N., Rosenblum, M. L. (1985). Stem cell studies of human malignant brain tumours, Part 2: Proliferation kinetics of brain tumour cells *in vitro* in early-passage cultures. *J. Neurosurg.* 63, 426-432.
- Peters, L. (1990). Inherent radiosensitivity of tumour and normal tissue cells as a predictor of human tumour response. *Radiotherapy Oncol.* 17, 177-190.

Pettersson, O. A., Carlsson, J., Grusell, E. (1992). Accumulation of the B-10 in the central degenerative area of human glioma and colon-carcinoma spheroids after sulfhydryl boron hydride administration. *Cancer Res.* 52, 1587-1591.

Pilkington, G. J. and Lantos, P. L. (1982). The role of glutamine synthesis in the diagnosis of cerebral tumours. *Neuropathol. Appl. Neurobiol.* 8, 227-236.

Ponten, J. and Westermark, B. (1978). Properties of human malignant glioma cells *in vitro*. *Med. Biol.* 56, 184-193.

Polednak, A. P. (1991). Time trends in incidence of brain and central nervous system cancers in Connecticut. *J. Natl. Cancer Inst.* 83, 1679-1681.

Ponten, J. and MacIntyre, E. H. (1968) Long term culture of normal and neoplastic human glia. *Acta. Pathol. Microbiol. Scand.* 74, 465-486.

Ponten, J. (1975). Neoplastic human glia cells in culture. In: J. Fogh (Ed.), Plenum. New York. pp 175-206

Prelich, G., Tan, C. K., Kostura, M., Mathews, M. B., So, A. G., Downey, K. M., Stillman, B. L. (1987). Functional identity of proliferating cell nuclear antigen and a DNA polymerase  $\delta$  auxiliary protein. *Nature.* 326, 517-520.

Prusoff, W. H. (1963). A review of some aspects of 5-<sup>125</sup>I-iododeoxyuridine and azauridine. *Cancer Res.* 23, 1246-1259.

Pucillo, C., Salzano, S., Pepe, S., Vitale, M., Formisano, S., Rossi, G. (1990). Regulation of expression of low-affinity IgE receptor (FceRII) in the human monocyte-like cell line (U937) by phorbol esters and TPA. *Int. Arch. Allergy. Immunol.* 93, 330-337.

Raaphorst, G. P., Feeley, M. M. Da, Silva Vfdanjoux, C. E. Gerig, L. H. (1989). A comparison of heat and radiation sensitivity of three human glioma cell lines. In. *J. Radiat. Oncol. Biol. Phys.* 17, 615-622.

Raben, D., Buchsbaum, D. J., Khazaeli, M. B., Rosenfeld, M. E., Gillespie, G. Y., Grizzel, W. E., Liu, T., Curiel, D. T. (1996). Enhancement of radiolabelled antibody binding and tumour localization through adenoviral transduction of the human carcinoembryonic antigen gene. *Gene Ther.* 3, 567-580.

Rak, J., Mitsuhashi, Y., Erdos, V., Huang, S.N., Filmus, J., Kerbel, R.S. (1995). Massive programmed cell death in intestinal epithelial cells induced by 3-dimensional growth conditions: suppression by mutant c-H-ras oncogene expression. *J. Cell Biol.* 131, 1587-1598.

Ramsey, R. G. and Brand, W. N. (1973). Radiotherapy of glioblastoma multiforme. *J. Neurosurg.* 39, 197-202.

Ransom, D. T., Ritland, S. R., Moertel, C. A., Dahl, R. J., O'Fallon, J. R., Scheithauer, B. W., et al. (1992). Correlation of cytogenetic analysis and loss of heterozygosity studies in human diffuse astrocytomas and mixed oligo-astrocytomas. *Genes Chromosome Cancer.* 5, 357-347.

Rasmussen, T. (1966). In: Radiation therapy of tumours and diseases of the nervous system. Editor, Bouchard, J. Philadelphia, PA: Lea and Febinger.

Reifenberger, G., Reifenberger, J., Ichimura, K., Meltzer, P. S., Collins, V. P. (1994). Amplification of multiple genes from chromosomal region 12 $\delta$ 13-14 in human malignant gliomas preliminary mapping of the amplicons shows preferential involvement of CDK4, SAS, and MDM2. *Cancer Res.* 54, 4299-4303.

Rey, R. and Kinsella, T. (1991). Halogenated pyrimidines as radio sensitizers for high grade glioma: Revisited. *Int. J. Radiat. Oncol. Biol. Phys.* 21, 859-862.

Rey, J. A., Bello, N. J, deCampos, J. M., Kusak, N. E., Ramos, C., Benitez, J. (1987) Chromosomal patterns in human malignant astrocytomas. *Cancer Genet. Cytogenet.* 29, 201-221.

Riva, P., Arista, A., Tison, V., Sturiale, C., Franceschi, G., Spinelli, A., Riva, N., Casi, M., et al. (1994). Intralesional radioimmunotherapy of malignant gliomas. An effective treatment in recurrent tumours. *Cancer.* 73, 1076-1082.

Rodriguez, A., Alpen, E. L., Mendonca, M., DeGuzman, R. J. (1988). Recovery from potentially lethal damage and recruitment time of noncycling clonogenic cells in 9L confluent monolayers and spheroids. *Radiat. Res.* 114, 515-527.

Rosenblum, M.L., Knebel, K. D., Wheeler, K. T., Barker, N., Wilson, C. B. (1975). Development of an *in vitro* colony formation assay for the evaluation of *in vivo* chemotherapy of a rat brain tumour. *In Vitro.* 11, 264-273.

Ross, G. M., Eady, J. J., Mithal, N. P., Bush, C., Steel, G. G., Jeggo, P. A., McMillan, T. J. (1995). DNA strand break rejoining defect in *xrs-6* is complemented by transfection with the human *ku80* gene. *Cancer Res.* 55, 1235-1238.

Ross, G. M. (1992). Cellular and molecular studies on the mechanistic basis of clinical radioresistance in human glioma. Ph.D thesis. University of Glasgow.

Roth, J. G. and Elvidge, A. R. (1960). Glioblastoma multiforme: a clinical survey. *J. Neurosurg.* 17, 736-750.

Rotmensch, J., Whitlock, J. L., Culbertson, S., Atcher, R. W., Schwartz, J. L. (1994). Comparison of sensitivities of cells to X-ray therapy, chemotherapy, and isotope therapy using a tumour spheroid model. *Gynecol. Oncol.* 52, 290-293.

Rowlinson-Busza, G., Bamias, A., Krausz, T., Epenetos, A. A. (1991a) Uptake and distribution of specific and control monoclonal antibodies in subcutaneous xenograft following intratumour injection. *Cancer Res.* 51, 3251-3256.

Russell, D. S. and Bland, J. O. W. (1933) Study of gliomas by method of tissue culture. *J. Pathol. Bacteriol.* 36, 273-283.

Rutka, J. T., Giblin, J. R., Dougherty, D. Y., Liu, H. C., McCulloch, J. R., Bell, C. W., Stern, R. S., Wilson, C. B., Rosenblum, M. L. (1987). Establishment and characterization of five cell lines derived from human malignant gliomas. *Acta Neuropathol.* 75, 92-103.

Rutka, W., Taghian, A., Gioioso, D., Fletcher, J. A., Preffer, F., Suit, H. D. (1996). Comparison between the *in vitro* intrinsic radiation sensitivity of human soft tissue sarcoma and breast cancer cell lines. *J. Surg. Oncol.* 61, 290-294.

Ryan, P., Lee, M. W., North, B., McMichael, A. J. (1992). Risk factors for tumours of the brain and meninges: results from the Adelaide adult brain tumours study. *Int. J. Cancer.* 51, 20-27.

Salazar, O. M. and Rubin, P. (1976). The spread of glioblastoma multiforme as a determining factor in the radiation treated volume. *Int. J. Radiat. Oncol. Biol. Phys.* 5, 1733-1740.

- Santos, O., Pant, K. D., Blank, E. W., Ceriani, R. L. (1992). 5-Iododeoxyuridine increases the efficacy of the radioimmunotherapy of human tumours growing in nude mice. *J. Nucl. Med.* 33, 1530-1534.
- Sastry, K. R. S., Rao, D. V. (1984). In: *Physics of nuclear medicine: recent advances*, Rao, D. V., Chandra, R., Graham, M. (eds). American Institute of Physics, New York. pp 169-208.
- Savitsky, K., Bar-Shira, A., Giald, S., Rotman, G., Ziv, Y., Vanagatie, L. (1995). A single ataxia telangiectasia gene with a product similar to P1-3 kinase. *Science.* 268, 1749-1753.
- Scharfen, C. O., Sneed, P. S., Wara, W. M., Larson, D. A., Phillips, T. L., Trados, M. D., Weaver, K. A. et al. (1992). High activity iodine-125 interstitial implant for gliomas. *Int. J. Radiat. Oncol. Biol. Phys.* 24, 583-591.
- Schneiderman, M. H. and Schneiderman, G. S. (1996). Radioiododeoxyuridine in cancer therapy: An in vitro approach to developing *in vivo* strategies. *J. Nucl. Med.* 37 (Suppl), 6S-9S.
- Schroder, R., Bien, K., Kott, R., Meyers, I., Vossing, R. (1991). The relationship between Ki67 labelling and mitotic index in gliomas and meningiomas: demonstration of the variability of the intermitotic cycle time. *Acta Neuropathol.* 82, 389-394.
- Schwachofer, J. H. M., Crooijmans, P. P. M. A., Hoogenhout, J., Jerusalem, C. R., Kal, H. B., Theeuwes, A. G. M. (1989). Radiosensitivity of different human tumour cell lines grown as multicellular spheroids derived from growth curves and survival data. *Int. J. Radiat. Oncol. Biol. Phys.* 17, 1015-1020.
- Schwartz, J. L., Mustafi, R., Hughes, A., Desomber, E. R. (1996). DNA and chromosome breaks by iodine-123 labelled oestrogen in chinese-hamster ovary cells. *Radiat. Res.* 146, 151-158.
- Shapiro, W. R., Green, S. B., Burger, P. C., Mahaley, M. S., Selker, R. G., Vangilder, J. C., Robertson, J. T., Ransohoff, J. et al. (1989). Randomized trial of three chemotherapy regimens and two radiotherapy regimens in post-operative treatment of malignant glioma. Brain Tumour Coop Group Trial 8001. *J. Neurosurg.* 71, 1-9.

Shapiro, J. R., Yung, W. K. A. and Shapiro, W. R. (1981). Isolation, karyotype and clonal growth of heterogeneous subpopulations of human malignant gliomas. *Cancer Res.* 41, 1349-2359.

Sheline, G. E. (1977). Radiation therapy of brain tumours. *Cancer.* 39, 873-881.

Shibuya, M., Saito, F., Miva, T., Davis, R. L., Wilson, C. B., Hoshino, T. (1992). Histochemical study of pituitary adenomas with Ki-67 and anti-DNA polymerase  $\alpha$  monoclonal antibodies, bromodeoxyuridine labelling, and nuclear organizer region counts. *Acta Neuropathol.* 84, 178-183.

Shrieve, D. C., Gutin, P. H., Larson, A. D. (1994). Brachytherapy. In: *Radiation Oncology, Technology and Biology.* Mauch, P., Loffler, J. S. Saunders, W. B. Philadelphia, pp 216-236.

Shrieve, D. C., Alexander, EIII., Wen, P. Y., Fine, H. A., Kooy, H. M., Black, P. M. L., Loeffler, J. S. (1995). Comparison of stereotactic radiosurgery and brachytherapy in the treatment of recurrent glioblastoma multiforme. *Neurosurgery.* 36, 275-284.

Slichenmyer, W. J., Nelson, W. G., Slebos, R. J., Kastan, M. B. (1993). Loss of a *p53* associated  $G_1$  checkpoint does not decrease cell survival following DNA damage. *Cancer Res.* 53, 4164-4168.

Stage, W. S. and Stein, J. J. (1974). Treatment of malignant astrocytomas. *Am. J. Roentgenol.* 120, 7-18.

Steel, G. G. (1991). Cellular sensitivity to low-dose rate irradiation focuses the problem of tumour radioresistance. *Radiother. Oncol.* 20, 71-83.

Steel, G.G. and Peacock, J. H. (1989). Why are some human tumours more radiosensitive than others? *Radiother. Oncol.* 15, 63-72.

Steel, G. G., Deacon, J. M., Duchesne, G. M., Horwich, A., Kelland, L. R., Peacock, J. H. (1987). The dose-rate effect in human tumour cells. *Radiother. Oncol.* 9, 299-310.

Steel, G. G., Down, J. D., Peacock, J. H., Stephens, T. C. (1986). Dose-rate effects and the repair of radiation damage. *Radiother. Oncol.* 5, 321-331.

- Steel, G. G. (1984). Therapeutic response of human tumour xenografts in immune-suppressed mice. In: Immune deficient animals. eds, Sordat, B. S. Karger, Basel. 409-415.
- Stewart, D. J. (1994). A critique of the role of the blood-brain-barrier in the chemotherapy of human brain-tumours. *J. Neuro. Oncol.* 20, 121-139.
- Strickland, D. K., Vaidyanathan, G., Zalutsky, M. R. (1994). Cytotoxicity of  $\alpha$ -particle-emitting m-<sup>211</sup>At-Astato-benzylguanidine on human neuroblastoma cells. *Cancer Res.* 54, 5414-5419.
- Stuschke, M., Budach, V., Sack, H. (1993). Radioresponsiveness of human glioma, sarcoma and breast-cancer spheroids depends on tumour differentiation. *Int. J. Radiat. Oncol. Biol. Phys.* 27, 627-636.
- Sullivan, F. J., Herscher, L. L., Cook, J. A., Smith, J., Steinberg, S. M., Epstein, A. H., Oldfield, E. H., Goffman, T. E. et al. (1994). National Cancer Institute (phase II) study of high-grade glioma treated with accelerated hyperfractionated radiation and iododeoxyuridine: results in anaplastic astrocytoma. *Int. J. Radiat. Biol. Phys.* 30, 583-590.
- Suresh, A., Tung, F., Moreb, J., Zucali, J. R. (1994). Role of manganese superoxide dismutase in radioprotection using gene transfer studies. *Cancer Gene Therapy.* 1, 85-90.
- Sutherland, R. M. (1988). Cell and environment interactions in tumour microregions: the multicell spheroid model. *Science.* 240, 177-184.
- Sutherland, R. M., Buchegger, F., Schreyer, M., Vacca, A., Mach, J. P. (1987). Penetration and binding of radiolabelled anti-carcinoembryonic antigen monoclonal-antibodies and their antigen-binding fragments in human colon multicellular tumour spheroids. *Cancer Res.* 47, 1627-1633.
- Sutherland, R. M., Inch, W. R., McCredie, J. A., Kruuv, J. (1970). A multi component radiation survival curve using an *in vitro* tumour model. *Int. J. Radiat. Biol.* 18, 491-495.
- Sutherland, R. M., McCredie, J. A., Inch, W. R. (1971). Multicellular spheroids: a new model target for *in vitro* studies of immunity to solid tumour allografts. *J. Natl. Cancer Inst.* 46, 113-120.

Taghian, A., Gioioso, D., Budach, W., Suit, H. (1993). In vitro split-dose recovery of glioblastoma multiforme. *Radiat. Res.* 134, 16-21.

Taghian, A., Suit, H., Phil, D., Pardo, F., Gioioso, D., Tomkinson, K., DuBois, W., Gerweck, L. (1992). In vitro intrinsic radiation sensitivity of glioblastoma multiforme. *Int. J. Radiat. Oncol. Biol. Phys.* 23, 55-62.

Tannock, I. F. (1996). Treatment of cancer with radiation and drugs. *J. Clin. Oncol.* 14, 3156-3174.

Tannock, I. F. (1978). Cell kinetics and chemotherapy: A critical review. *Cancer Treat. Rep.* 62, 1117-1133.

Taratuto, A. L., Sevlever, G., Piccardo, P. (1991). Clues and pitfalls in stereotaxic biopsy of the central-nervous system. *Arch. pathol. lab. Med.* 115, 596-602.

Taveras, J. M., Thompson Jr. H. G., Pool, J. L. (1962). Should we treat glioblastoma multiforme? A study of survival in 425 cases. *Am. J. Roentgenol.* 87, 473-479.

Tsurumi, Y., Kameyama, M., Ishiwata, K., Katakura, R., Monma, M., Ido, T., Suzuki, J. (1990). <sup>18</sup>F-fluoro-2'-deoxyuridine as a tracer of nucleic acid metabolism in brain tumours. *J. Neurosurg.* 72,110-113.

Uihlein, A., Colby Jr, M. Y., Layton, D. D., Parsons, W. R., Carter, T. L. (1966). Comparison of surgery and surgery plus irradiation in the treatment of supratentorial gliomas. *Acta Radiol. Ther. Phys. Biol.* 5, 67-78.

Urtasun, R. C., Cosmatos, D., DelRowe, J., Kinsella, T. J., Lester, S., Wasserman, T., Fulton, D. S. (1993). Iododeoxyuridine (IUdR) combined with radiation in the treatment of malignant glioma: A comparison of short versus long intravenous dose schedules (RTOG 86-12). *Int. J. Radiat. Oncol. Biol. Phys.* 27, 207-214.

Urtasun, R. C., Band, P., Chapman, J. D., Harvey, R. R., Wilson, A. F., Fryer, C. G. (1977). Clinical phase I study of the hypoxic cell radiosensitizer RO-07-0582, a 2-nitroimidazole derivative. *Radiology.* 122, 801-804.

Urtasun, R. C., Feldstein, M. L., Partington, J., Tanasichuk, H., Miller, J. D. R., Russell, D. B., Agboola, O., Mielke, B. (1982). Radiation and nitroimidazoles in supratentorial high grade gliomas: a second clinical trial. *Br. J. Cancer.* 46, 101-108.

Vaeth, J. M. and Meyer, J. L (Eds). (1990). The present and future role of monoclonal antibodies in the management of cancer. In: *Frontiers of Radiation Therapy*. 24, Karger; Basel.

Vaidyanathan, G., Larsen, R. H., Zalutsky, M. R. (1996). 5-[<sup>211</sup>At]astato-2'-deoxyuridine, an alpha particle-emitting endoradiotherapeutic agent undergoing DNA incorporation. *Cancer Res.* 56, 1204-1209.

Von Deimling, A., Eibl, R. H., Louis, D. N., Von Ammon, H., Petersen, I., Kleihues, P., Chung, R. Y., Wiestler, O. D., Seizinger, B. R. (1992a). *p53* mutations are associated with 17p allelic loss in grade II and grade III astrocytoma. *Cancer Res.* 52, 2987-2990.

Von Deimling, A., Louis, D. N., Von Ammon, K., Petersen, I., Wiestler, O. D., Seizinger, B. R. (1992b). Evidence for a tumour suppressor gene on chromosome 19q associated with astrocytomas, oligodendrogliomas and mixed gliomas. *Cancer Res.* 52, 31-38.

Von Deimling, A., Louis, D. N., Von Ammon, H., Petersen, I., Hoell, T., Chung, R. Y., Martuza, R. L., Schoenfeld, D. A., Yasargil, G., Wiestler, O. D., Seizinger, B. R. (1992c). Association of epidermal growth factor receptor gene amplification with loss of chromosome 10 in human glioblastoma multiform. *J. Neurosurg.* 77, 295-301.

Voute, P. A., Hoefnagel, C. A., de Kraker, J., Valdes-Omas, R., Bakker, D. J., van de Kleu, A. J. (1991). Results of treatment with meta-iodo-benzylguanidine (<sup>131</sup>I-mIBG) in patients with neuroblastoma : Future prospects of zeto therapy. In: *Advances in neuroblastoma research*. Evans, A.E. D'Angio, G. J. Kundson, A. G. and Seeger, R.C. Wiley-Liss, New York. pp 439-446.

Walker, M. D., Green, S. B., Byer, D. P., Alexander, E., Batzdorf, U., Brooks, W. H., Hunt, W. E., Collins, M. D. et al. (1980). Comparisons of radiotherapy and nitrosoureas for the treatment of malignant glioma after surgery. *N. Eng. J. Med.* 303, 1323-1329.

Walker, M. D., Alexander E. Jr., Hunt, W. E., MacCarty, C. S., Mahaley, M. S. Jr., Mealey, J. Jr., Norrell, H. A., Owens, G. et al. (1978). Evaluation of BCNU and /or radiotherapy in the treatment of anaplastic gliomas. A cooperative clinical trial. *J. Neurosurg.* 49, 333-343.

- Walker, K. A., Murray, T., Hilditch, T. E., Wheldon, T. E., George, A., Hann, I. M. (1988). A tumour spheroid model for antibody-targeted therapy of micrometastases. *Br. J. Cancer.* 58, 13-16.
- Wallner, K. E., Galicich, J. H., Krol, G., Arbit, E., Malkin, M. G. (1989). Patterns of failure following treatment for glioblastoma multiforme and anaplastic astrocytoma. *Int. J. Radiat. Oncol. Phys.* 16, 1405-1409.
- Ward, J. (1990). The yield of DNA double-strand breaks produced intracellularly by ionizing radiation: a review. *Int. J. Radiat. Biol.* 57, 1141-1150.
- Weichselbaum, R. R. and Little, J. B. (1982). The differential response of human tumours to fractionated radiation response of human tumours to fractionated radiation may be due to a post-irradiation repair process. *Br. J. Cancer.* 46, 532-537.
- Weichselbaum, R. R., Hallahan, D. E., Becket, M. A., Mauceri, H. J., Lee, H., Sukhatme, V. P., Kufe, D. W. (1994). Gene therapy targeted by radiation preferentially radiosensitises tumour cells. *Cancer Res.* 54, 4266-4269.
- Weingerg, R. G. (1989). Positive and negative controls on cell growth. *Biochemistry.* 28, 8264-9.
- Wessels, B. W. and Rogus, K. D. (1984). Radionuclide selection and model absorbed dose calculation for radiolabelled tumour associated antibodies. *Med. Phys.* 11, 638-644.
- Westermark, B., Ponten, J. Hugosson, R. (1973). Determinants for the establishment of permanent tissue culture lines from human gliomas. *Acta Path. Microbiol. Scand. A,* 81, 191-805.
- Westphal, M., Nausch, H., Herrmann, H. D. (1990). Antigenic staining patterns of human glioma cultures: Primary cultures, long-term cultures and cell lines. *J. Neurocytol.* 19, 466-477.
- Westphal, M. and Herrmann, H. D. (1989). Growth-factor biology and oncogene activation in human gliomas and their implications for specific therapeutic concepts. *Neurosurg.* 25, 681-694.

- Whately, T. L., Falton, P. A., Robertson, L., Rampling, R (1995). *In vitro* study of PLGA implants for sustained delivery of carboplatin and etoposide to the brain. Proc. Contr. Rel. Soc. 22, 582-583.
- Wheldon, T.E., Livingstone, A., Wilson, L., O'Donoghue, J., Gregor, A. (1985). The radiosensitivity of human neuroblastoma cells estimated from regrowth curves of multicellular tumour spheroids. Br. J. Radiol. 58, 661-664.
- Wheldon, T. E. and O'Donoghue, J. A. (1990). The radiobiology of targeted radiotherapy. Int. J. Radiat. Biol. 58, 1-21.
- Wheldon, T. E. (1994). Targeting radiation to tumours. Int. J. Radiat. Biol. 65, 109-116.
- Wheldon, T. E. and O'Donoghue, J. A. (1997). Microdosimetric considerations in the targeted radiotherapy of cancer. In: Proceedings 12th International Symposium on Microdosimetry. London: Royal Institute of Chemistry Publications, in press.
- Whittle, I. R. and Gregor, A. (1991). The treatment of primary malignant brain-tumours. J. Neuro. Neurosurg. Psych. 54, 101-103.
- Williams, M., Denekamp, J., Fowler, J. (1985). A review of  $\alpha/\beta$  ratios for experimental tumours: implications for clinical studies of altered fractionation. Int. J. Radiat. Oncol. Biol. Phys. 11, 87-96.
- Withers, H. R. (1992). Biological basis of radiation therapy for cancer. Science and practice. 339, 156-163.
- Wong, A. J., Ruppert, J. M., Bigner, S. H., Grzeschik, C. H., Humphery, A. P., Bigner, D. D., Vogelstein, B. (1992). Structural alterations of the epidermal growth factor receptor gene in human gliomas. Proc. Natl. Acad. Sci. U S A. 89, 2965-2969.
- Zalutsky, M. R., Moseley, R. P., Benjamin, J. C., Colpinto, E. V., Fuller, G. N., Coakham, H. P., Binger, D. D. (1990). Monoclonal antibody and F(ab')<sub>2</sub> fragment delivery to tumours in patients with glioma: comparison of intracarotid and intravenous administration. Cancer Res. 50, 4105-4110.